2013

Structure and function of class one non-symbiotic plant hemoglobins

Ryan Thomas Sturms
Iowa State University

Structure and function of class one non-symbiotic plant hemoglobins

by

Ryan Thomas Sturms

A dissertation submitted to the graduate faculty

in partial fulfillment of the requirements for the degree of

DOCTOR OF PHILOSOPHY

Major: Biochemistry

Program of Study Committee:
Mark Hargrove, Major Professor
Alan DiSpirito
Don Beitz
John Robyt
Laura Jarboe

Iowa State University
Ames, Iowa
2013

TABLE OF CONTENTS

ACKNOWLEDGEMENTS

I would like to thank my program of study committee: Dr. Alan DiSpirito, Dr. Don Beitz, Dr. John Robyt, Dr. Laura Jarboe, and especially my major professor Dr. Mark Hargrove. Without their support and guidance none of this work would have been possible.

I would like to thank all of the faculty and the staff in the Roy J. Carver Department of Biochemistry, Biophysics, and Molecular Biology. Your dedication to students and fostering an atmosphere of learning is something I hope to be able to carry forward in my career. Thank you to all of my lab mates, past and present. Dr. James Trent III, Dr. Benoit Smagghe, Dr. Julie Hoy, and Dr. Smita Kakar for helping me learn many techniques related to studying hemoglobins and Navjot Singh and Xiaoguang Wang for always working hard and helping to maintain an optimistic outlook in the lab, even when things got tough.

Thank you to all of the friends and colleagues that I have had the pleasure of working with. Your support and friendship both in the lab and outside of it have meant the world to me. To my family, Mom, Dad, Matt, Natalie, and Elizabeth; you have been the most loving and encouraging family I could ask for. Thank you for pushing me to set and achieve lofty goals. Finally, thank you to Madeline. I am blessed to have met such a loving and supportive person. Through all of the struggles you were always at my side to encourage me and help me through, and in all of the good times you were the

first one to help me celebrate. Your patience during these last 4 years has been amazing and has meant so much. I could not have done this without you.

ABSTRACT

Plants contain at least three kinds of hemoglobins. Those plants that carry out symbiotic nitrogen fixation use oxygen transport hemoglobins to deliver oxygen to the aerobic nitrogen fixing bacteria in their roots. The functions of other plant hemoglobins are not yet known with confidence, but are thought to also have roles in nitrogen metabolism. This dissertation examines plant hemoglobin structure and function in two distinct classes: oxygen transport hemoglobins and what we believe to be hemoglobins that function as dissimilatory nitrite reductases.

The capacity for oxygen transport arose twice independently in two distinct phylogenetic classes of plant hemoglobins. From "Class 2" hemoglobins arose the "leghemoglobins" common in many species of legumes including soybeans. From "Class 1" hemoglobins arose an individual oxygen transport hemoglobin in the species *Parasponia andersonii* (ParaHb). ParaHb and leghemoglobins have convergently evolved the clear physical properties supporting oxygen transport. Hemogobin from a closely related species, *Trema tomentosa*, is not an oxygen transporter, in spite of > 90% sequence identity to one another. The first part of this dissertation examines how such a small number of amino acid substitutions could result in the pronounced physical differences conferring a change in physiological function.

The second part of the dissertation presents evidence establishing dissimilatory nitrogen reduction as a physiological function for Class 1 plant hemoglobins. These proteins are able to efficiently reduce nitrite and hydroxylamine *in vitro*, in contrast to most other

hemoglobins. It is shown that the unique structure of Class 1 plant hemoglobins facilitates catalytic reduction of nitrite and hydroxylamine by providing a ligand binding site and enhancing intermolecular electron transfer in support of multi-electron reduction reactions.

CHAPTER 1.

INTRODUCTION

Introduction

The relationship between protein structure and physiological function is question that is actively being addressed in many areas of biochemical research. Computational models are developed to predict protein functionality based on amino acid sequence [1-6], therapeutic targets are being developed based on structural information [7-11], and enzymes are being engineered to specifically alter substrate preference and end product identity [12, 13]. All of these efforts require a basic understanding of the relationship between structure and function and many of them rely on the assumption that homologous structures will lead to homologous function. However, this assumption is not always the case in living organisms as has been demonstrated most clearly in the globin superfamily of proteins.

This family of proteins comprises some of the most extensively studied proteins in all of science. The first three dimensional crystal structure of a protein ever solved was that of myoglobin in 1958 by John Kendrew [14]. Since then, nearly 400 structures of globin proteins, their liganded forms, and their mutants have been solved. These structures range from the familiar hemoglobin and myoglobin proteins to the Hell's Gate globin found in thermophillic acidophilic obligate methanotrophic bacteria [14-16]. They

come from organisms that inhabit environments that span the vertical space of earth from deep sea vents to the air over Mount Everest [17-20].

All of these globins share a homologous fold, one that is typically comprised of eight alpha helices sandwiched together in a canonical "3-on-3" fold, though there is some variation in this which is observed in the "2-on-2" truncated globins, which lack two helices normally found in the classical globin fold [21]. Despite the broad similarity observed in the tertiary structure of members of the globin family of proteins, the functions of each individual member of the family vary widely [21].

A drastic example of differing function despite structural similarity comes from comparing myoglobin to another globin found in mammals, neuroglobin. Despite belong to the same family of proteins and being structurally homologous, neuroglobin does not participate in oxygen transport [22]. Additionally, a histidine present in the distal pocket of neuroglobin forms a sixth coordinate bond to the heme iron, a bond which is not formed by the same residue in myoglobin or hemoglobin [23].

Another, well defined, system for studying functional differences among structurally homologous proteins in the members of the globin family is plants. All plants encode and express hemoglobin genes that can be phylogeneticly grouped into distinct classes. These classes are the symbiotic leghemoglobins, the class 1 non-symbiotic hemoglobins, the class 2 non-symbiotic hemoglobins, and the class 3 non-symbiotic hemoglobins [21, 24, 25]. Of these classes, only the leghemoglobins have been assigned a known function, which is to bind and transport oxygen in root nodules of plants that symbiotically fix atmospheric nitrogen [26, 27]. However, based on the

phylogenetic tree of plant hemoglobins and kinetic and structural studies, this oxygen transport function is not the original function of the globin family of proteins and furthermore these proteins acquired the oxygen transport function associated with globins more recently on an evolutionary time scale than the globins in mammalian systems [21, 25].

In an effort to understand the evolution of oxygen transport in plant hemoglobins and to assign an ancient function to globins, the class one non-symbiotic hemoglobins have been extensively studied through x-ray crystallography and detailed *in vitro* biochemical analyses. These studies have helped to generate hypotheses for the primordial function of these proteins that range from nitric oxide scavenging via a nitric oxide dioxygenase reaction [28-33] to nitrite reductase activity to provide a source of nitric oxide [34].

The work presented in this dissertation is focused on this central question in the field of plant hemoglobin biochemistry: "What is the function of non-symbiotic plant hemoglobins?" The work comprises two aspects of this question. The first deals with the evolution of oxygen transport, a well-known, but evolutionarily newer function of plant hemoglobins, and the second aims to address what other functions non-symbiotic hemoglobins may be carrying out. It will present evidence in support of our hypothesis that non-symbiotic hemoglobins are serving in the hypoxic root as an alternate respiration system in which nitrogenous ligands serve as the terminal electron acceptor. These types of reactions have previously been described in bacterial species [35-43]. This work provides an *in vitro* basis for individual steps in a similar reaction cycle in plants.

Dissertation Organization

Chapters two and three focus on the evolution of oxygen transport in plant hemoglobins by examining a pair of hemoglobin proteins from the plants *Trema tomentosa* (TremaHb), a non-nitrogen fixing plant, and *Parasponia andersonii* (ParaHb), a nitrogen fixing plant, that are nearly identical in primary sequence (differing by only eleven amino acids), yet based on previous studies and expression profiles *in planta* would be predicted to function very differently. ParaHb has characteristics of typical oxygen transport hemoglobins: high concentration, moderate oxygen affinity, a pentacoordinate heme and a rapid oxygen dissociation rate. These characteristics contrast with TremaHb, which is present in low concentrations and based on phlogeny would be predicted to have a hexacoordinate heme iron, a high affinity for oxygen and a slow oxygen dissociation rate.

Chapter two presents detailed kinetic characterizations of both ParaHb and TremaHb in both the ferric and ferrous oxidation states to address the question of whether or not two hemoglobins with such high sequence similarity can actually be so different in functional behavior. The results from these experiments indicate that the two proteins differ from each other only in oxygen affinity and oxygen dissociation rate constants, two factors key to their different functions. These results demonstrate distinct mechanisms for convergent evolution of oxygen transport in different phylogenetic classes of plant hemoglobins. The contributions of the authors in chapter two were as follows: Ryan Sturms- primary experimenter and writer, Smita Kakar- helped prepare proteins and phylogenetic materials, James Trent- provided instruction on the techniques

used and feedback on written materials, and Mark Hargrove- principal investigator and corresponding author.

Chapter three is a structural investigation of these same hemoglobins from *Trema* and *Parasponia* that aims to further address how these hemoglobins could differ in function despite their shared sequence identity. Additionally, redox potential measurements and analytical ultracentrifuge measurements made in chapter two suggest that both of these proteins exist as dimers and that there may be some inequality in the hemes of the subunits of ParaHb. To determine the cause of subunit heterogeneity in ParaHb, we have measured their crystal structures in the ferric oxidation state. Furthermore, we have made a monomeric ParaHb mutant protein (I43N) and measured its ferrous/ferric heme redox potential to test links between quaternary structure and heme heterogeneity in wild type ParaHb. The results of these studies are presented in chapter three. Author contributions for chapter three were as follows: Smita Kakar- crystallographer and primary author, Ryan Sturms- generated mutant proteins and carried out all ultracentrifugation and redox titration measurements, Andrea Tiffany- purified proteins and made initial efforts at crystallization, Jay C. Nix- beamline scientist, Alan DiSpirito- contributing author, and Mark Hargrove- principal investigator and corresponding author.

Chapter four begins the second aspect of answering the question of function for non-symbiotic plant hemoglobins, "what other functions could non-symbiotic hemoglobin serve?" Research into the reaction of nitrite with mammalian hemoglobin, myoglobin, neuroglobin, and cytoglobin, demonstrated that deoxy forms of these

proteins are able to reduce nitrite to nitric oxide [44, 45]. The authors of these studies postulate that hemoglobin serves as an additional source of nitric oxide that can carry out signaling and protective vasodilatory effects. However, the concentrations of nitrite that are typically found in cells (low micromolar) combined with the fact that endothelial cells produce nitric oxide at a much higher rate, suggest that this may not be a significant function of these mammalian globins [46, 47].

In plants though, the concentrations of nitrite can rise drastically under hypoxic conditions, both conditions when expression of non-symbiotic hemoglobin is induced [48, 49]. This led me to test the ability of non-symbiotic plant hemoglobin and *Synechocystis* cyanoglobin to reduce nitrite and the results are presented in chapter four. Author contributions for chapter four are as follows: Ryan Sturms- primary experimenter and author, Alan DiSpirito- provided the use of the anaerobic chamber used in the experiments and valuable discussion points, and Mark Hargrove- principal investigator and corresponding author.

Chapter five continues to investigate the reduction of nitrogenous ligands as a possible function of non-symbiotic plant hemoglobins. Previous studies have shown that the nitrogenous ligand, hydroxylamine, is also reduced by deoxy hemoglobin and myoglobin[50, 51]. Studies into the mechanism of nitrite reductase have postulated that hydroxylamine is an intermediate in the reduction of nitrite to ammonium that is carried out by this enzyme [52, 53]. Given the propensity of non-symbiotic hemoglobin to reduce nitrite [34, 54], and the hypothesis that nitrite may build up due to a failure of nitrite

reductase to complete its reaction cycle [55], we hypothesize that under hypoxic conditions, non-symbiotic hemoglobin may be an alternative means of reducing a potentially toxic build-up of hydroxylamine in support of continued energy production. We measure the final product of this reaction using NMR spectroscopy and compare the rates of reaction with hydroxylamine for deoxy non-symbiotic hemoglobin, myoglobin, neuroglobin, cytoglobin, and *Synechocystis* cyanoglobin. The results of these studies are presented in chapter five. Author contributions for chapter five are as follows: Ryan Sturms- primary experimenter and author, Alan DiSpirito- provided the use of the anaerobic chamber used in the experiments and valuable discussion points, Bruce Fulton- NMR scientist, and Mark Hargrove- principal investigator and corresponding author.

Chapter six is a manuscript that is to be submitted, and it addresses a specific question that is raised in chapter five, namely "How does deoxy hemoglobin reduce hydroxylamine by two electrons without forming any observable intermediate?" I hypothesize that intermolecular electron transfer may be occurring during multi-electron reduction events and that the relative rates of this transfer may be influencing the overall reaction rate. To test this hypothesis, we developed a new method for observing electron self-exchange (ESE) in hemoglobins. Typically, the rates of ESE are measured by using NMR spectroscopy, but this technique requires the addition of a bulky ligand to the heme protein [56]. Other methods include creating an excited population of ruthenium modified molecules and watching inter-molecular electron transfer [57]. Both of these methods introduce an unwanted variable when trying to determine the relative rates of

ESE in a ground state, unliganded protein. To overcome this challenge, we use deuteroheme reconstituted proteins, in which the protoporphyrin heme has been replaced with a deuteroporphryin heme, one that is missing the vinyl groups. This substitution results in approximately a 10 nanometer blue shift of the absorbance spectrum and a minimal difference in reduction potential [(58)]. This spectroscopic difference allows us to simply mix one population of reduced proto-heme protein with an equal population of oxidized deutero-heme protein and monitor the approach to equilibrium. The relative rates of ESE for myoglobin and rice non-symbiotic hemoglobin are presented in chapter six. Author contributions for chapter six are as follows: Ryan Sturms- primary experimenter and author, Alan DiSpirito- provided the use of the anaerobic chamber used in the experiments and valuable discussion points, and Mark Hargrove- principal investigator and corresponding author.

Chapter seven is a manuscript that is to be submitted, and it addresses mechanistic questions regarding multi-electron reduction of hydroxylamine. Structural comparisons of non-symbiotic hemoglobin with bacterial ammonifying nitrite reductases reveal surprising similarities between the two proteins. Bacterial ammonifying nitrite reductases contain multiple heme centers, one or more that is low spin bis-histidyl coordinated and one that is a high spin pentacoordinate (lysine coordinated) center with an open binding site [(35-43)]. By comparison, non-symbiotic hemoglobins typically exist in a fractionally hexacoordinated state, which would functionally mimic the active site of the bacterial ammonifying nitrite reductases. In the bacterial ammonification systems, the pentacoordinate center serves as the ligand binding site and the bis-histidyl

hexacoordinate center serves as an electron donor [40]. The experiments presented in chapter six test the hypothesis that non-symbiotic hemoglobins may be functioning in a manner similar to the bacterial ammonifying nitrite reductases through mutational studies. By tightening or abolishing hexacoordination in non-symbiotic hemoglobins, we should disrupt the ability of the protein to carry out the multi-electron reduction of hydroxylamine through elimination of the ligand binding site or the electron donor. Through mixing experiments similar to those presented in chapter six, we aim to address the directionality of electron flow in this system. Additionally, we test the role of the transient dimer that is typically formed by non-symbiotic hemoglobins in the reaction with hydroxylamine. The results of these experiments are presented in chapter seven. Author contributions for chapter seven are as follows: Ryan Sturms- primary experimenter and author, Alan DiSpirito- provided the anaerobic chamber and thoughtful discussion points, and Mark Hargrove- principal investigator and corresponding author.

References

1. Clark, W. T., and Radivojac, P. (2011) Analysis of protein function and its prediction from amino acid sequence, *Proteins 79*, 2086-2096.

2. Erdin, S., Venner, E., Lisewski, A. M., and Lichtarge, O. (2013) Function prediction from networks of local evolutionary similarity in protein structure, *BMC Bioinformatics 14 Suppl 3*, S6.

3. Pierri, C. L., Parisi, G., and Porcelli, V. (2010) Computational approaches for protein function prediction: a combined strategy from multiple sequence alignment to molecular docking-based virtual screening, *Biochimica et Biophysica Acta 1804*, 1695-1712.

4. Roy, A., Kucukural, A., and Zhang, Y. (2010) I-TASSER: a unified platform for automated protein structure and function prediction, *Nature Protocols 5*, 725-738.

5. Sadowski, M. I., and Jones, D. T. (2009) The sequence-structure relationship and protein function prediction, *Current Opinion in Structural Biology 19*, 357-362.

6. Sael, L., Chitale, M., and Kihara, D. (2012) Structure- and sequence-based function prediction for non-homologous proteins, *Journal of Structural and Functional Genomics 13*, 111-123.

7. Cheng, H., Hoffman, J. E., Le, P. T., Pairish, M., Kania, R., Farrell, W., Bagrodia, S., Yuan, J., Sun, S., Zhang, E., Xiang, C., Dalvie, D., and Rahavendran, S. V. (2013) Structure-based design, SAR analysis and antitumor activity of PI3K/mTOR dual inhibitors from 4-methylpyridopyrimidinone series, *Bioorganic & Medicinal Chemistry Letters*.

8. Huang, X., Cheng, C. C., Fischmann, T. O., Duca, J. S., Richards, M., Tadikonda, P. K., Reddy, P. A., Zhao, L., Arshad Siddiqui, M., Parry, D., Davis, N., Seghezzi, W., Wiswell, D., and Shipps, G. W., Jr. (2013) Structure-based design and optimization of 2-aminothiazole-4-carboxamide as a new class of CHK1 inhibitors, *Bioorganic & Medicinal Chemistry Letters*.

9. Junior, M. C., de Assis, S. A., Goes-Neto, A., Duarte, A. A., Alves, R. J., Junior, M. C., and Taranto, A. G. (2013) Structure-based drug design studies of UDP-N-acetylglucosamine pyrophosphosrylase, a key enzyme for the control of witches' broom disease, *Chemistry Central Journal 7*, 48.

10. Neves, B. J., Bueno, R. V., Braga, R. C., and Andrade, C. H. (2013) Discovery of new potential hits of Plasmodium falciparum enoyl-ACP reductase through ligand- and structure-based drug design approaches, *Bioorganic & Medicinal Chemistry Letters 23*, 2436-2441.

11. Urich, R., Wishart, G., Kiczun, M., Richters, A., Tidten-Luksch, N., Rauh, D., Sherborne, B., Wyatt, P. G., and Brenk, R. (2013) De Novo Design of Protein Kinase Inhibitors by in Silico Identification of Hinge Region-Binding Fragments, *ACS Chemical Biology*.

12. Woolston, B. M., Edgar, S., and Stephanopoulos, G. (2013) Metabolic Engineering: Past and Future, *Annual Review of Chemical and Biomolecular Engineering*.

13. Yoon, J. M., Zhao, L., and Shanks, J. V. (2013) Metabolic Engineering with Plants for a Sustainable Biobased Economy, *Annual Review of Chemical and Biomolecular Engineering*.

14. Kendrew, J. C., Bodo, G., Dintzis, H. M., Parrish, R. G., Wyckoff, H., and Phillips, D. C. (1958) A three-dimensional model of the myoglobin molecule obtained by x-ray analysis, *Nature 181*, 662-666.

15. Perutz, M. F., Rossmann, M. G., Cullis, A. F., Muirhead, H., Will, G., and North, A. C. (1960) Structure of haemoglobin: a three-dimensional Fourier synthesis at 5.5-A. resolution, obtained by X-ray analysis, *Nature 185*, 416-422.

16. Teh, A. H., Saito, J. A., Baharuddin, A., Tuckerman, J. R., Newhouse, J. S., Kanbe, M., Newhouse, E. I., Rahim, R. A., Favier, F., Didierjean, C., Sousa, E. H., Stott, M. B., Dunfield, P. F., Gonzalez, G., Gilles-Gonzalez, M. A., Najimudin, N., and Alam, M. (2011) Hell's Gate globin I: an acid and thermostable bacterial hemoglobin resembling mammalian neuroglobin, *FEBS Letters 585*, 3250-3258.

17. de Haas, F., Zal, F., You, V., Lallier, F., Toulmond, A., and Lamy, J. N. (1996) Three-dimensional reconstruction by cryoelectron microscopy of the giant hemoglobin of the polychaete worm Alvinella pompejana, *Journal of Molecular Biology 264*, 111-120.

18. Liang, Y., Hua, Z., Liang, X., Xu, Q., and Lu, G. (2001) The crystal structure of bar-headed goose hemoglobin in deoxy form: the allosteric mechanism of a hemoglobin species with high oxygen affinity, *Journal of Molecular Biology 313*, 123-137.

19. Liu, X. Z., Li, S. L., Jing, H., Liang, Y. H., Hua, Z. Q., and Lu, G. Y. (2001) Avian haemoglobins and structural basis of high affinity for oxygen: structure of bar-headed goose aquomet haemoglobin, *Acta Crystallographica. Section D, Biological Crystallography 57*, 775-783.

20. Zhang, J., Hua, Z., Tame, J. R., Lu, G., Zhang, R., and Gu, X. (1996) The crystal structure of a high oxygen affinity species of haemoglobin (bar-headed goose haemoglobin in the oxy form), *Journal of Molecular Biology 255*, 484-493.

21. Kakar, S., Hoffman, F. G., Storz, J. F., Fabian, M., and Hargrove, M. S. (2010) Structure and reactivity of hexacoordinate hemoglobins, *Biophysical Chemistry 152*, 1-14.

22. Trent, J. T., 3rd, Watts, R. A., and Hargrove, M. S. (2001) Human neuroglobin, a hexacoordinate hemoglobin that reversibly binds oxygen, *The Journal of Biological Chemistry 276*, 30106-30110.

23. Pesce, A., Dewilde, S., Nardini, M., Moens, L., Ascenzi, P., Hankeln, T., Burmester, T., and Bolognesi, M. (2003) Human brain neuroglobin structure reveals a distinct mode of controlling oxygen affinity, *Structure 11*, 1087-1095.

24. Hoy, J. A., Robinson, H., Trent, J. T., 3rd, Kakar, S., Smagghe, B. J., and Hargrove, M. S. (2007) Plant hemoglobins: a molecular fossil record for the evolution of oxygen transport, *Journal of Molecular Biology 371*, 168-179.

25. Smagghe, B. J., Hoy, J. A., Percifield, R., Kundu, S., Hargrove, M. S., Sarath, G., Hilbert, J. L., Watts, R. A., Dennis, E. S., Peacock, W. J., Dewilde, S., Moens, L., Blouin, G. C., Olson, J. S., and Appleby, C. A. (2009) Review: correlations between oxygen affinity and sequence classifications of plant hemoglobins, *Biopolymers 91*, 1083-1096.

26. Wittenberg, J. B. (1974) Facilitated oxygen diffusion. The role of leghemoglobin in nitrogen fixation by bacteroids isolated from soybean root nodules, *The Journal of Biological Chemistry 249*, 4057-4066.

27. Wittenberg, J. B., Appleby, C. A., Bergersen, F. J., and Turner, G. L. (1975) Leghemoglobin: the role of hemoglobin in the nitrogen-fixing legume root nodule, *Annals of the New York Academy of Sciences 244*, 28-34.

28. Hebelstrup, K. H., Igamberdiev, A. U., and Hill, R. D. (2007) Metabolic effects of hemoglobin gene expression in plants, *Gene 398*, 86-93.

29. Igamberdiev, A. U., Baron, K., Manac'h-Little, N., Stoimenova, M., and Hill, R. D. (2005) The haemoglobin/nitric oxide cycle: involvement in flooding stress and effects on hormone signalling, *Annals of Botany 96*, 557-564.

30. Igamberdiev, A. U., Bykova, N. V., Shah, J. K., and Hill, R. D. (2010) Anoxic nitric oxide cycling in plants: participating reactions and possible mechanisms, *Physiologia Plantarum 138*, 393-404.

31. Igamberdiev, A. U., and Hill, R. D. (2004) Nitrate, NO and haemoglobin in plant adaptation to hypoxia: an alternative to classic fermentation pathways, *Journal of Experimental Botany 55*, 2473-2482.

32. Igamberdiev, A. U., Seregelyes, C., Manac'h, N., and Hill, R. D. (2004) NADH-dependent metabolism of nitric oxide in alfalfa root cultures expressing barley hemoglobin, *Planta 219*, 95-102.

33. Smagghe, B. J., Trent, J. T., 3rd, and Hargrove, M. S. (2008) NO dioxygenase activity in hemoglobins is ubiquitous in vitro, but limited by reduction in vivo, *PloS One 3*, e2039.

34. Tiso, M., Tejero, J., Kenney, C., Frizzell, S., and Gladwin, M. T. (2012) Nitrite reductase activity of nonsymbiotic hemoglobins from Arabidopsis thaliana, *Biochemistry 51*, 5285-5292.

35. Atkinson, S. J., Mowat, C. G., Reid, G. A., and Chapman, S. K. (2007) An octaheme c-type cytochrome from Shewanella oneidensis can reduce nitrite and hydroxylamine, *FEBS Letters 581*, 3805-3808.

36. Einsle, O. (2011) Structure and function of formate-dependent cytochrome c nitrite reductase, NrfA, *Methods in Enzymology 496*, 399-422.

37. Einsle, O., Messerschmidt, A., Stach, P., Bourenkov, G. P., Bartunik, H. D., Huber, R., and Kroneck, P. M. (1999) Structure of cytochrome c nitrite reductase, *Nature 400*, 476-480.

38. Einsle, O., Stach, P., Messerschmidt, A., Simon, J., Kroger, A., Huber, R., and Kroneck, P. M. (2000) Cytochrome c nitrite reductase from Wolinella succinogenes. Structure at 1.6 A resolution, inhibitor binding, and heme-packing motifs, *The Journal of Biological Chemistry 275*, 39608-39616.

39. Kern, M., Eisel, F., Scheithauer, J., Kranz, R. G., and Simon, J. (2010) Substrate specificity of three cytochrome c haem lyase isoenzymes from Wolinella succinogenes: unconventional haem c binding motifs are not sufficient for haem c attachment by NrfI and CcsA1, *Molecular Microbiology 75*, 122-137.

40. Kern, M., and Simon, J. (2009) Electron transport chains and bioenergetics of respiratory nitrogen metabolism in Wolinella succinogenes and other Epsilonproteobacteria, *Biochimica et Biophysica Acta 1787*, 646-656.

41. Mowat, C. G., Rothery, E., Miles, C. S., McIver, L., Doherty, M. K., Drewette, K., Taylor, P., Walkinshaw, M. D., Chapman, S. K., and Reid, G. A. (2004) Octaheme tetrathionate reductase is a respiratory enzyme with novel heme ligation, *Nature Structural & Molecular Biology 11*, 1023-1024.

42. Pittman, M. S., Elvers, K. T., Lee, L., Jones, M. A., Poole, R. K., Park, S. F., and Kelly, D. J. (2007) Growth of Campylobacter jejuni on nitrate and nitrite: electron transport to NapA and NrfA via NrfH and distinct roles for NrfA and the globin Cgb in protection against nitrosative stress, *Molecular Microbiology 63*, 575-590.

43. Stach, P., Einsle, O., Schumacher, W., Kurun, E., and Kroneck, P. M. (2000) Bacterial cytochrome c nitrite reductase: new structural and functional aspects, *Journal of Inorganic Biochemistry 79*, 381-385.

44. Petersen, M. G., Dewilde, S., and Fago, A. (2008) Reactions of ferrous neuroglobin and cytoglobin with nitrite under anaerobic conditions, *Journal of Inorganic Biochemistry 102*, 1777-1782.

45. Tiso, M., Tejero, J., Basu, S., Azarov, I., Wang, X., Simplaceanu, V., Frizzell, S., Jayaraman, T., Geary, L., Shapiro, C., Ho, C., Shiva, S., Kim-Shapiro, D. B., and Gladwin, M. T. (2011) Human neuroglobin functions as a redox-regulated nitrite reductase, *The Journal of Biological Chemistry 286*, 18277-18289.

46. Chen, K., and Popel, A. S. (2006) Theoretical analysis of biochemical pathways of nitric oxide release from vascular endothelial cells, *Free Radical Biology & Medicine 41*, 668-680.

47. Chen, K., and Popel, A. S. (2007) Vascular and perivascular nitric oxide release and transport: biochemical pathways of neuronal nitric oxide synthase (NOS1) and endothelial nitric oxide synthase (NOS3), *Free Radical Biology & Medicine 42*, 811-822.

48. Ohwaki, Y., Kawagishi-Kobayashi, M., Wakasa, K., Fujihara, S., and Yoneyama, T. (2005) Induction of class-1 non-symbiotic hemoglobin genes by nitrate, nitrite and nitric oxide in cultured rice cells, *Plant & Cell Physiology 46*, 324-331.

49. Sowa, A. W., Guy, P. A., Sowa, S., and Hill, R. D. (1999) Nonsymbiotic haemoglobins in plants, *Acta Biochimica Polonica 46*, 431-445.

50. Bazylinski, D. A., Arkowitz, R. A., and Hollocher, T. C. (1987) Decomposition of hydroxylamine by hemoglobin, *Archives of Biochemistry and Biophysics 259*, 520-526.

51. Colter, J. S., and Quastel, J. H. (1950) Catalytic decomposition of hydroxylamine by hemoglobin, *Archives of Biochemistry 27*, 368-389.

52. Kuznetsova, S., Knaff, D. B., Hirasawa, M., Lagoutte, B., and Setif, P. (2004) Mechanism of spinach chloroplast ferredoxin-dependent nitrite reductase: spectroscopic evidence for intermediate states, *Biochemistry 43*, 510-517.

53. Kuznetsova, S., Knaff, D. B., Hirasawa, M., Setif, P., and Mattioli, T. A. (2004) Reactions of spinach nitrite reductase with its substrate, nitrite, and a putative intermediate, hydroxylamine, *Biochemistry 43*, 10765-10774.

54. Sturms, R., DiSpirito, A. A., and Hargrove, M. S. (2011) Plant and cyanobacterial hemoglobins reduce nitrite to nitric oxide under anoxic conditions, *Biochemistry 50*, 3873-3878.

55. Gupta, K. J., Fernie, A. R., Kaiser, W. M., and van Dongen, J. T. (2011) On the origins of nitric oxide, *Trends in Plant Science 16*, 160-168.

56. Brunel, C., Bondon, A., and Simonneaux, G. (1992) Electron-transfer self-exchange kinetics of trimethylphosphine horse-heart myoglobin, *Biochimica et Biophysica Acta 1101*, 73-78.

57. Crutchley, R. J., Ellis, W. R., and Gray, H. B. (1985) Long-distance electron transfer in pentaammineruthenium (histidine-48)-myoglobin. Reorganizational energetics of a high-spin heme, *Journal of the American Chemical Society 107*, 5002-5004.

58. Brunori, M., Saggese, U., Rotilio, G. C., Antonini, E., and Wyman, J. (1971) Redox equilibrium of sperm-whale myoglobin, Aplysia myoglobin, and Chironomus thummi hemoglobin, *Biochemistry 10*, 1604-1609.

CHAPTER 2.

TREMA AND *PARASPONIA* HEMOGLOBINS REVEAL CONVERGENT EVOLUTION OF OXYGEN TRANSPORT IN PLANTS

Modified from a paper published in *Biochemistry*

Ryan Sturms[1,2], Smita Kakar[1,3], James Trent, III[1,3], and Mark S. Hargrove[1,4]

Abstract

All plants contain hemoglobins that fall into distinct phylogenetic classes. The subset of plants that carry out symbiotic nitrogen fixation express hemoglobins that scavenge and transport oxygen to bacterial symbiotes within root nodules. These "symbiotic" oxygen transport hemoglobins are distinct in structure and function from the non-oxygen transport ("nonsymbiotic") Hbs found in all plants. Hemoglobins found in two closely related plants present a paradox concerning hemoglobin structure and function. *Parasponia andersonii* is a nitrogen fixing plant that expresses a symbiotic hemoglobin (ParaHb) characteristic of oxygen transport hemoglobins in having a pentacoordinate ferrous heme iron, moderate oxygen affinity, and a relatively rapid oxygen dissociation rate constant. A close relative that does not fix nitrogen, *Trema tomentosa*, expresses hemoglobin (TremaHb) sharing 93% amino acid identity to ParaHb, but its phylogeny predicts a typical nonsymbiotic hemoglobin with a hexacoordinate heme iron, high oxygen affinity, and slow oxygen dissociation rate constant. Here we characterize heme coordination and oxygen binding in TremaHb and ParaHb to investigate whether or not two hemoglobins with such high sequence

similarity are actually so different in functional behavior. Our results indicate that the two proteins resemble nonsymbiotic hemoglobins in the ferric oxidation state, and symbiotic hemoglobins in the ferrous oxidation state. They differ from each other only in oxygen affinity and oxygen dissociation rate constants, two factors key to their different functions. These results demonstrate distinct mechanisms for convergent evolution of oxygen transport in different phylogenetic classes of plant hemoglobins.

Introduction

The history of hemoglobins (Hbs) predates the photosynthetic oxygenation of earth (*1-3*). The "oxygen catastrophe" that occurred approximately two billion years ago greatly increased atmospheric oxygen, forcing organisms to avoid, tolerate, or exploit this change in their physiochemical environments. Thus, early Hbs probably protected cells from oxygen toxicity (*4, 5*). As aerobic organisms grew larger and evolved more specialized tissues, their surface-to-volume ratios decreased, and passive oxygen diffusion became limiting. In response to this pressure, oxygen transport mechanisms evolved nearly 500 million years ago enabling organisms to grow to unprecedented size, complexity, and diversity (*2*). The modern day forms of these proteins are the hemocyanins in mollusks and arthropods, hemerythrins in marine worms, and oxygen transport Hbs in animals and plants. However, oxygen transport is certainly not the primordial, or even the most common function of Hbs (*6, 7*). Bacterial and yeast Hbs destroy toxic molecules like nitric oxide encountered in their environments (*8*), and animals contain specialized Hbs in neural and other tissues that are suggested to do the same (*9-11*). Although a few plant species contain oxygen transport Hbs, all plants

contain Hbs unrelated to oxygen transport (*12*). The fact that the majority of Hbs do not function in oxygen transport suggests that the capacity for oxygen transport is a fairly recent development in the Hb evolutionary timeline.

A comparison of oxygen transport Hbs in plants and animals to the other Hbs present in the same organisms reveal distinct differences in structure and behavior (*13*). Oxygen transport Hbs are present in high millimolar concentrations, and their rate constants for oxygen release are relatively rapid (greater than 1 s^{-1}). Moreover, their association equilibrium constants are moderate, enabling them to bind oxygen when it is present, yet release it when needed. The heme groups in known oxygen transporters are "pentacoordinate" with an open binding site to the iron, characterized by a single histidine coordinating the "proximal" side of the heme, leaving the "distal" site open for reversible oxygen binding (Figure 1). The distal site often houses another histidine (called the "distal" histidine) that does not coordinate the heme iron, but is in close proximity to and interacts with bound oxygen.

Hbs not involved in oxygen transport, including the "nonsymbiotic" (nsHbs) found in all plants, as well as neuroglobin (*14-16*) and cytoglobin (*17, 18*) found in animals, have a second histidine reversibly coordinating the ligand binding site (Figure 1). While these proteins share globin folds, their heme active sites resemble that of cytochrome *b5*. These Hbs are known as "hexacoordinate" Hbs (hxHbs), and their structures and chemistries are subjects of increasing attention due to potential roles in sensing and detoxifying nitric oxide and other environmental challenges.

It has been hypothesized that oxygen transport Hbs evolved from hxHbs independently in both plants and animals (*14, 19, 20*). In both cases, the chemical challenge was to express hemoglobin with stable pentacoordinate heme coordination. This is a difficult task to achieve because the change in spin state of the iron d-shell electrons upon histidine coordination is energetically very favorable (*21-23*), and holding a histidine near the heme iron without allowing it to bind presents a formidable thermodynamic challenge. Thus, an oxygen transport Hb must provide a protein scaffold that can offset this coordination energy in order to stabilize a pentacoordinate heme center.

The evolution of oxygen transport function in plant Hbs occurred more recently (around 200 million years ago (*20, 24-26*)) than in animal Hbs, making them a useful system for investigating protein structural elements that are instrumental in this change of function. The phylogeny of plant Hbs can be divided into three general classes, two of which are known predecessors of oxygen transport globins (*12*). The familiar oxygen transport "leghemoglobins" (Lbs) common to the legume family evolved from "Class 2" nsHbs, and still share ~ 40% sequence identity with nsHbs (compared to less than 20% for red blood cell Hb and non-oxygen transport Hbs in animals) (*13*). Plant oxygen transport Hbs have also evolved independently and much more recently from "Class 1" nsHbs (*19, 24, 25*) (Figure 1). This more recent event has left pairs of proteins that have different functions, but share very similar primary structures. An extreme example is found in *Parasponia andersonii* (*27*) (a non-legume which fixes N_2 in root nodules) and *Trema tomentosa* (*28*) (which does not fix N_2). Their Hbs are 93% identical (differing in

only 11 positions with no primary sequence gaps), yet *Parasponia andersonii* Hb (ParaHb) is a pentacoordinate oxygen transporter and *Trema tomentosa* (TremaHb) is predicted to be a typical hexacoordinate nsHb (Figure 1).

ParaHb has been shown to be pentacoordinate in the ferrous oxidation state, and to have rate and affinity constants for oxygen that are appropriate for transport (*29*, *30*). However, little is known about TremaHb or ferric ParaHb. The comparative experiments presented here were designed to test whether these proteins are truly as divergent in structure and chemistry as their physiological expression would suggest, or whether their behavior mirrors the similarity of their sequence identity. The former result would reveal a surprising difference in physical behavior for two proteins sharing such high sequence identity, and the latter would suggest that pentacoordinate oxygen transporters could play the role of nsHbs, and that hexacoordination *per se* is not an important structural feature for their physiological function.

Experimental Procedures.

Production of Proteins- Recombinant rice nsHb1 and soybean Lba were produced as described previously (*31, 32*). Codon-optimized cDNA for *Parasponia andersonii* (genebank number u27194) and *Trema tomentosa* hemoglobins (genebank number 1402313a) were synthesized by Epoch Biolabs using assembly PCR. These cDNAs were inserted in to a pET 28a plasmid for expression in the BL21 Star DE3 *E. coli* strain. A second sequence for *Trema tomentosa* hemoglobin (genebank number y00296) was deposited more recently that differs from the former by lacking the

conserved Val^{117} amino acid. Both Trema cDNAs were expressed in E. coli, but only the former (which included Val^{117}) produced soluble hemoglobin.

The BL21 Star DE3 host strain was grown in 2-liter Erlenmeyer flasks that were inoculated using a 100 milliliter starter culture grown overnight to saturation. The expression media used was 1 liter of Terrific Broth supplemented with 1 milliliter of 50 milligram/milliliter Kanamycin per flask. The flasks were cultured at 37° C while being shaken for 18-20 hours at 250 rpm without induction before being harvested by centrifugation (9,000 rpm for 10 minutes). The collected cells were lysed by homogenization before being purified in a three-step process: (1) ammonium sulfate fractionation (60 and 90 percent), (2) immobilized metal affinity chromatography (BD TALON), and (3) Size exclusion chromatography (HiPrep 26/60 Sephacryl S-100 High Resolution). Collected fractions were dialyzed into 10 millimolar TRIS buffer and concentrated using Amicon Millipore concentrators. Purification efficiency was measured by spectroscopic analysis of Soret/280 ratios. All absorbance spectra were measured using either a Cary-50 Bio or an Ocean Optics USB4000 Spectrophotometer. Ferric protein was made by oxidizing each Hb with potassium ferricyanide followed by desalting over a G-25 column. Ferrous hemoglobins were generated by reducing ferric samples with sodium dithionite.

Kinetic Experiments- Flash Photolysis and stopped-flow reactions were used to measure CO binding for all proteins as described previously (*33, 34*). Oxygen association and dissociation rate constants were measured by flash photolysis and rapid mixing with CO, respectively (*35*). All kinetic traces were fit to exponential decays

using Igor Pro. Calculation of rate constants for hexacoordination and CO binding used the method described by Smagghe et al. (*34*). Affinity constants for azide were measured using previously described methods (*36*).

Electrochemical and quaternary structure analysis- Midpoint reduction potentials were measured by potentiometric titration using an apparatus described in detail previously (*37*). The biphasic reduction curve exhibited by ParaHb was evident under a range of conditions. This prompted our analysis of the oligomeric state of the ferric proteins by equilibrium analytical ultracentrifugation. This procedure followed one published earlier (*38*) with the exception that a newer model Beckman Coulter ProteomeLab XLA ultracentrifuge was used. Molecular mass was calculated from the linear portions of the plots in Figure 4 Equation 1 where M is molecular mass, r is the radial position of the sample, v is partial specific volume (fixed at 0.72 ml/g), r is solvent density (fixed at 0.9982 g/ml), the angular velocity ω= 3,099 radians/s (29,600 rpm), R = 8.31441 x 10^7 (g cm^2)/(s^2 k mole), and T was 293 ° K

$$\ln(Abs) = \frac{M(1-v\rho)\omega^2}{2RT} r^2 \qquad \text{Equation 1.}$$

Results

The experiments presented here are designed to measure three characteristics that distinguish the structure and reactivity of oxygen transport proteins from those of nsHbs. These characteristics are endogenous histidine coordination in the ferric oxidation state, endogenous histidine coordination in the ferrous oxidation state, and the kinetics of

oxygen binding. NsHbs are hexacoordinate in both oxidation states, as described by the following reaction (*33*).

$$Hb_{Hex} \underset{k_H}{\overset{k_{-H}}{\leftrightarrow}} Hb_{Pent} + L \underset{k_L}{\overset{k'_L}{\leftrightarrow}} Hb_L \qquad \text{Equation 2.}$$

In this equation, Hb_{Hex} and Hb_{Pent} are the hexacoordinate and pentacoordinate forms of the Hb, and the rate constants for distal histidine coordination (H) and exogenous ligand (L) binding are written at the top (for association) and bottom (for dissociation) of each step. The influence of distal histidine coordination on equilibrium binding affinity can be evaluated by the following equation.

$$K_{eff} = \frac{K_{L,pent}}{1 + K_H} \qquad \text{Equation 3.}$$

Here $K_{L,pent}$ is k'_L/k_L (the affinity constant in the absence of the influence of histidine coordination), and K_H (k_H/k_{-H}) is the affinity constant for endogenous histidine coordination. Equation 3 predicts a decrease in affinity for exogenous ligand binding when histidine coordination is tight.

The rates of exogenous ligand binding can be influenced by histidine coordination as described by Equation 4, which allows measurement of k_H and k_{-H} using appropriate ligands in the ferric and ferrous oxidation states (*33*).

$$k_{obs} = \frac{k_{-H} k'_L [L]}{k_H + k_{-H} + k'_L [L]}$$ Equation 4.

Equation 4 predicts a limited rate of exogenous ligand binding when coordinated histidine dissociation is slow.

Coordination and ligand binding in the ferric oxidation state- A principal distinction between oxygen transport Hbs and nsHbs is hexacoordination in the latter, which is generally much stronger in the ferric than the ferrous oxidation state (*21*, *37*). Coordination state is evident from the visible-region absorbance spectra in both oxidations states (*39, 40*) as exemplified for hxHbs by rice nsHb, and for pentacoordinate Hbs by soybean Lba (Figure 2). The prominent band at 529 nm and shoulder at 560 nm of rice nsHb is characteristic of a ferric, low-spin hemichrome heme center. In contrast, the larger degree of absorbance at 484 nm, and the peak at 620 nm in the spectrum of Lba are characteristic charge-transfer bands found in high-spin, pentacoordinate ferric heme proteins. The absorbance spectra of recombinant ParaHb is (as shown by Appleby et al. (*19*) for the native protein) largely low-spin (hexacoordinate), but with a measurable fraction of high-spin character evident from a minor 620 nm absorbance band. However, TremaHb is entirely low-spin and functionally indistinguishable from rice nsHb.

To measure the impact of hexacoordination in ParaHb and TremaHb, equilibrium affinities for the ferric ligand, azide, were measured along with soybean Lba and rice nsHb as pentacoordinate and hexacoordinate controls, respectively. The binding curves

for each are shown in Figure 2B. In these experiments, Lba binds azide stoichiometrically with an affinity constant precluding measurement at this protein concentration (5 μM). The other three proteins however, bind azide with much lower affinities (each constant is on the order of 3 mM), as would be expected from Equation 3 for hxHbs with higher values of K_H. The data in Figure 2 reveal that TremaHb and ParaHb are predominately hexacoordinate in the ferric oxidation states. Thus, they share similarity to nsHbs rather than Lbs for this property.

Coordination and ligand binding in the ferrous oxidation state- Heme coordination in the ferrous oxidation state is evident from splitting of the visible bands seen in low-spin complexes. *Bis*-histidyl ferrous heme coordination results in prominent peaks at 528 and 556 nm that resemble the visible spectrum of cytochrome *b5*. Figure 3A shows the absorbance spectra of rice nsHb, ParaHb, and TremaHb in this region. To provide a reference for the degree of histidine coordination in these proteins, absorbance spectra for human neuroglobin (Ngb) (fraction of coordination ~ 1) and Lba (fraction of coordination ~ 0) are included. The ratio of absorbance at 555nm to that at 540nm has been shown to reflect the fraction of hexacoordination (*34*) (Figure 3B). The line in Figure 3B was established empirically for this relationship (*34*). These data estimate that both TremaHb and ParaHb are fractionally coordinated at a ratio less than 0.2.

The low degree of ferrous hexacoordination in TremaHb and ParaHb is supported by the kinetics of CO binding. Figure 3C demonstrates the effect of histidine coordination in rice nsHb, showing CO binding time courses for [CO] ranging from 12 to 500 μM. In each case (Figures 3C-E), the y-axes are normalized to absorbance

change expected for the reaction. The time courses for rice nsHb are relatively slow, show appreciable loss of amplitude only at the highest [CO], and coalesce to a concentration-independent rate constant as [CO] is raised (Figure 3F). These phenomena are characteristic of hexacoordination as exhibited by rice nsHb, described by Equation 4 when KH is appreciable, and k_H and k_{-H} are on the order of k'_{CO} (*34*). In contrast, CO binding to ParaHb (Figure 3D) and TremaHb (Figure 3E) is much faster, and the majority of the absorbance change is lost in the dead time of the reaction at even moderate [CO] (the maximum [CO] in Figures 3D and E is 125 μM). Furthermore, there is a linear relationship between the observed rate constants and [CO]. Lba is not included in Figure 3 because its rate of CO binding is too fast for analysis by rapid mixing. These characteristics are common to bimolecular CO binding in the absence of appreciable K_H, and demonstrate that ParaHb and TremaHb resemble Lba and other pentacoordinate Hbs in the ferrous oxidation state.

Values of k_{-H2} can be estimated from the data in Figure 3 by examination of the rate constant for binding to the slower fraction (~15%) at the highest [CO] (*34*). These values are reported in Table 1 along with the bimolecular rate constants for CO association. Knowing k_{-H2} and K_H allows an estimation of the rate constant for histidine binding (k_{H2}), which is also reported in Table 1.

Electrochemical analysis- Binding of the distal histidine to form a *bis*-histidyl heme complex is generally favored more in the ferric oxidation state than the ferrous (*21*). The data above suggest that hexacoordination is significant in ferric TremaHb and ParaHb, but not in the ferrous forms of each protein. As is the case for other

hexacoordinate heme proteins, this should result in midpoint reduction potentials that are more negative than for Hbs that are strictly pentacoordinate (*37*). To test this hypothesis, potentiometric titration was used to measure the midpoint reduction potentials for Para and Trema Hbs compared to Lba and rice nsHb. As demonstrated previously (*37*), the midpoint reduction potential for rice nsHb is -132 mv (versus SHE), and that of Lba is +13 mv. As expected for histidine coordination preferentially in the ferric oxidation state, the midpoint reduction potential for TremaHb is -138 mv. Surprisingly, the ParaHb redox titration is biphasic, with 50% of the population having a midpoint reduction potential of 0 mv, and 50% at -150 mv.

There are many ways that heme coordination by histidine could influence midpoint reduction potentials in hxHbs. Differential coordination strength in the ferric and ferrous oxidation states leads to lower reduction potentials in all hxHbs due to tighter binding in the ferric oxidation state (*37*). However, none of these reactions can account for biphasic equilibrium redox titration curves, as they are at rapid-exchange on the time scale of the experiment. A mechanistic explanation requires dissimilar heme sites that are not inter-converting, or that are exchanging so slowly that it is not detected in the experiment (which normally takes eight hours or more to complete).

Two dissimilar heme sites is difficult to rationalize with a monomeric Hb (like Lba). Likewise, rice nsHb has a dissociation equilibrium constant for dimerization of 86 µM (*38*), leaving it mostly monomeric in our experiments (5 µM in Hb concentration). However, the original purification of native ParaHb reported it as a "readily dissociable dimer" (*19*). Our potentiometric titration results would be easier to explain if in fact

ParaHb had a much lower K_D for dimerization. This possibility was measured using equilibrium analytical ultracentrifugation to analyze the quaternary structure of ferric ParaHb and TremaHb (Figure 4B). In this experiment, rice nsHb, TremaHb, and ParaHb were analyzed at a concentration of 5 μM (in heme). At this concentration, rice nsHb is mainly monomeric and has an apparent molecular mass of 17.3 kD. However, at the same concentration, TremaHb and ParaHb have molecular masses of 32.8 and 31 kD respectively, indicating that they are largely dimeric even at this low concentration. From these data and Equation 1, it can be estimated that K_D values for dimerization for these proteins are no greater than 1 μM. These results show that ParaHb is in fact dimeric in our potentiometric titration experiments, and make asymmetric heme sites a plausible cause of the biphasic redox titration curve observed for this protein.

Oxygen binding- Our results so far suggest that in the ferric oxidation state, TremaHb and ParaHb resemble nsHbs; but in the ferrous state, they both share more similarity with pentacoordinate oxygen transporters like Lba. Our final test to distinguish between oxygen transport Hbs and typical hexacoordinate Hbs is a measurement of oxygen affinity and kinetics. ParaHb has kinetic and affinity constants for oxygen similar to Lbs (*12, 19*). To compare these results with those of TremaHb, Figure 5A shows oxygen binding (following flash photolysis), and Figure 5B time courses for oxygen dissociation for both proteins (again with Lba and rice nsHb as controls). The association rate constants for TremaHb and ParaHb are similar (210 and 170 $\mu M^{-1}s^{-1}$, respectively). However, the oxygen dissociation rate constants are quite distinct at 0.38 and 12 s^{-1}, respectively. This 30-fold difference in respective oxygen

dissociation rate constants is a clear functional distinction between ParaHb and TremaHb. The oxygen dissociation rate constant for TremaHb (0.38 s^{-1}) groups it with the nsHbs, and the rate constant for Para Hb (12 s^{-1}) is consistent with the oxygen transport function of the Lbs (Table 2).

Discussion

The rationale for this investigation was the high level of sequence similarity between ParaHb, a typical plant oxygen transport protein, and TremaHb, which is predicted to be distinct from known oxygen transporters in heme coordination and oxygen binding kinetics. There were two possible outcomes anticipated. The first was that TremaHb could have been identical to ParaHb in its behavior implying that the physical differences between nsHbs and oxygen transport Hbs are not necessary for nsHb function, which would mean that oxygen transporters could possibly function as nsHbs. The second possible outcome was a difference between the two proteins, demonstrating that a surprisingly small number of amino acid changes are responsible for a large shift in structure and function. With respect to oxygen binding, our results support the latter conclusion. The oxygen affinity and binding kinetics of TremaHb are not suitable for oxygen transport, and completely in line with Class 1 nsHbs. However, with respect to hexacoordination, the conclusions are mixed; both Hbs are predominately hexacoordinate in the ferric oxidation state, and mostly pentacoordinate in the ferrous oxidation state. They are distinct from other nsHbs in having ~ 20 (Class 1) or ~ 800 (Class 2) fold lower affinities for ferrous distal histidine coordination. Furthermore, in contrast to both Lbs and Class 1 nsHbs, ParaHb and TremaHb are tightly associated

dimers. The implications of these results to the evolution of oxygen transport Hbs is discussed below.

Independent evolution of oxygen transport Hbs in plants: Class 1 versus Class 2 oxygen transport hemoglobins- The two phylogenetic Classes of nsHbs that have given rise to oxygen transport globins have distinct physical attributes, including the degree of hexacoordination found in each, and their affinity constants for oxygen (Table 3) (*12*). In contrast, ParaHb and Lbs (which evolved from Class 1 and Class 2 nsHbs, respectively) are similar in their affinities for oxygen, and both lack significant histidine coordination in the ferrous oxidation state. The convergence of similar oxygen transport globins from dissimilar starting points required different molecular changes in each Class of nsHb. In an effort to compare the molecular mechanisms that lead to the development of plant oxygen transport globins, average values for the rate and affinity constants for ferrous hexacoordination and oxygen binding for each nsHb Class are provided in Table 3 along with rate and affinity constants for oxygen binding to the plant oxygen transport Hbs (taken from Smagghe *et al.* (*12*)).

If we choose to define the requirements of an oxygen transport Hb based solely on affinity and kinetics of oxygen binding, Class 2 nsHbs are not far off the mark. With equilibrium constants averaging 3 μM^{-1}, and dissociation rate constants averaging 1.1 s^{-1}, they would require only slight modification to attain the values shared by the Lbs. On the other hand, Class 1 nsHbs would have to significantly lower their affinity for oxygen (by ~ 20-fold) and increase their oxygen dissociation rate constants (~10-fold). In addition to these changes, is the apparent requirement of a pentacoordinate ferrous heme,

based on the knowledge that all observed oxygen transporter Hbs are pentacoordinate in this oxidation state.

One possibility for overcoming the challenges of designing affinity, kinetics, and coordination is to change the distal histidine to an amino acid that cannot coordinate the heme iron. In fact, the mutant protein E7L of rice nsHb (in which the distal histidine is replaced by leucine) meets all of these requirements for oxygen transport (*41*) (Table 3). Likewise, histidine substitution mutations in soybean Lba are well-suited for oxygen transport based on these criteria (*35*) (Table 3). However, all oxygen transport Hbs in plants (and in nearly all other organisms) are not only pentacoordinate, but also contain histidine at position E7 near the ligand binding site. When considering the constraints of pentacoordinate ferrous heme and a nearby distal histidine, the act of converting both classes of nsHbs to oxygen transporters involves reducing the oxygen affinity values presented in Table 3 for Class 1 and Class 2 nsHbs ($K_{O2,pent}$) to ~ 20 μM^{-1}. The oxygen affinities can be lowered by increasing the oxygen dissociation rate constant by ~ 90 and ~ 12-fold for Class 1 and 2 nsHbs, respectively.

The molecular details resulting in the changes in oxygen dissociation rate constants are still unclear, though some hints are provided from biophysical studies of Lbs and nsHbs. Oxygen release can be controlled by hydrogen bonding with the distal histidine (*42*), by the nature of the proximal histidine-heme bond (*43-45*), and by control of geminate rebinding through cavities and tunnels in the protein matrix surrounding the heme (*46, 47*). Previous research indicates that the distal histidine in Class 2 nsHbs hydrogen bonds with bound oxygen (*12*), but the distal histidine present in soybean Lba

does not form this same hydrogen bond (*31, 35*). This suggests that the evolution of oxygen transport in Class 2 Hbs resulted, at least in part, from the loss of oxygen stabilization by the distal histidine. However, until other Class 2 nsHbs and Lbs are examined, this conclusion is tentative because of potentially different mechanisms for regulating oxygen affinity in other Lbs (*30, 48*).

It is also known that Class 1 nsHbs use a hydrogen bond to stabilize bound oxygen (*49, 50*). Whether loss of this hydrogen bond causes the decrease in oxygen affinity in ParaHb has not been addressed, but could be tested by analysis of ParaHb and TremaHb distal His mutant proteins. If the loss of this hydrogen bond were key to modulating oxygen affinity, it would be expected that distal His mutation in TremaHb would increase the oxygen dissociation rate constant, but that in ParaHb would not. However, a comparison of the amino acid sequences of these proteins reveals no obvious suspects that might influence oxygen dissociation rate constants between the two, or that would suggest a mechanism for regulating oxygen affinity (Figure 1). Both have Phe at position B10 (*36*), an apolar side chain at position F7 (*45, 51*), and there are no substitutions predicted to be closer than ~10 Å to the distal heme pocket. Thus, a molecular explanation for the nearly 50-fold difference in oxygen affinity between ParaHb and TremaHb will require a detailed study of the structures of these Hbs and the behavior of key mutant proteins derived from each.

Why are oxygen transport Hbs pentacoordinate, and why do they retain a distal histidine? It has been proposed that oxygen transport Hbs evolved from hexacoordinate hemoglobins (hxHbs) in both plants and animals (*19, 20, 52*). In both

cases, the functions of the precursor hxHbs are not yet clear, and the necessity of hexacoordination is accordingly unknown (*12, 53*). The oxygen transport Hbs that evolved from them share similar features of pentacoordinate ferrous heme, relatively rapid oxygen dissociation, and in nearly all cases a distal histidine. The few exceptions among known oxygen transporters have substitutions of glutamine, which is capable of electrostatic interactions with ligands similar to, but somewhat weaker than histidine (*54-56*). The requirement of a pentacoordinate ferrous heme is probably due to the effect of hexacoordination on heme oxidation, as it has been shown that both plant and animal hxHbs oxidize significantly faster than oxygen transport Hbs (*15, 36*). For example, a *bis*-histidyl myoglobin mutant protein oxidizes much more rapidly than the wild type protein (*57*). The reason for this could be due to the ability of the *bis*-histidyl heme center to more rapidly transfer electrons (*58*), or to the more negative reduction potentials that accompany disproportionately strong ferric distal histidine coordination (*15, 37*).

The requirement for a distal histidine arises from the need for stabilization of bound oxygen (in some Hbs), ligand discrimination, and slowing of heme oxidation and subsequent hemin dissociation (*59, 60*). The examples given above of the HisE7L mutant proteins of rice nsHb and soybean Lba have appropriate kinetic and equilibrium constants for oxygen transport, but they are much poorer than their respective wild-type proteins in discriminating for oxygen against other potential ligands like carbon monoxide (*41*). Likewise, replacement of the distal histidine in most Hbs increases heme oxidation due to lower oxygen affinity and increased solvent access to the heme

pocket (*42*, *61*). Thus, oxygen transport Hbs require that histidine be located precariously near the ligand binding site, but not so near as to coordinate the ferrous heme iron. This requirement of the cognate globin reveals that the architecture of oxygen transport proteins is a delicate balance of structure and coordination that is highlighted in comparison to their hxHb evolutionary precursors.

References

1. Hardison, R. C. (1996) A brief history of hemoglobins: Plant, animal, protist, and bacteria, *PNAS 93*, 5675-5679.

2. Hardison, R. C. (1999) The evolution of hemoglobins, *American Scientist 87*, 126-133.

3. Hardison, R. C. (1998) Hemoglobins from bacteria to man: evolution of different patterns of gene expression, *J. Exp. Bot. 201*, 1099-1117.

4. Raymond, J., and Segre, D. (2006) The Effect of Oxygen on Biochemical Networks and the Evolution of Complex Life, *Science 311*, 1764-1767.

5. Falkowski, P. (2006) Tracing Oxygen's Imprint on Earth's Metabolic Evolution, *Science 311*, 1724-1725.

6. Hankeln, T., Ebner, B., Fuchs, C., Gerlach, F., Haberkamp, M., Laufs, T. L., Roesner, A., Schmidt, M., Weich, B., Wystub, S., Saaler-Reinhardt, S., Reuss, S., Bolognesi, M., De Sanctis, D., Marden, M. C., Kiger, L., Moens, L., Dewilde, S., Nevo, E., Avivi, A., Weber, R. E., Fago, A., and Burmester, T. (2005) Neuroglobin and cytoglobin in search of their role in the vertebrate globin family, *J Inorg Biochem 99*, 110-119.

7. Wittenberg, J. B., Wittenberg, B. A., and Guertin, M. (2002) Truncated Hemoglobins: A New Family of Hemoglobins Widely Distributed in Bacteria, Unicellular Eukaryotes, and Plants, *J. Biol. Chem. 277*, 871-874.

8. Gardner, P. R., Gardner, A. M., Martin, L. A., and Salzman, A. L. (1998) Nitric oxide dioxygenase: an enzymatic function for flavohemoglobin, *Proc. Natl. Acad. Sci. USA 95*, 10378-10383.

9. Sun, Y., Jin, K., Mao, X., Zhu, Y., and Greenberg, D. A. (2001) Neuroglobin is up-regulated by and protects neurons from hypoxic-ischemia injury, *Proc. Natl. Acad. Sci. U.S.A. 98*, 15306-15311.

10. Sun, Y., Jin, K., Peel, A., Mao, X. O., Xie, L., and Greenberg, D. A. (2003) Neuroglobin protects the brain from experimental stroke invivo, *PNAS 100*, 3497-3500.

11. Khan, A. A., Wang, Y., Sun, Y., Mao, X. O., Xie, L., Miles, E., Graboski, J., Chen, S., Ellerby, L. M., Jin, K., and Greenberg, D. A. (2006) Neuroglobin-overexpressing transgenic mice are resistant to cerebral and myocardial ischemia, *Proc Natl Acad Sci U S A 103*, 17944-17948.

12. Smagghe, B. J., Hoy, J. A., Percifield, R., Kundu, S., Hargrove, M. S., Sarath, G., Hilbert, J. L., Watts, R. A., Dennis, E. S., Peacock, W. J., Dewilde, S., Moens, L., Blouin, G. C., Olson, J. S., and Appleby, C. A. (2009) Review: Correlations between oxygen affinity and sequence classifications of plant hemoglobins, *Biopolymers 91*, 1083-1096.

13. Kundu, S., Trent, J.T., III, and Hargrove, M.S. (2003) Plants, humans, and hemoglobins, *Trends in Plant Sc. 8*, 387-393.

14. Burmester, T., Welch, B., Reinhardt, S., and Hankeln, T. (2000) A vertebrate globin expressed in the brain, *Nature 407*, 520-523.

15. Dewilde, S., Kiger, L., Burmester, T., Hankeln, T., Baudin-Creuza, V., Aerts, T., Marden, M., Caubergs, R., and Moens, L. (2001) Biochemical characterization and ligand-binding properties of neuroglobin, a novel member of the globin family, *J. Biol. Chem. 276*, 38949-38955.

16. Trent, J. T., III., Watts, R. A., and Hargrove, M. S. (2001) Human neuroglobin, a hexacoordinate hemoglobin that reversibly binds oxygen, *J. Biol. Chem. 276*, 30106-30110.

17. Burmester, T., Ebner, B., Weich, B., and Hankeln, T. (2002) Cytoglobin: A Novel Globin Type Ubiquitously Expressed in Vertebrate Tissues, *Mol Biol Evol 19*, 416-421.

18. Trent, J. T., III., and Hargrove, M. S. (2002) A Ubiquitously Expressed Human Hexacoordinate Hemoglobin, *J. Biol. Chem. 277*, 19538-19545.

19. Appleby, C. A., Tjepkema, J. D., and Trinick, M. J. (1983) Hemoglobin in a Nonleguminous Plant, *Parasponia:* Possible Genetic Origin and Function in Nitrogen Fixation, *Science 220*, 951-953.

20. Trevaskis, B., Watts, R. A., Andersson, C. R., Llewellyn, D. J., Hargrove, M. S., Olson, J. S., Dennis, E. S., and Peacock, W. J. (1997) Two hemoglobin genes in Arabidopsis thaliana: the evolutionary origins of leghemoglobins, *Proc Natl Acad Sci U S A 94*, 12230-12234.

21. Cowley, A. B., Kennedy, M. L., Silchenko, S., Lukat-Rodgers, G. S., Rodgers, K. R., and Benson, D. R. (2006) Insight into heme protein redox potential control and functional aspects of six-coordinate ligand-sensing heme proteins from studies of synthetic heme peptides, *Inorg Chem 45*, 9985-10001.

22. Nesset, M., Shokhirev, N., Enemark, P., Jacobson, S., and Walker, F. (1996) Models of the Cytochromes. Redox Properties and Thermodynamic Stabilities of Complexes of "Hindered" Iron(III) and Iron(II) Tetraphenylporphyrinates with Substituted Pyridines and Imidazoles, *Inorg. Chem. 35*, 5188-5200.

23. Safo, M., Nesset, M., Walker, F., Debrunner, P., and Robert Scheidt, W. (1997) Models of the Cytochromes. Axial Ligand Orientation and Complex Stability in Iron(II) Porphyrinates: The Case of the Noninteracting d Orbitals, *J. Am. Chem. Soc. 119*, 9438-9448.

24. Guldner, E., Desmariais, E., Galtier, N., and Godelle, B. (2004) Molecular evolution of plant haemoglobin: two haemoglobin genes in nymphaeaceae *Euryale ferox*, *J. Evol. Biol.*, 48-54.

25. Guldner, E., Godelle, B., and Galteir, N. (2004) Molecular Adaptation in Plant Hemoglobin, a Duplicated Gene Involved in Plant–Bacteria Symbiosis, *J. Mol. Evol. 59*, 416-425.

26. Hunt, P. W., Watts, R. A., Trevaskis, B., Llewellyn, D. J., Burnell, J., Dennis, E. S., and Peacock, W. J. (2001) Expression and evolution of functionally distinct haemoglobin genes in plants, *Plant Mol. Bio. 47*, 677-692.

27. Kortt, A., Trinick, M., and Appleby, C. (1988) Amino acid sequences of hemoglobins I and II from root nodules of the non-leguminous Parasponia rigida-rhizobium symbiosis, and a correction of the sequence of hemoglobin I from Parasponia andersonii., *Eur. J. Biochem 175*, 141-149.

28. Bogusz, D., Appleby, C. A., Landsmann, J., Dennis, E. S., Trinick, M. J., and Peacock, W. J. (1988) Functioning haemoglobin genes in non-nodulating plants, *Nature 331*, 178-180.

29. Wittenberg, J. B., Wittenberg, B. A., Gibson, Q. H., Trinick, M. J., and Appleby, C. A. (1986) The kinetics of the reactions of *Parasponia andersonii* hemoglobin

with oxygen, carbon monoxide, and nitric oxide, *J. Biol. Chem. 261*, 13624–13631.

30. Gibson, Q. H., Wittenberg, J. B., Wittenberg, B. A., Bogusz, D., and Appleby, C. A. (1989) The kinetics of ligand binding to plant hemoglobins: structural implications, *J. Biol. Chem. 264*, 100–107.

31. Hargrove, M. S., Barry, J. K., Brucker, E. A., Berry, M. B., Phillips, G. N., Jr., Olson, J. S., Arredondo-Peter, R., Dean, J. M., Klucas, R. V., and Sarath, G. (1997) Characterization of recombinant soybean leghemoglobin a and apolar distal histidine mutants, *J. Mol. Biol. 266*, 1032-1042.

32. Hargrove, M., Brucker, E., Stec, B., Sarath, G., Arredondo-Peter, R., Klucas, R., Olson, J., and Phillips, G. (2000) Crystal structure of a nonsymbiotic plant hemoglobin, *Structure Fold. Des. 8*, 1005-1014.

33. Smagghe, B. J., Halder, P., and Hargrove, M. S. (2008) Measurement of distal histidine coordination equilibrium and kinetics in hexacoordinate hemoglobins, *Methods Enzymol 436*, 359-378.

34. Smagghe, B. J., Sarath, G., Ross, E., Hilbert, J. L., and Hargrove, M. S. (2006) Slow ligand binding kinetics dominate ferrous hexacoordinate hemoglobin reactivities and reveal differences between plants and other species, *Biochemistry 45*, 561-570.

35. Kundu, S., and Hargrove, M. S. (2003) Distal Heme Pocket Regulation of Ligand Binding and Stability in Soybean Leghemoglobin, *Proteins 50*, 239-248.

36. Smagghe, B. J., Kundu, S., Hoy, J. A., Halder, P., Weiland, T. R., Savage, A., Venugopal, A., Goodman, M., Premer, S., and Hargrove, M. S. (2006) Role of phenylalanine B10 in plant nonsymbiotic hemoglobins, *Biochemistry 45*, 9735-9745.

37. Halder, P., Trent, J. T., III., and Hargrove, M. S. (2007) The Influence of the Protein Matrix on Histidine Ligation in Ferric and Ferrous Hexacoordinate Hemoglobins, *PROTEINS: Structure, Function, and Bioinformatics 66*, 172-182.

38. Goodman, M. D., and Hargrove, M. S. (2001) Quaternary structure of rice nonsymbiotic hemoglobin, *J. Biol. Chem. 276*, 6834-6839.

39. Appleby, C. A. (1969) The separation and properties of low-spin (haemochrome) and native, high-spin forms of leghaemoglobin from soybean nodule extracts, *Biochim Biophys Acta 189*, 267-279.

40. Yonetani, T., Iizuka, T., and Waterman, M. R. (1971) Studies on modified hemoglobins. 3. Spin states of ferric hemoglobin, semi-hemoglobin, and isolated subunit chains, *J Biol Chem 246*, 7683-7689.

41. Arredondo-Peter, R., Hargrove, M. S., Sarath, G., Moran, J. F., Lohrman, J., Olson, J. S., and Klucas, R. V. (1997) Rice hemoglobins. Gene cloning, analysis, and O_2-binding kinetics of a recombinant protein synthesized in *Escherichia coli*, *Plant Physiol. 115*, 1259-1266.

42. Springer, B. A., Egeberg, K. D., Sligar, S. G., Rohlfs, R. J., Mathews, A. J., and Olson, J. S. (1989) Discrimination between oxygen and carbon monoxide and inhibition of autooxidation by myoglobin. Site-directed mutagenesis of the distal histidine, *J. Biol. Chem. 264*, 3057-3060.

43. Perutz, M. F. (1970) Stereochemistry of cooperative effects in haemoglobin, *Nature 228*, 726–739.

44. Smerdon, S. J., Krzywda, S., Wilkinson, A. J., Brantley, R. E., Jr., Carver, T. E., Hargrove, M. S., and Olson, J. S. (1993) Serine92 (F7) contributes to the control of heme reactivity and stability in myoglobin, *Biochemistry 32*, 5132-5138.

45. Kundu, S., Snyder, B., Das, K., Chowdhury, P., Park, J., Petrich, J. W., and Hargrove, M. S. (2002) The leghemoglobin proximal heme pocket directs oxygen dissociation and stabilizes bound heme, *Proteins 46*, 268-277.

46. Scott, E. E., Gibson, Q. H., and Olson, J. S. (2001) Mapping the pathways for O2 entry into and exit from myoglobin, *J Biol Chem 276*, 5177-5188.

47. Salter, M. D., Nienhaus, K., Nienhaus, G. U., Dewilde, S., Moens, L., Pesce, A., Nardini, M., Bolognesi, M., and Olson, J. S. (2008) The apolar channel in Cerebratulus lacteus hemoglobin is the route for O2 entry and exit, *J Biol Chem 283*, 35689-35702.

48. Kundu, S., Blouin, G., Premer, S., Sarath, G., Olson, J., and Hargrove, M. (2004) TyrB10 Inhibits Stabilization of Bound Oxygen in Soybean Leghemoglobin, *Biochemistry 43*, 6241-6252.

49. Arredondo-Peter, R., Moran, J. F., Sarath, G., Luan, P., and Klucas, R. V. (1997) Molecular cloning of the cowpea leghemoglobin II gene and expression of its cDNA in *Escherichia coli*. Purification and characterization of the recombinant protein., *Plant Physiol. 114*, 493-500.

50. Watts, R. (1999) Characterisation of Non-symbiotic Haemoglobins from Dicotyledonous Plants, *Division of Biochemistry and Molecular Biology Australian National University*, PhD thesis.

51. Smerdon, S. J., Dodson, G. G., Wilkinson, A. J., Gibson, Q. H., Blackmore, R. S., Carver, T. E., and Olson, J. S. (1991) Distal pocket polarity in ligand binding to myoglobin: Structural and functional characterization of a threonine^{68} (E11) mutant, *Biochemistry 30*, 6252–6260.

52. Burmester, T., Weich, B., Reinhardt, S., and Hankeln, T. (2000) A vertebrate globin expressed in the brain, *Nature 407*, 520-523.

53. Hankeln, T., Ebner, B., Fuchs, C., Gerlach, F., Haberkamp, M., Laufs, T., Roesner, A., Schmidt, M., Weich, B., Wystub, S., Saaler-Reinhardt, S., Reuss, S., Bolognesi, M., De Sanctis, D., Marden, M., Kiger, L., Moens, L., Dewilde, S., Nevo, E., Avivi, A., Weber, R., Fago, A., and Burmester, T. (2005) Neuroglobin and cytoglobin in search of their role in the vertebrate globin family, *J. Inorg. Biochem. 99*, 110-119.

54. Rohlfs, R. J., Mathews, A. J., Carver, T. E., Olson, J. S., Springer, B. A., Egeberg, K. D., and Sligar, S. G. (1990) The effects of amino acid substitution at position E7 (residue 64) on the kinetics of ligand binding to sperm whale myoglobin, *J. Biol. Chem. 265*, 3168-3176.

55. Olson, J. S., and Phillips, G. N., Jr. (1997) Myoglobin discriminates between O_2, NO, and CO by electrostatic interactions with the bound ligand, *J. Biol. Inorg. Chem. 2*, 544-552.

56. Dikshit, K. L., Orii, Y., Navani, N., Patel, S., Huang, H. Y., Stark, B. C., and Webster, D. A. (1998) Site-directed mutagenesis of bacterial hemoglobin: the role of glutamine (E7) in oxygen-binding in the distal heme pocket, *Arch. Biochem. Biophys. 349*, 161-166.

57. Dou, Y., Admiraal, S. J., Ikeda-Saito, M., Krzywda, S., Wilkinson, A. J., Li, T., Olson, J. S., Prince, R. C., Pickering, I. J., and George, G. N. (1995) Alteration of axial coordination by protein engineering in myoglobin. Bisimidazole ligation in the His64-->Val/Val68-->His double mutant, *J. Biol. Chem. 270*, 15993-16001.

58. Weiland, T., Kundu, S., Trent, J., Hoy, J., and Hargrove, M. (2004) Bis-histidyl hexacoordination in hemoglobins facilitates heme reduction kinetics, *J. Am. Chem. Soc. 126*, 11930-11935.

59. Hargrove, M. S., and Olson, J. S. (1996) The stability of holomyoglobin is determined by heme affinity, *Biochemistry 35*, 11310-11318.

60. Aranda, R. t., Cai, H., Worley, C. E., Levin, E. J., Li, R., Olson, J. S., Phillips, G. N., Jr., and Richards, M. P. (2009) Structural analysis of fish versus mammalian

hemoglobins: effect of the heme pocket environment on autooxidation and hemin loss, *Proteins 75*, 217-230.

61. Brantley, R. E., Jr., Smerdon, S. J., Wilkinson, A. J., Singleton, E. W., and Olson, J. S. (1993) The mechanism of autooxidation of myoglobin, *J. Biol. Chem. 268*, 6995-7010.

Tables

Table 1

Ferrous Ligand Binding and Hexacoordination Values

Protein	$k'_{CO,pent}$ ($\mu M^{-1}s^{-1}$)	k_{H2} (s^{-1})	k_{-H2} (s^{-1})	K_{H2}
Lba	13			~ 0
Rice Hb	6.8	75	40	1.9
Para Hb	10	~ 7[3]	~ 70[2]	~ 0.1[1]
Trema Hb	43	~ 5[3]	~ 50[2]	~ 0.1[1]

[1] is estimated from the ferrous absorption spectrum and the amplitude of CO binding at high [CO]

[2] is k_{obs} at high [CO]

[3] is estimated from K_H and k_{-H}

Table 2

Protein	$k'_{O2,pent}$ ($\mu M^{-1}s^{-1}$)	k_{O2} (s^{-1})	$K_{O2,pent}$ (μM^{-1})	K_{O2} (μM^{-1})
Rice Hb1	60	0.038	1600	540
Soybean Lba	130	5.6	23	23
T. tomentosa	210	0.38	550	500
P. andersonii (native)	165	15	11	11
P. andersonii (recombinant)	170	12	14	13

Table 3

Protein	k_{H2} (s^{-1})	k_{-H2} (s^{-1})	K_{H2}	$k'_{O2,pent}$ ($\mu M^{-1}s^{-1}$)	k_{O2} (s^{-1})	$K_{O2,pent}$ (μM^{-1})	K_{O2} (μM^{-1})
Class 1 nsHbs	130	75	1.7	67	0.14	1200	410
Rice Hb E7L				620	51	12	12
Class 2 nsHbs	1500	25	84	76	1.1	260	2.9
Plant Oxygen Transporters				230	13	20	20
Lba E7V				400	24	17	17

Figure Legends

Figure 1. The phylogeny of oxygen transport hemoglobins in plants. Oxygen transport Hbs have evolved from two phylogenetic Classes of nonsymbiotic Hbs (nsHbs). In each case, the oxygen transport proteins are pentacoordinate in the ferrous state (top inset structure), while the precursor nsHbs are hexacoordinate (bottom inset structure). The oxygen transport leghemoglobins (Lbs) evolved from "Class 2" nonsymbiotic Hb (nsHbs), while *Parasponia andersonii* is a Class 1-derived oxygen transport Hb (ParaHb) that is 93% identical to the nsHb from *Trema tomentosa*. The amino acid sequences for ParaHb, TremaHb, rice nsHb, and soybean Lba are shown at the bottom, with the 11 differences between ParaHb and TremaHb highlighted in blue. Also indicated on the sequences are the distal (E7) and proximal (F8) histidines, phenylalanine at position B10, and the positions of conserved dimer interface amino acids (Int.).

Figure 2. Coordination and ligand binding in the ferric oxidation state. A) Absorbance spectra of oxidized TremaHb and rice nsHb are typical of hexacoordinate, low spin ferric hemoglobins. That of soybean Lba is characteristic of a high spin, pentacoordinate complex. The ParaHb spectrum represents a mixture of high and low spin heme. B) Azide binding to each protein shows that TremaHb, ParaHb, and rice nsHb bind with much lower affinity than soybean Lba, indicating competition from histidine coordination in the former three Hbs.

Figure 3. Coordination and ligand binding in the ferrous oxidation state. A) Absorbance spectra of each Hb in the ferrous oxidation state is compared to human neuroglobin (Ngb) which is completely hexacoordinate in ferrous oxidation state. B) Empirical quantification of the ratio of absorbance at 555nm/540nm indicates that ParaHb and TremaHb have a fraction of histidine coordination of < 0.2. C-E) Time courses for CO binding to each Hb at varying [CO] reveal the fraction of hexacoordinate Hb and the rate constants for histidine binding and dissociation. F) The concentration dependence of the observed rate constant for the fast phase of CO binding to each Hb shows that ParaHb and TremaHb are predominately pentacoordinate, and rice nsHb has an appreciable fraction of hexacoordinate heme.

Figure 4. Potentiometric titrations and equilibrium analytical ultracentrifugation analysis. A) Nernst plots of potentiometric titrations were used to

measure the ferrous/ferric redox potential for each Hb. B) Each Hb was analyzed at 5 μM by equilibrium analytical ultracentrifugation monitored at 410 nm. The slopes of the plots for ParaHb and TremaHb indicate a tighter dimer than that observed for rice nsHb.

Figure 5. The kinetics of oxygen binding to ParaHb and TremaHb A) Time courses for oxygen association and B) dissociation for ParaHb, TremaHb, rice nsHb, and soybean Lba in air. The dissociation curves in B were measured against displacement by 1 mM CO.

Figure 1.

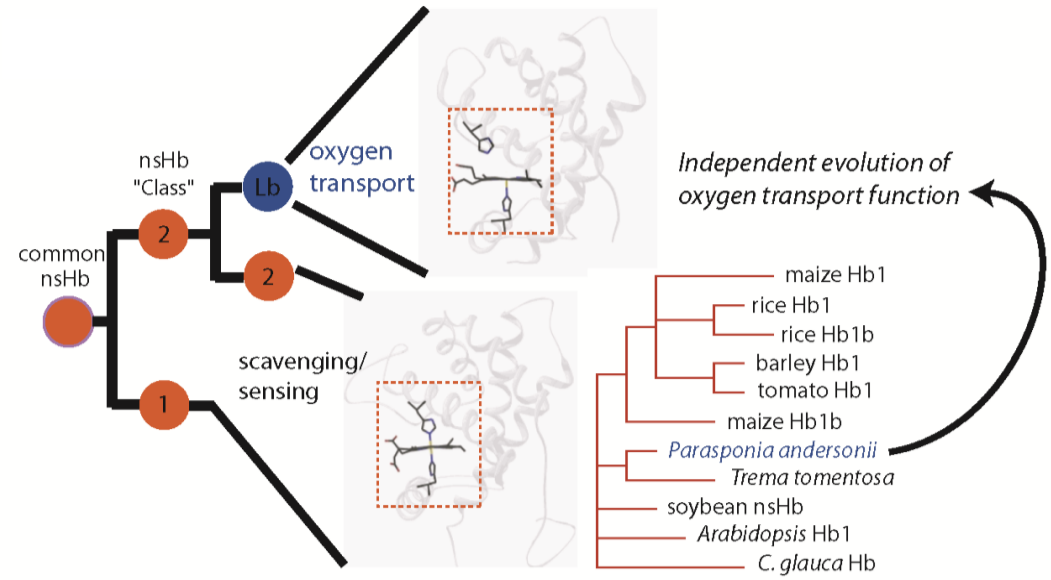


```
                                                    Phe"B10"
TremaHb MSSSE----VDKVFTEEQEALVVKSWAVMKKNSAELGLKFFLKIFEIAPSAKNLFSYLKD 56
ParaHb  MSSSE----VNKVFTEEQEALVVKAWAVMKKNSAELGLQFFLKIFEIAPSAKNLFSYLKD 56
Rice Hb1 MALVEDNNAVAVSFSEEQEALVLKSWAILKKDSANIALRFFLKIFEVAPSASQMFSFLRN 60
Lba     ----------MVAFTEKQDALVSSSFEAFKANIPQYSVVFYTSILEKAPAAKDLFSFLAN 50
                                                        Int.

TremaHb SPIPLEQNPKLKPHAMTVFVMTCESAVQLRKAGKVTVRESNLKRLGAIHFKNGVVNEHFE 116
ParaHb  SPVPLEQNPKLKPHATTVFVMTCESAVQLRKAGKVTVKESDLKRIGAIHFKTGVVNEHFE 116
Rice Hb1 SDVPLEKNPKLKTHAMSVFVMTCEAAAQLRKAGKVTVRDTTLKRLGATHLKYGVGDAHFE 120
Lba     GVDPT--NPKLTGHAEKLFALVRDSAGQLKASGTVVADAA----LGSVHAQKAVTDPQFV 104
                      His"E7"                               His"F8"

TremaHb VTRFALLETIKEAVP-EMWSPEMKNAWGEAYDQLVAAIKSEMKPSST 162
ParaHb  VTRFALLETIKEAVP-EMWSPEMKNAWGVAYDQLVAAIKFEMKPSST 162
Rice Hb1 VVKFALLDTIKEEVPADMWSPAMKSAWSEAYDHLVAAIKQEMKPAE- 166
Lba     VVKEALLKTIKAAVG-DKWSDELSRAWEVAYDELAAAIKKA------ 144
        Int. Int.
```

Figure 2.

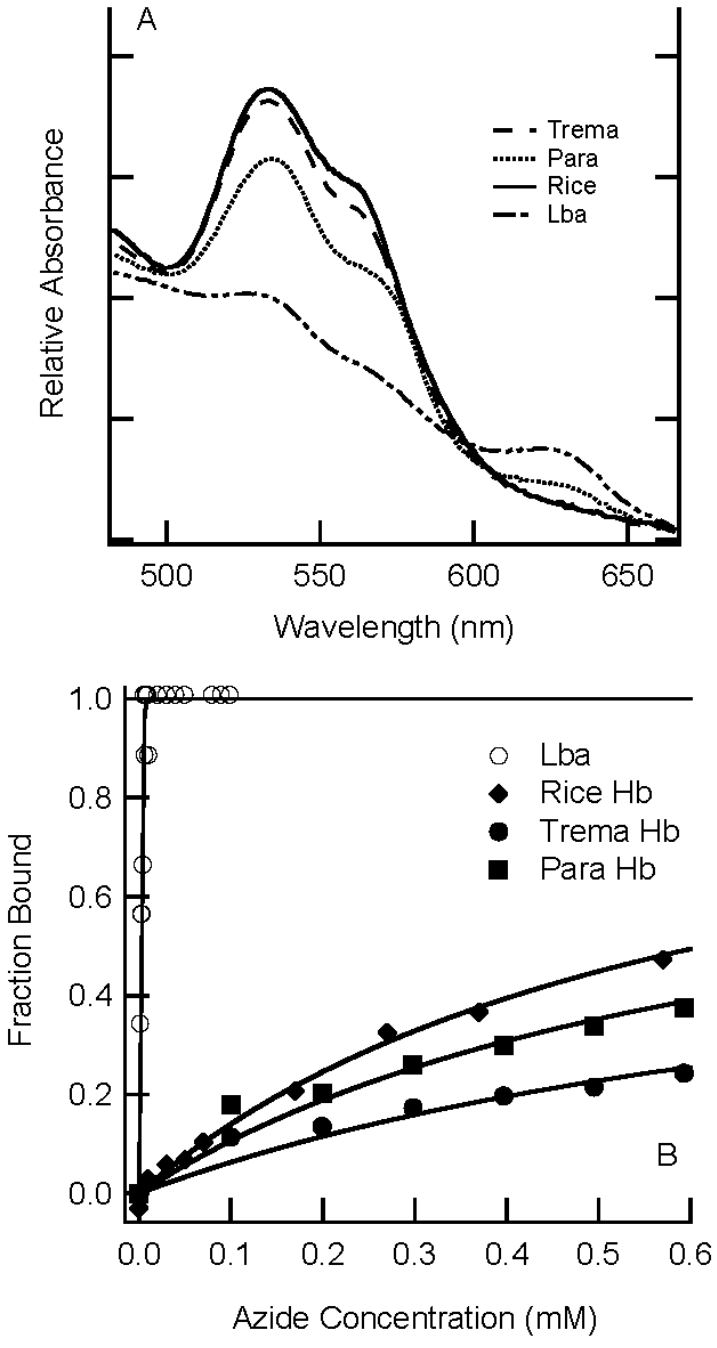
A
Relative Absorbance
Trema
Para
Rice
Lba
500
550
600
650
Wavelength (nm)
1.0
0.8
0.6
0.4
0.2
0.0
Fraction Bound
Lba
Rice Hb
Trema Hb
Para Hb
B
0.0
0.1
0.2
0.3
0.4
0.5
0.6
Azide Concentration (mM)

Figure 3.

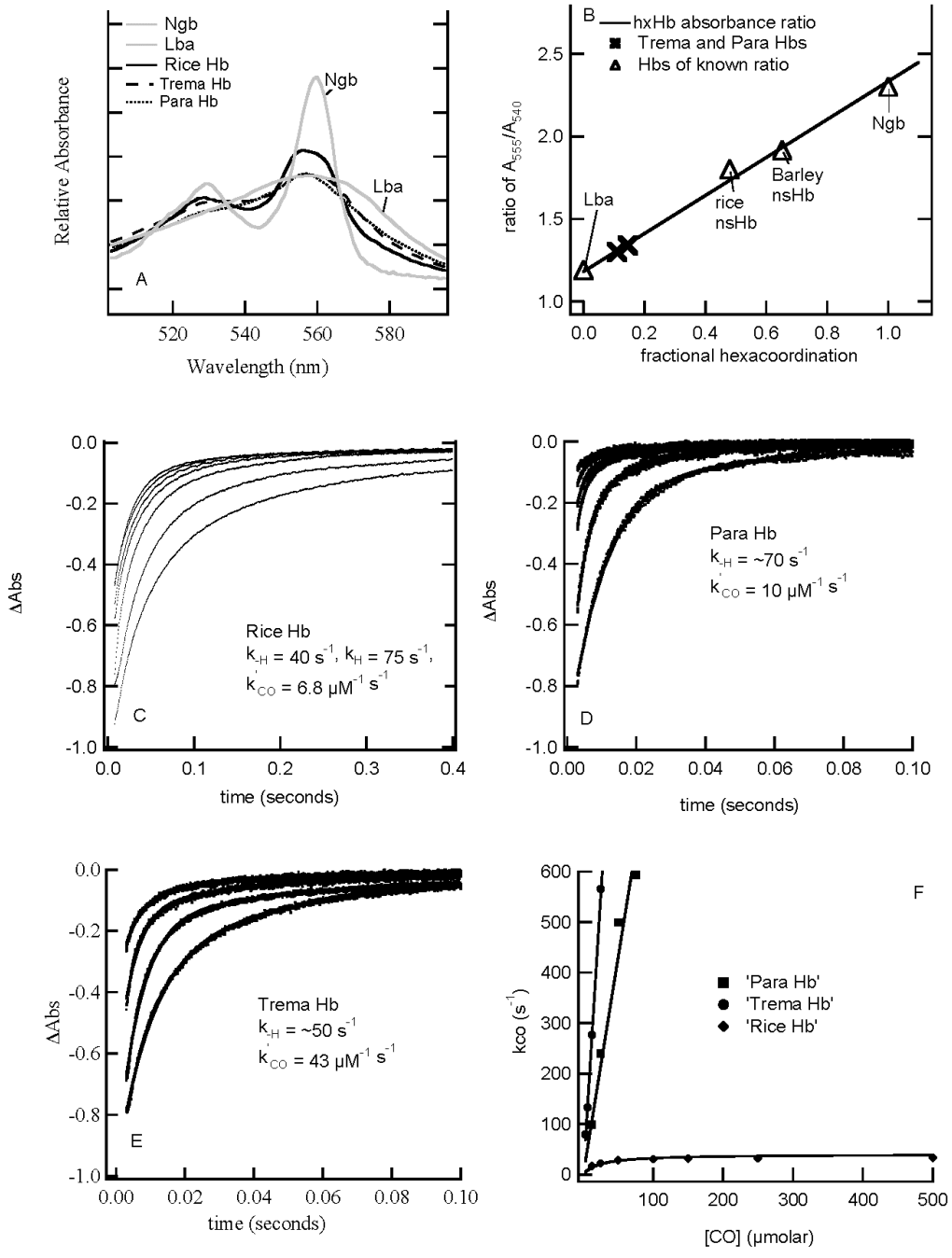
Ngb
Lba
Rice Hb
Trema Hb
Para Hb
Relative Absorbance
Wavelength (nm)
A
B
hxHb absorbance ratio
Trema and Para Hbs
Hbs of known ratio
ratio of A555/A540
fractional hexacoordination
Barley nsHb
rice nsHb
C
Rice Hb
k-H = 40 s-1, kH = 75 s-1,
k'CO = 6.8 µM-1 s-1
ΔAbs
time (seconds)
D
Para Hb
k-H = ~70 s-1
k'CO = 10 µM-1 s-1
E
Trema Hb
k-H = ~50 s-1
k'CO = 43 µM-1 s-1
F
'Para Hb'
'Trema Hb'
'Rice Hb'
kco (s-1)
[CO] (µmolar)

Figure 4.

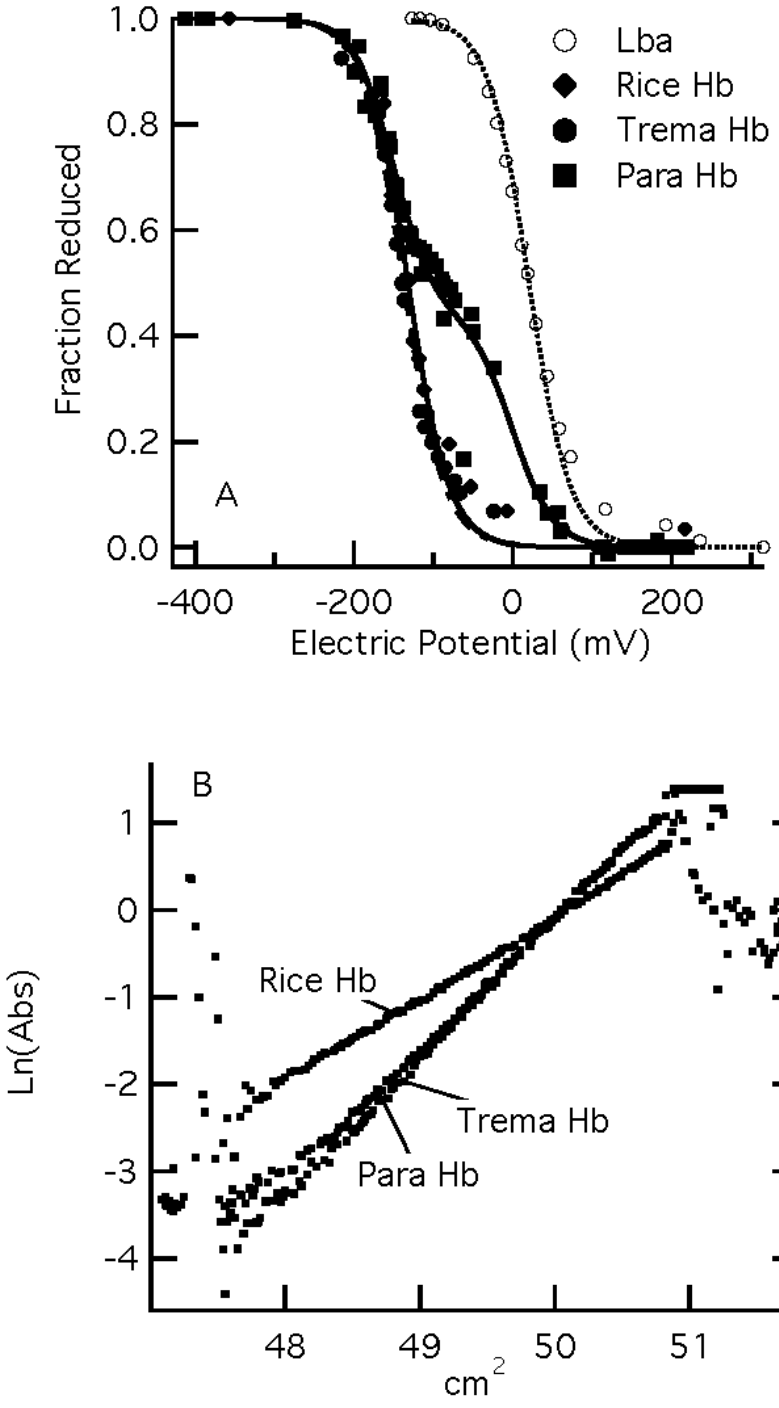
1.0
0.8
0.6
0.4
0.2
0.0
Fraction Reduced
A
-400
-200
0
200
Electric Potential (mV)
Lba
Rice Hb
Trema Hb
Para Hb
B
1
0
-1
-2
-3
-4
Ln(Abs)
Rice Hb
Trema Hb
Para Hb
48
49
50
51
cm2

Figure 5.

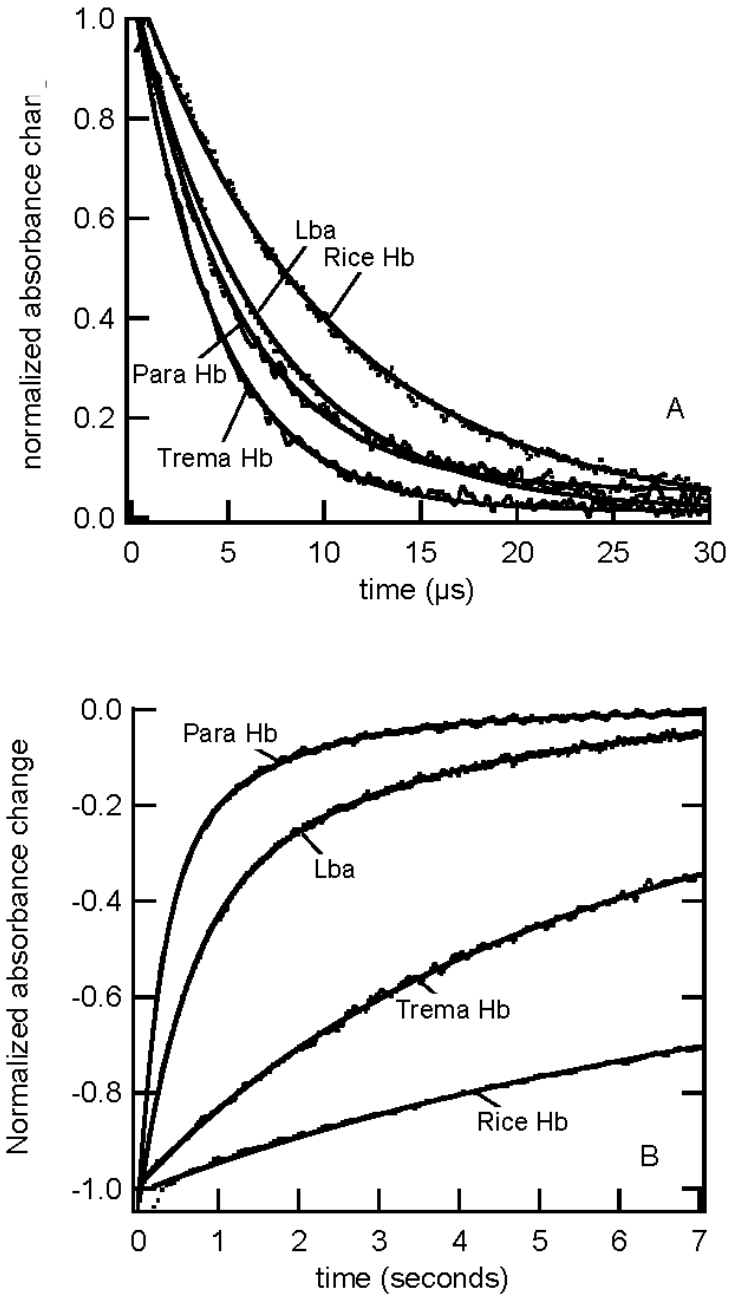
1.0
0.8
0.6
0.4
0.2
0.0
normalized absorbance char
Lba
Rice Hb
Para Hb
Trema Hb
A
0
5
10
15
20
25
30
time (μs)
0.0
-0.2
-0.4
-0.6
-0.8
-1.0
Normalized absorbance change
Para Hb
Lba
Trema Hb
Rice Hb
B
0
1
2
3
4
5
6
7
time (seconds)

CHAPTER 3.

CRYSTAL STRUCTURES OF *PARASPONIA* AND *TREMA* HEMOGLOBINS; DIFFERENTIAL HEME COORDINATION IS LINKED TO QUATERNATY STRUCTURE

Modified from a paper published in *Biochemistry*

Smita Kakar, Ryan Sturms, Andrea Tiffany, Jay C. Nix, Alan DiSpirito, and Mark S. Hargrove

Abstract

Hemoglobins from the plants *Parasponia andersonii* (ParaHb) and *Trema tomentosa* (TremaHb) are 93% identical in primary structure but differ in oxygen binding constants in accordance with their distinct physiological functions. Additionally, these proteins are dimeric, and ParaHb exhibits the unusual property of having different heme redox potentials for each subunit. To investigate how these hemoglobins could differ in function despite their shared sequence identity and to determine the cause of subunit heterogeneity in ParaHb, we have measured their crystal structures in the ferric oxidation state. Furthermore, we have made a monomeric ParaHb mutant protein (I43N) and measured its ferrous/ferric heme redox potential to test the hypothesized link between quaternary structure and heme heterogeneity in wild type ParaHb. Our results demonstrate that TremaHb is a symmetric dimeric hemoglobin similar to other class 1 nonsymbiotic plant hemoglobins, but that ParaHb has structurally distinct heme coordination in each of its two subunits that is absent in the monomeric I43N mutant

protein. A mechanism for achieving structural heterogeneity in ParaHb is proposed, in which the $Ile^{101(F4)}$ side chain contacts the proximal $His^{105(F8)}$ in one subunit but not the other. These results are discussed in the context of the evolution of plant oxygen transport hemoglobins, and other potential functions of plant hemoglobins.

Introduction

Plants and animals contain different classes of hemoglobins (Hbs) with distinct structures and functions (*1, 2*). Animals have oxygen transport Hbs along with others whose functions are not completely clear (*3*). In plants, the class 1 nonsymbiotic Hbs (nsHbs) are believed to scavenge nitric oxide during nitrate assimilation under hypoxic conditions (*4, 5*), while the leghemoglobins are transporters and scavengers of oxygen inside the root nodules of legumes capable of symbiotic nitrogen fixation (*6*). Oxygen transport is not the original function of Hbs in plants or animals (*3, 7*), and understanding the structural changes that accompanied its development will reveal clues about molecular evolution and protein design in the globin scaffold.

Oxygen transport Hbs evolved in animals nearly 500 million years ago, and the resulting proteins, myoglobin and the subunits of red blood cell hemoglobin, share < 20 % sequence identity with their non-transport counterparts, including neuroglobin and cytoglobin (*8-10*). In plants, oxygen transport Hbs evolved twice (*2, 11-14*). The first time, around 200 million years ago, resulted in the production of the leghemoglobins from class 2 nsHbs, which share ~ 40% sequence identity. The second event, originating from class 1 nsHbs, produced the oxygen transport Hb found in the root nodules of

Parasponia, a non-legume capable of symbiotic nitrogen fixation. This more recent occurrence has left pairs of proteins with very high (> 90%) sequence identity, but clearly distinct physiological function (*12*).

A comparison of *Parasponia* Hb (ParaHb) to that from *Trema tomentosa* (TremaHb), a class 1 nsHb sharing 93% sequence identity, showed that these two proteins have distinct oxygen affinities and kinetics that are characteristic of their physiological functions (*15*). Furthermore, both Hbs are tightly dimeric in quaternary structure compared to other Class 1 nsHbs (*16*), and ParaHb is unusual in displaying two Fe^{3+}/Fe^{2+}redox potentials, presumably resulting from different values for each subunit. In contrast, most other Hbs, including TremaHb and the $\alpha_2\beta_2$ heterotetramer found in mammalian red bloods cells, exhibit a single redox midpoint indicative of thermodynamic exchange between the subunits (*15, 17*).

To investigate the proposed linkage of quaternary structure and heme chemistry in ParaHb, and to provide a clearer structural framework for studying the evolutionary gain of oxygen transport function, we have used X-ray crystallography to examine the structures of ParaHb and TremaHb. We have also used site-directed mutagenesis to produce a monomeric version of ParaHb, and measured its midpoint reduction potential in comparison to wild-type ParaHb. Our results reveal that the ParaHb subunits are indeed structurally distinct and that the biphasic redox potential is linked to quaternary structure, and not observed in monomeric ParaHb.

Materials and Methods

Protein preparation- Codon optimized cDNAs for *P. andersonii* (Genbank number u27194) and *T. tomentosa* Hbs (GenBank number 1402313a) were synthesized and cloned as described previously (*15*). The cDNA for ParaHb I43N was constructed using the Quickchange mutagenesis system from Agilent Technologies. TremaHb was expressed, and purification was achieved using a three-step process as described earlier (*15*). ParaHb and its mutant were expressed in host strain BL21 Star DE3 cells. Purification included ammonium sulfate fractionation, DEAE-cellulose, and CM-Sephadex column chromatography. The purification efficiency for the proteins used for crystallization was measured by the ratio of absorbance at the Soret peak and that at 280 nm, and was 3.2 and 2.9 for Trema Hb and Para Hb, respectively. The proteins were oxidized by addition of a slight molar excess of potassium ferricyanide that was removed by passage through a G-25 size exclusion column equilibrated with 10 mM HEPES buffer, pH 7.0. Ferrous hemoglobins were generated by reducing ferric samples with sodium dithionite. Absorbance spectra were measured by using a Cary-50 Bio Spectrophotometer.

Crystallization and data collection- Crystals were grown using the hanging drop vapor diffusion method at 25 ºC. Single crystals of TremaHb grew after 3 days from drops containing 1 µl of 3 mM ferric protein and 1 l crystallization buffer composed of 1.6 M ammonium sulfate and 0.1 M Hepes buffer pH 7.0. ParaHb crystals grew overnight from drops containing 1 l of 3 mM ferric protein and 1 l of well buffer containing 1.6 M ammonium sulfate, 10% dioxane, 0.1 M MES pH 7.0 with 0.1 M

phenol as an additive. Native diffraction datasets for TremaHb and ParaHb crystals were collected at 100K on a Rigaku/MSC home source generator in the Iowa State University Macromolecular X-ray Crystallography Facility. Phasing of the TremaHb data set was accomplished by using single wavelength anomalous dispersion (SAD) at the iron atom, collected at the Advanced Light Source (beamline 4.2.2).

Structure determination and refinement- Diffraction data were integrated and processed using d*TREK (*18*). Atomic positions for two iron atoms in the asymmetric unit of TremaHb SAD data set were located by HKL2MAP (SHELXD) (*19*) and the phases were calculated with SOLVE (*20*). Automated model building was performed using RESOLVE (*21*), and manual model rebuilding with O (*22*) and PDB Viewer (*23*), followed by refinement with REFMAC5 from the CCP4 suite (*24*). The resolution for TremaHb structure was extended to 1.84 Å using a native data set and further refinement using REFMAC5. The ParaHb structure was solved by molecular replacement starting with the TremaHb dimeric asymmetric unit. The final ParaHb structure resulted from refinement in CCP4. The final models have been deposited in the Protein Data Bank as 3QQR (for ParaHb) and 3QQQ (for TremaHb).

Quaternary structure and electrochemical analysis of ParaHb I43N- The oligomeric state of the ferric ParaHb I43N mutant protein was determined by equilibrium analytical ultracentrifugation using the procedure published wild type ParaHb and TremaHb (*15*). Molecular mass was calculated from the linear portions of the plots in Figure 4A using Equation 1, where M is molecular mass, r is the radial position of the sample, v is partial specific volume (fixed at 0.72 mL/g), r is solvent

density (fixed at 0.9982 g/mL), the angular velocity ω = 3099 rad/s (29600 rpm), R = 8.31441 × 10^7 (g cm^2)/ (s^2 K mol), and T is 293 K.

$$\ln(Abs) = \frac{M(1-v\rho)\omega^2}{2RT} r^2 \quad \text{Equation 1}$$

Midpoint reduction potentials were measured using an apparatus described previously (*25*), but with the following modifications. Rather than relying on nitrogen positive pressure to exclude oxygen, the titration apparatus was completely housed in an argon-purged inert box (Coy Laboratory Products). The anaerobic conditions were maintained using a palladium catalyst and 5% hydrogen/argon gas mix. Midpoint potentials were obtained by fitting absorbance data to the following equation:

$$F_{reduced} = \frac{e^{-\left(\frac{nF(E_{obs}-E_{mid})}{RT}\right)}}{1+e^{-\left(\frac{nF(E_{obs}-E_{mid})}{RT}\right)}} \quad \text{Equation 2}$$

For wild type ParaHb, which has two distinct redox transitions, was fit to a sum of two midpoint potentials with the amplitude of each fixed at 50%. However, allowing the amplitudes of each transition to float during the fitting routine yields the same results.

Results

The structures of ferric TremaHb and ParaHb- Crystals of ferric TremaHb and ParaHb diffracted to 1.8 Å and 2.15 Å, respectively. Neither home-source data set could be phased by molecular replacement using other nsHb structures as starting models, so phases were calculated experimentally for TremaHb, leading to a starting molecule for the refinement of the TremaHb structure, which in turn was a successful

molecular replacement starting-model for ParaHb. The best TremaHb model has two molecules in the asymmetric unit that can be refined using noncrystallographic symmetry (NCS) restraints (*26*). The ParaHb model, however, was significantly improved by removing NCS restraints and allowing the subunits to adopt distinct structures (Table 1).

Quaternary structure and subunit interface- The general organization of subunits in the dimeric structures of ParaHb and TremaHb resemble the asymmetric unit of rice nsHb (Figure 1) (*27*), having a symmetric group of hydrophobic contacts between the middle of the G helix of one subunit and the C helix of the other, and a hydrogen bond between the side chain of a Ser on the C helix of one subunit and a polar side chain on the G helix of the other (Figure 2). The total buried surface in the TremaHb and ParaHb dimers is ~600 $Å^2$ per subunit, slightly larger than that of rice nsHb1 (554 $Å^2$) (*27*), but still low compared to values for other stable dimers (*28*). The increased stability of the TremaHb and ParaHb dimer (K_D < 1 μM) compared to other nsHbs (K_D ~ 80 μM) can be attributed to an additional symmetric pair of tight (2.7 Å) hydrogen bonds directly between the G helices of each subunit, created by the side chains of Glu^{113} and His^{114}. Another contributing factor could be that Ser^{46} hydrogen bonds with Asn^{112} in TremaHb and ParaHb, which is one turn of the G helix toward the N terminus of the protein compared to the Glu side chain contacting this Ser side chain in other in other nsHbs (*16*).

ParaHb has structurally distinct subunits- While the TremaHb model did not improve much from the removal of NCS constraints (only 1.2% in R_{free} (Table 1)), that

of ParaHb improved nearly 4% in both. A comparison of electron density in the two subunits of ParaHb reveals the most notable difference at the proximal histidines ($His^{105(F8)}$) (Figure 3). The ParaHb Chain A proximal His is typical of Hbs (and similar to the subunits of TremaHb), with proper coordination geometry and a Nε-heme iron distance of 1.99 Å, but that of Chain B is unusual. The electron density defining Chain B $His^{105(F8)}$ clearly indicates the position of the main-chain atoms and the side-chain Cβ, but rotation of the side chain about χ2 (the rotational orientation of the imidazole ring) is not as well defined.

Our efforts to resolve the position of the Chain B $His^{105(F8)}$ side chain are presented in Figure 3. Based on the electron density, there are two χ2 rotamers of the Chain B $His^{105(F8)}$ side chain that must be considered. The best fit to the density results from rotating the Chain A $His^{105(F8)}$ side chain by 117°, but this puts Nε into a position from which it cannot coordinate the heme iron. To illustrate the necessity of fitting $His^{105(F8)}$ differently in Chains A and B of ParaHb, the electron density for the hemes and the distal and proximal histidines for each are shown in Figure 3. Figure 3A shows the Chain A heme pocket (blue) fit into Chain A electron density. Figure 3B shows the Chain B model (red) and its accompanying electron density. In Figures 3C and D, the models and densities are swapped, showing the resulting poor fits of each model in the other's electron density.

An alternative Chain B $His^{105(F8)}$ conformation that allows Nε-heme coordination (at 2.1 Å) results from χ2 rotation of 73° of the Chain A His position, but it extends the Nδ and Cε atoms outside of the electron density (Figure 3E). In support of this

conformation is weak but continuous electron density between the Chain B $His^{105(F8)}$ side chain and the heme iron. Thus, the density immediately around the side chain supports the former (non-coordinated) conformation, but that between the side chain and the heme iron supports the latter (coordinated). Including both rotamers in the model did not improve model statistics, and fitting for the occupancy of both returned 100% of the former (non-coordinated) conformation. However, the density in this area of Chain B and resolution of the structure (2.15 Å) leave the exact nature of the $His^{105(F8)}$-heme interaction somewhat ambiguous. A prudent interpretation of these results (in combination with the ParaHb solution spectral data) is that the Chain B $His^{105(F8)}$ side chain is distinct from that in Chain A, and is partially disrupted from heme coordination.

ParaHb heme pocket heterogeneity is linked to quaternary structure- In order to test whether the asymmetric hemes in the structure of ParaHb are the root of the biphasic reduction potentials observed for the wild-type protein, a point mutation (I43N) was created in the hydrophobic core of the dimer interface with the goal of producing a monomeric ParaHb protein. This particular substitution was chosen because a homologous mutation in rice nsHb was previously used to disrupt quaternary structure without otherwise affecting the protein (*16*). To measure the effects of the I43N mutation on the quaternary structure of ParaHb, the molecular mass of the mutant protein was measured by equilibrium analytical ultracentrifugation (Figure 4A). The experiment was conducted with 5μM (in heme) wild-type and I43N ParaHb, and molecular masses were calculated to be 31.1 and 14.3 KD, respectively, indicating that the mutant protein is monomeric at this concentration.

The consequences of disrupting the ParaHb dimer were measured by comparing the ferric and ferrous absorption spectra of the wild type and I43N proteins, and by measuring the reduction potential of the heme iron using potentiometric titration while monitoring the absorption spectra. Figure 4B and C shows the absorbance spectra of wild type and I43N ParaHb in the ferric and ferrous oxidation states, respectively. The ferric absorption spectra are similar, exhibiting the mixed-spin state associated with the shoulder at 625 nm, and the lower absorbance at 540 nm compared to rice nsHb1, which is fully low-spin. However, the ferrous absorbance spectra of these proteins are different. Wild type ParaHb is largely high spin, with a slight (~15%) contribution of low spin character. In contrast, the I43N mutant protein is completely high spin, with no indication of hexacoordination by the distal His. In Figure 4, Rice nsHb1 again serves as the control for hxHb with a low spin spectrum.

The spectrochemical redox titrations for wild type and I43N ParaHb are shown in Figure 4D. As previously described, wild type ParaHb exhibits the unusual phenomenon of two discrete midpoint potentials at 0 and -150 mv (*15*). However, the reduction of the monomeric ParaHb I43N mutant protein is monophasic with a midpoint reduction potential of +17 mv, which is different from either of the wild-type mid-point potentials, and supportive of a linkage between quaternary structure and heme heterogeneity.

Discussion

The crystal structures of ParaHb and TremaHb reflect the relationship between their primary structures and *in vitro* biochemistry; these are two proteins sharing many

general similarities along with a few key differences that are critical to their distinct physiological functions. Similarities include tight dimeric quaternary structure and relatively weak *bis*-histidyl coordination in the ferrous oxidation state. Functional differences include lower oxygen affinity and a faster oxygen dissociation rate constant in ParaHb, consistent with its function as an oxygen transporter. TremaHb, on the other hand, exhibits oxygen binding constants on-par with those of other class 1 nsHbs (*1*, *15*). The structures of these proteins are very similar and do not offer an immediate explanation for the differences in their oxygen binding abilities.

A comparison of the ParaHb and TremaHb structures presents some other differences between the proteins that could be linked to oxygen binding, but the mechanism of linkage is not readily evident. The subunits of ferric ParaHb have distinct heme sites; one resembles a typical *bis*-histidyl Hb and the other is largely pentacoordinate with the proximal histidine ($His^{105(F8)}$) dissociated from the heme iron. These observations bring to the forefront several questions related to plant Hb structure and function.

How could the structure of ParaHb cause asymmetric heme sites and affect oxygen affinity? Absorbance spectra of ParaHb suggest that it is an equal mixture of pentacoordinate and hexacoordinate heme in the ferric oxidation state. The biphasic redox potentials and structural differences between the subunits support the hypothesis that the mixture of high and low spin hemes results from discrete and non-exchanging heme environments, rather than equivalent subunits at equilibrium between high and low spin states. There are no indications from kinetic measurements of oxygen or CO

binding that the ferrous subunits behave differently, suggesting that heme site asymmetry may be relieved when the protein is reduced. However, the possibility of heterogeneous ligand binding to the distinct chains of ferric ParaHb (or even binding to the proximal side of the heme group in Chain B) cannot yet be discounted.

It is clear that heme asymmetry is induced by the subunit interface, as the monomeric mutant protein ParaHb I43N does not exhibit biphasic redox titration. The absorbance spectrum of ferric I43N ParaHb is a mixture of high and low spin hemes, suggesting that the monomeric ParaHb heme pocket does not favor either state completely in the absence of influence from the subunit interface. However when reduced, the I43N mutant protein is completely high spin, indicating that the residual (~10%) low-spin character in wild type ferrous ParaHb is induced by the dimer interface.

There are only eleven differences between the primary structures of ParaHb and TremaHb (*15*). None of them are near the subunit interface, and six are remote from the heme and present no obvious mechanism for influencing heme chemistry. The other five are located on (or near) the F helix around the proximal $His^{105(F8)}$ and are the most likely to affect coordination to the heme iron (Figure 5). Of these, the amino acid at sequence position 101(F4) in each protein contacts $His^{105(F8)}$ and provides a plausible mechanism for displacing the ParaHb Chain B $His^{105(F8)}$ side chain from the heme iron.

The $His^{105(F8)}$ side chain of TremaHb is coordinated to the heme iron in both subunits, and steric contact between the $Leu^{101(F4)}$ and $His^{105(F8)}$ side chains is minimal, with the closest contact (between the Cδ and Nδ of each side chain) being 4.6 Å. The substitution of Ile at this position in ParaHb creates a much closer contact between the

$His^{105(F8)}$ side chain and the Cγ ("beta-branched") $Ile^{101(F4)}$ methyl group. In ParaHb Chain A, which has $His^{105(F8)}$ side coordination like TremaHb, there is a close (but acceptable) 3.44 Å contact between $Ile^{101(F4)}$ Cγ and $His^{105(F8)}$ Nδ. However, if the same orientation of $His^{105(F8)}$ were found in Chain B this distance would be 2.8 Å, causing a severe steric clash (*29*) (Figure 5 B-D). Instead, the $His^{105(F8)}$ is found at the observed position, creating an acceptable 4.0 Å contact between $Ile^{101(F4)}$ Cγ and $His^{105(F8)}$ Cδ (Figure 5E).

It is not completely clear how the differential interactions between $Ile^{101(F4)}$ and $His^{105(F8)}$ in ParaHb might be influenced by the subunit interface. However, there are some significant differences between the subunit interfaces in ParaHb and TremaHb in comparison to other nsHbs that are probably important (*1*, *27*, *30*). In ParaHb and TremaHb, there are three successive side chains at the beginning of the G helix that are directly involved in the subunit interface: Asn^{112}, Glu^{113}, and His^{114} (Figure 2). The inter-subunit contact between Glu^{113} and His^{114} is not present in any other nsHbs structures to date, and serves as a direct interaction between the G helices of the subunits. The contact between Asn^{112} and Ser^{46} is also different from other nsHbs, where the homologous Ser instead contacts a Glu side chain two turns further down the G helix, away from the F helix.

Thus, ParaHb and TremaHb have unique subunit contacts at the beginning of the G helix that could influence the environment of the F helix and $His^{105(F8)}$. In the context of ParaHb, this unique subunit interface could work in concert with $Ile^{101(F4)}$ to stimulate the differences in coordination between the two subunits, and potentially influence the

observed differences in oxygen affinity between the two proteins. Detailed studies of site directed mutations of ParaHb and TremaHb are required to investigate this hypothesis.

What is the role of quaternary structure in nsHb function? Not all Hbs have quaternary structure, and it seems logical that those exhibiting it do so for a reason. Many, including red blood cell Hb, use subunit interactions to achieve cooperative oxygen binding. Others, such as many extracellular Hbs, probably do so for stability as well as cooperativity (*31*, *32*). Quaternary structure in plant Hbs includes dimers ($K_{D,dimer}$ < 1μM) in the cases of ParaHb and TremaHb, "loose" dimers ($K_{D,dimer}$ ~80 μM) in other nsHbs (*16, 33*), and monomeric leghemoglobins (*6*). The quaternary structures of Class 2 and Class 3 nsHbs have not yet been measured.

Possible reasons for quaternary structure include cooperative ligand binding, stability, and electron transport events involving more than one electron, or electron transfer at different redox potentials. A role for quaternary structure in protein stability seems unlikely, as nsHbs and leghemoglobins are naturally stable in different quaternary states, and monomeric mutant proteins (like I43N ParaHb, and others (*16*)), have not been challenging to make in the laboratory. There is no evidence of cooperative ligand binding in nsHbs, although equilibrium oxygen binding curves have not been measured directly. Until recently, it was believed that their high oxygen affinities precluded direct observation of equilibrium constants, but recent estimations of affinity for Class 2 nsHbs and ParaHb suggest that these might be suited for this measurement (*1*, *15*).

The involvement of quaternary structure in electron transfer reactions cannot be firmly evaluated without first knowing the biochemical function of nsHbs. This dimerization could be important in redox biochemistry involving nitrogen (*34*), including nitric oxide scavenging (*35*), by influencing heme reduction kinetics or redox chemistry with a substrate. Rather than being limited to a one-electron redox event such as nitric oxide dioxygenase mediated nitric oxide scavenging (*36*), dimeric nsHbs could also facilitate two-electron redox events. The distinct redox potentials of ParaHb subunits are intriguing, as this is not observed in other Hb systems. Normally, the hemes of multidomain Hbs are linked electronically, manifesting a single redox potential for the protein (*17*).

How do the structures of ParaHb and TremaHb impact our understanding of the evolution of plant oxygen transport Hbs? The fact that leghemoglobins and ParaHb differ in quaternary structure indicates that oxygen transport can be achieved in either quaternary structure, and suggests that Class 1 nsHbs (from which ParaHb is derived) and Class 2 nsHbs (which gave rise to the leghemoglobins) followed different pathways in their independent evolution of this function. If we consider pre-oxygen transport Hbs to be similar to the Class 1 and Class 2 nsHbs, then there were different challenges to building an oxygen transporter from each (*1, 15*). The conversion of Class 2 nsHbs to leghemoglobins required an increase in oxygen affinity, an increase in oxygen dissociation rate constant, and settled on a monomeric protein. Conversion of a typical Class 1 nsHb into ParaHb requires a lower oxygen affinity, a faster oxygen dissociation rate constant, and a tighter dimeric structure. Clearly, the formation of a

tight dimer alone is not sufficient to make these changes, as TremaHb is also dimeric but retains the physical properties of Class 1 nsHbs. The most likely explanation is that the tight dimer interface is involved in the mechanism of raising the oxygen dissociation rate constant, causing a lower oxygen affinity in ParaHb. Thus, as in the comparison of myoglobin to leghemoglobin (*11*), the physical requirements for oxygen transport can be implemented using different chemical mechanisms even in similar protein structures.

References

1. Smagghe, B., Hoy, J., Percifield, R., Kundu, S., Hargrove, M., Sarath, G., Hilbert, J., Watts, R., Dennis, E., Peacock, W., Dewilde, S., Moens, L., Blouin, G., Olson, J., and Appleby, C. (2009) Review: correlations between oxygen affinity and sequence classifications of plant hemoglobins., *Biopolymers 91*, 1083-1096.

2. Kakar, S., Hoffman, F. G., Storz, J. F., Fabian, M., and Hargrove, M. S. (2010) Structure
and reactivity of hexacoordinate hemoglobins., *Biophys Chem 152*, 1-14.

3. Hankeln, T., Ebner, B., Fuchs, C., Gerlach, F., Haberkamp, M., Laufs, T. L., Roesner, A., Schmidt, M., Weich, B., Wystub, S., Saaler-Reinhardt, S., Reuss, S., Bolognesi, M., De Sanctis, D., Marden, M. C., Kiger, L., Moens, L., Dewilde, S., Nevo, E., Avivi, A., Weber, R. E., Fago, A., and Burmester, T. (2005) Neuroglobin and cytoglobin in search of their role in the vertebrate globin family, *Journal of Inorganic Biochemistry 99*, 110-119.

4. Sowa, A., Duff, S., Guy, P., and Hill, R. (1998) Altering hemoglobin levels changes energy status in maize cells under hypoxia., *Proc Natl Acad Sci U S A 95*, 10317-10321.

5. Nie, X., and Hill, R. D. (1997) Mitochondrial Respiration and Hemoglobin Gene Expression in Barley Aleurone Tissue, *Plant Physiol 114*, 835-840.

6. Appleby, C. A. (1984) Leghemoglobin and Rhizobium Respiration, *Annual Review of Plant Physiology 35*, 443-478.

7. Wittenberg, B. (2001) Truncated Hemoglobins: A New Family of Hemoglobins Widely Distributed in Bacteria, Unicellular Eukaryotes, and Plants, *Journal of Biological Chemistry 277*.

8. Burmester, T., Welch, B., Reinhardt, S., and Hankeln, T. (2000) A vertebrate globin expressed in the brain, *Nature 407*, 520-523.

9. Burmester, T., Ebner, B., Weich, B., and Hankeln, T. (2002) Cytoglobin: a novel globin type ubiquitously expressed in vertebrate tissues., *Mol Biol Evol 19*, 416-421.

10. Trent, J. T., 3rd, and Hargrove, M. S. (2002) A ubiquitously expressed human hexacoordinate hemoglobin, *Journal of Biological Chemistry 277*, 19538-19545.

11. Kundu, S., Trent, J. r., and Hargrove, M. (2003) Plants, humans and hemoglobins., *Trends Plant Sci 8*, 387-393.

12. Appleby, C. A., Tjepkema, J. D., and Trinick, M. J. (1983) Hemoglobin in a Nonleguminous Plant, Parasponia: Possible Genetic Origin and Function in Nitrogen Fixation, *Science 220*, 951-953.

13. Guldner, E., Desmarais, E., Galtier, N., and Godelle, B. (2004) Molecular evolution of plant haemoglobin: two haemoglobin genes in Nymphaeaceae Euryale ferox, *Journal of Evolutionary Biology 17*, 48-54.

14. Guldner, E., Godelle, B., and Galtier, N. (2004) Molecular adaptation in plant hemoglobin, a duplicated gene involved in plant-bacteria symbiosis, *Journal of Evolutionary Biology 59*, 416-425.

15. Sturms, R., Kakar, S., Trent, J., 3rd, and Hargrove, M. S. (2010) Trema and parasponia hemoglobins reveal convergent evolution of oxygen transport in plants, *Biochemistry 49*, 4085-4093.

16. Goodman, M. D., and Hargrove, M. S. (2001) Quaternary structure of rice nonsymbiotic hemoglobin, *Journal of Biological Chemistry 276*, 6834-6839.

17. Eraldo Antonini, J. W., Maurizio Brunori, John Fuller Taylor, Alessandro Rossi-Fanelli and Antonio Caputo. (1964) Studies on the Oxidation-Reduction Potentials of Heme Proteins, *The Journal of Biological Chemistry 239*, 907-912.

18. Pflugrath, J. W. (1999) The finer things in X-ray diffraction data collection, *Acta Crystallogr D Biol Crystallogr 55*, 1718-1725.

19. Pape, T., Schneider, T. R. (2004) HKL2MAP: a graphical user interface for macromolecular phasing with SHELX programs, *Journal of Applied Crystallography 37*, 843-844.

20. Terwilliger, T. C., and Berendzen, J. (1999) Automated MAD and MIR structure solution, *Acta Crystallographica. Section D, Biological Crystallography 55*, 849-861.

21. Terwilliger, T. C. (2000) Maximum likelihood density modification, *Acta Crystallographica. Section D, Biological Crystallography D56*, 965-972.

22. Jones, T. A., Zou, J. Y., Cowan, S. W., and Kjeldgaard. (1991) Improved methods for building protein models in electron density maps and the location of errors in these models, *Acta Crystallographica. Section D, Biological Crystallography 47 (Pt 2)*, 110-119.

23. Schwede, T., Kopp, J., Guex, N., and Peitsch, M. (2003) SWISS-MODEL: An automated protein homology-modeling server., *Nucleic Acids Res 31*, 3381-3385.

24. CCP4. (1994) The CCP4 suite: programs for protein crystallography, *Acta Crystallographica. Section D, Biological Crystallography 50*, 760-763.

25. Halder, P., Trent, J. r., and Hargrove, M. (2007) Influence of the protein matrix on intramolecular histidine ligation in ferric and ferrous hexacoordinate hemoglobins., *Proteins 66*, 172-182.

26. Adams P.D., G.-K. R. W., Hung L.-W., Ioerger T.R., McCoy A.J., Moriarty N.W., Read R.J., Sacchettini J.C., Sauter N.K. and Terwilliger T.C. (2002) PHENIX: building new software for automated crystallographic structure determination, *Acta Cryst. D58 D58*, 1948-1954.

27. Hargrove, M. S., Brucker, E. A., Stec, B., Sarath, G., Arredondo-Peter, R., Klucas, R. V., Olson, J. S., Phillips, G. N., Jr. (2000) Crystal structure of a nonsymbiotic plant hemoglobin, *Structure Folding and Design 8*, 1005-1014.

28. Janin, J., Miller, S., and Chothia, C. (1988) Surface, Subunit Interfaces and Interior of Oligomeric Proteins, *J. Mol. Biol. 204*, 155-164.

29. Li, A. J., and Nussinov, R. (1998) A set of van der Waals and coulombic radii of protein atoms for molecular and solvent-accessible surface calculation, packing evaluation, and docking., *Proteins 32*, 111-127.

30. Hoy, J., Robinson, H., Trent, J. r., Kakar, S., Smagghe, B., and Hargrove, M. (2007) Plant hemoglobins: a molecular fossil record for the evolution of oxygen transport., *J Mol Biol 371*, 168-179.

31. Zhu, H., Hargrove, M., Xie, Q., Nozaki, Y., Linse, K., Smith, S. S., Olson, J. S., and Riggs, A. F. (1996) Stoichiometry of subunits and heme content of

hemoglobin from the earthworm Lumbricus terrestris, *J Biol Chem 271*, 29999-30006.

32. Royer, W. E., Jr., Hendrickson, W. A., and Chiancone, E. (1989) Structural transitions upon ligand binding in a cooperative dimeric hemoglobin, *Science 249*, 518鳖521.

33. Duff, S. M., Wittenberg, J. B., and Hill, R. D. (1997) Expression, purification, and properties of recombinant barley (Hordeum sp.) hemoglobin. Optical spectra and reactions with gaseous ligands, *Journal of Biological Chemistry 272*, 16746-16752.

34. Gupta, K. J., Fernie, A. R., Kaiser, W. M., and van Dongen, J. T. (2010) On the origins of nitric oxide., *Trends Plant Sci*.

35. Igamberdiev, A., and Hill, R. (2004) Nitrate, NO and haemoglobin in plant adaptation to hypoxia: an alternative to classic fermentation pathways., *J Exp Bot 55*, 2473-2482.

36. Eich, R. F., Li, T., Lemon, D. D., Doherty, D. H., Curry, S. R., Aitken, J. F., Mathews, A. J., Johnson, K. A., Smith, R. D., Phillips, G. N., Jr., and Olson, J. S. (1996) Mechanism of NO-induced oxidation of myoglobin and hemoglobin, *Biochemistry 35*, 6976-6983.

Tables

Table 1. Data collection and refinement statistics

Data Collection Statistics	Native Trema Hb	SAD Trema Hb	Para Hb
Wavelength (nm)	1.54	1.72	1.54
Resolution (Å)	31.3-1.84 (1.9-1.84)[a]	50-2.01 (2.08-2.01)	39.19-2.15 (2.25-2.15)
R-merge (%)	0.064 (0.297)	0.056 (0.273)	0.043 (0.307)
Completeness (%)	75.7 (14.9)	87.8 (52.4)	95.0 (90.0)
Unique, total reflections	23821, 150655	89616, 619984	18471, 109909
Redundancy	6.31 (2.10)	7.0 (3.80)	5.94 (5.05)
Refinement/Quality Statistics			
Space group	P212121		P212121
Unit cell			
Bond lengths (Å)	a = 55.87,b = 70.74,c = 89.59		a = 55.04,b = 72.04, c = 88.32
Bond angles(°)	α = 90,β = 90, γ = 90		α = 90,β = 90, γ = 90
Molecules in Asymmetric Unit	2		2
Refined residues, Waters	310, 250		310, 148
R_{cryst} (%)- no NCS restraints	21.31		22.44
R_{cryst} (%)- with NCS restraints	22.09		25.06
R_{free} (%)[b]- no NCS restraints	24.85		28.56
R_{free} (%)- with NCS restraints	26.07		32.50
Average B factor (Å^2)	27.2		41.58
Ramachandran Plot			
Most favored (%)	99.0		98.9
Additionally allowed (%)	1.0		1.1
Generously allowed (%)	0		0
Rmsd			
Bond lengths (Å)	0.008		0.013
Bond angles (°)	1.10		1.468

[a] Outer shell statistics are shown in parentheses.
[b] Calculated using 5% of reflections.

Figure Legends.

Figure 1. Crystal structures of *Parasponia* and *Trema* hemoglobins. A) An overlay of the structures of ParaHb and TremaHb, and B) ParaHb and RiceHb1.

Figure 2. A detailed view of the dimer interface in ParaHb and TremaHb. The amino acid side chains constructing the interface of ParaHb and TremaHb include a hydrophobic cluster consisting of I43, V117, and F120 of each subunit that is conserved in other nsHbs, H-bonds between S49 and N112 of each subunit, and H-bonds between H114 and E113 off each subunit that are unique to these structures.

Figure 3. Heme pocket electron density of ParaHb subunits justifying distinct proximal histidine conformations. A) Chain A model with Chain A density; B) Chain B model with Chain B density; C) Chain A model with Chain B density; D) Chain B model with Chain A density. E) A stereo-view comparison of two possible chi2 rotamers of the Chain B $His^{105(F8)}$ side chain fit into the Chain B electron density. The orientation used in the A-D is shown in red, the other, with Ne coordinating the heme iron, is shown in blue. All electron density maps are contoured at 2.5 s.

Figure 4. Physical analysis of wild type and I43N ParaHb. A) Each ferric Hb was analyzed by equilibrium analytical ultracentrifugation at 410 nm, at a concentration of 5μM. The slopes of these plots yield molecular masses of 31.1 and 14.3 kD, respectively, for wild type and I43N ParaHb. B) Absorbance spectra of ferric and ferrous

(C) ParaHb and ParaI43N along with riceHb1 as a control. D) Potentiometric titrations of wild type and I43N ParaHbs. These curves were fit to Equation 2 to extract midpoint redox potentials for each protein. For wild type ParaHb, the curve fit to a sum of two midpoints at 0 and -150 mv (versus SHE), and for the I43N mutant protein, a single midpoint is observed at +17 mv.

Figure 5. A potential role for ParaHb Ile^{101} in stimulating heme asymmetry. A) Five of the eleven differences between ParaHb (green structure) and TremaHb (lavender structure) are on or near the F helix. Each is labeled with the ParaHb amino acid first, and TremaHb second (for example, I,L means that ParaHb has Ile at this position, and TremaHb has a Leu). B) ParaHb Chain B compared to TremaHb. C) A space filling representation of ParaHb Chain A showing an acceptable van der Waals contact between Ile$^{101(F4)}$ and His$^{105(F8)}$. D) A space filling representation of ParaHb Chain B with His$^{105(F8)}$ from Chain A, showing the steric clash that would result if His$^{105(F8)}$ of Chain B adopted this orientation. E) A space filling representation of ParaHb Chain B, showing the acceptable van der Waals contact between Ile$^{101(F4)}$ and His$^{105(F8)}$ observed when the His$^{105(F8)}$ side chain is displaced from the heme iron.

Figure 1.

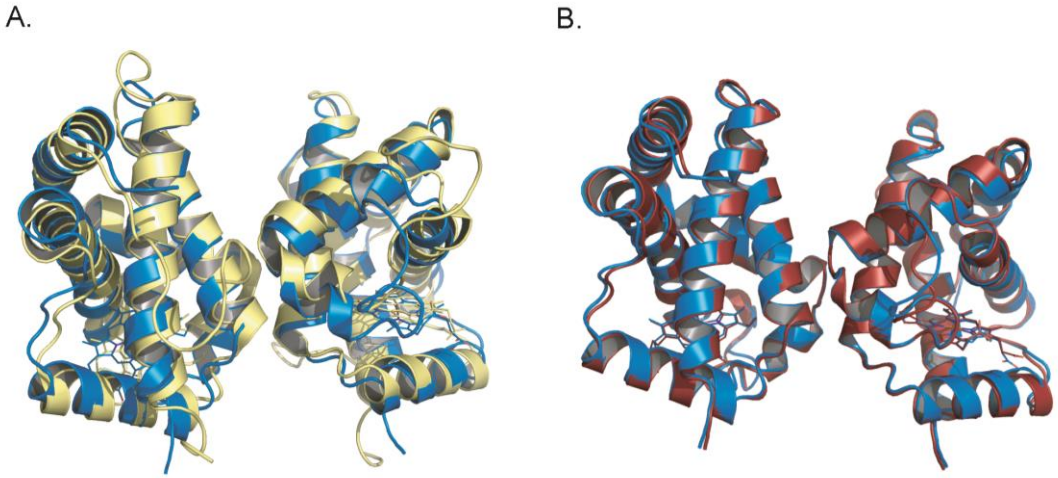

Figure 2.

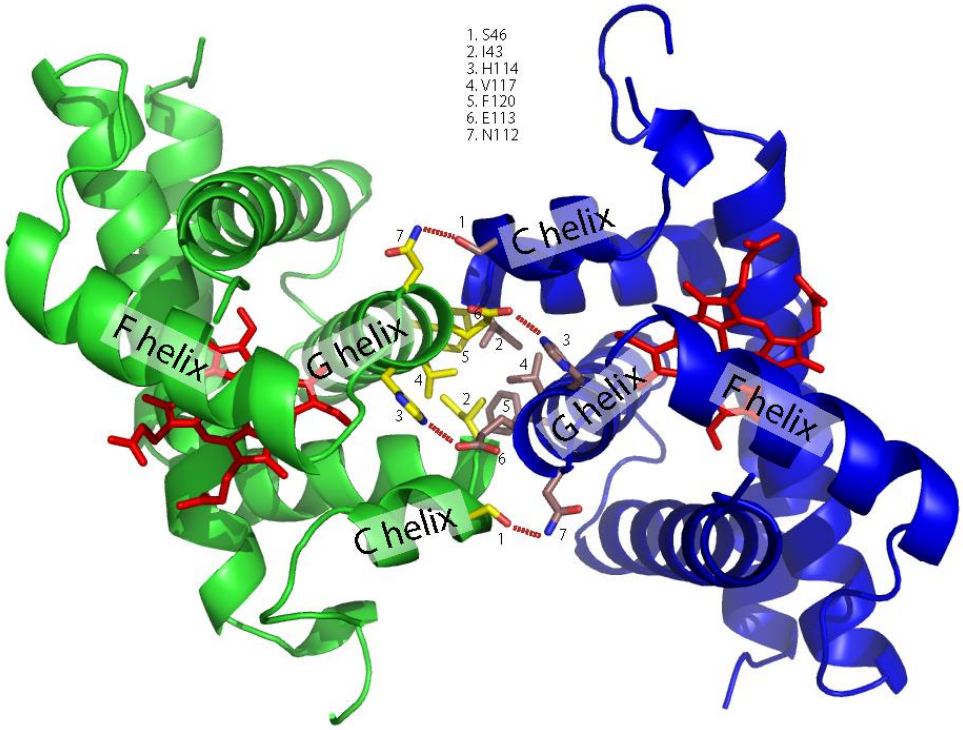
1. S46
2. I43
3. H114
4. V117
5. F120
6. E113
7. N112
C helix
F helix
G helix
G helix
F helix
C helix

Figure 3.

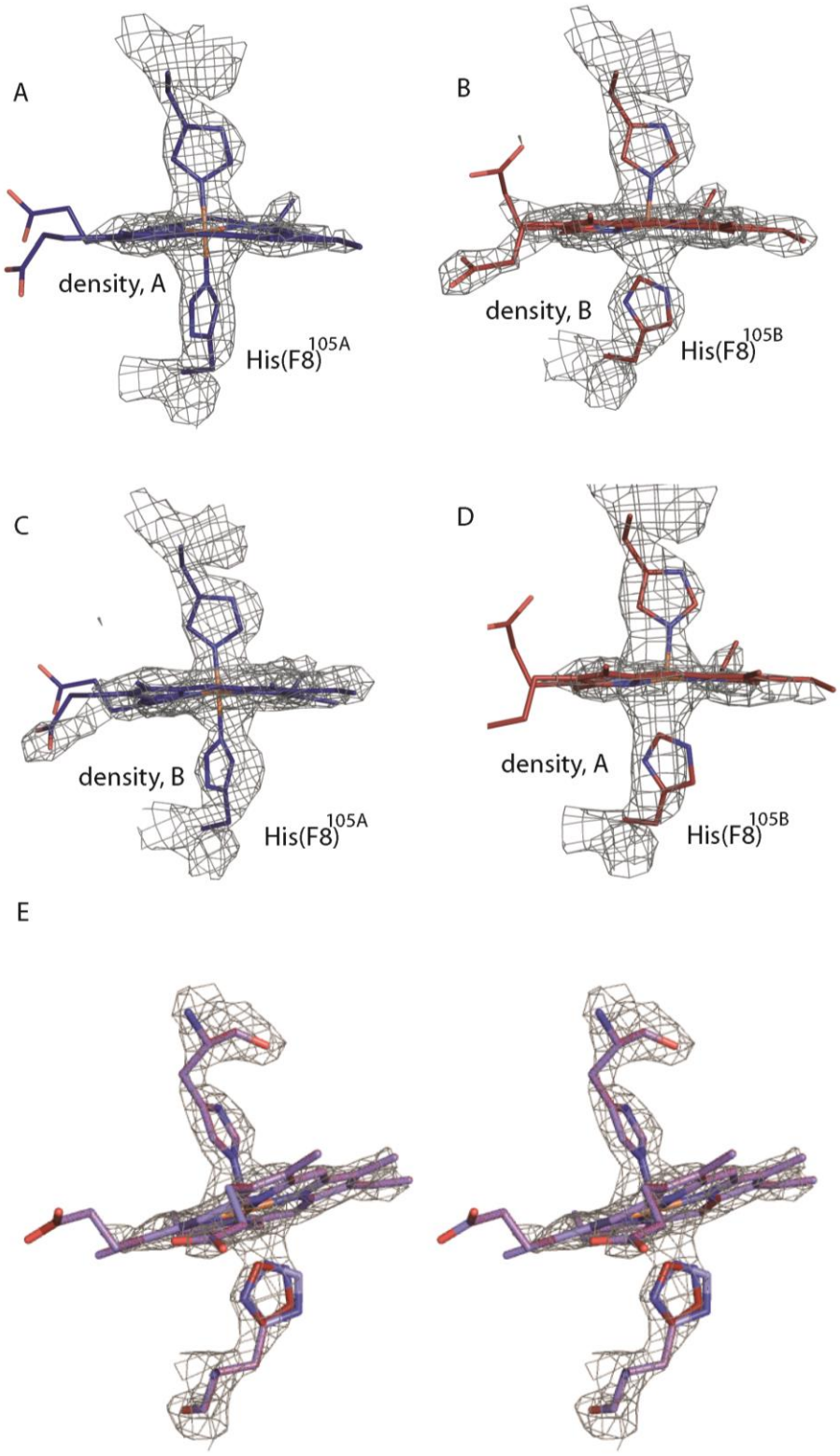
A
density, A
His(F8)105A
B
density, B
His(F8)105B
C
density, B
His(F8)105A
D
density, A
His(F8)105B
E

Figure 4.

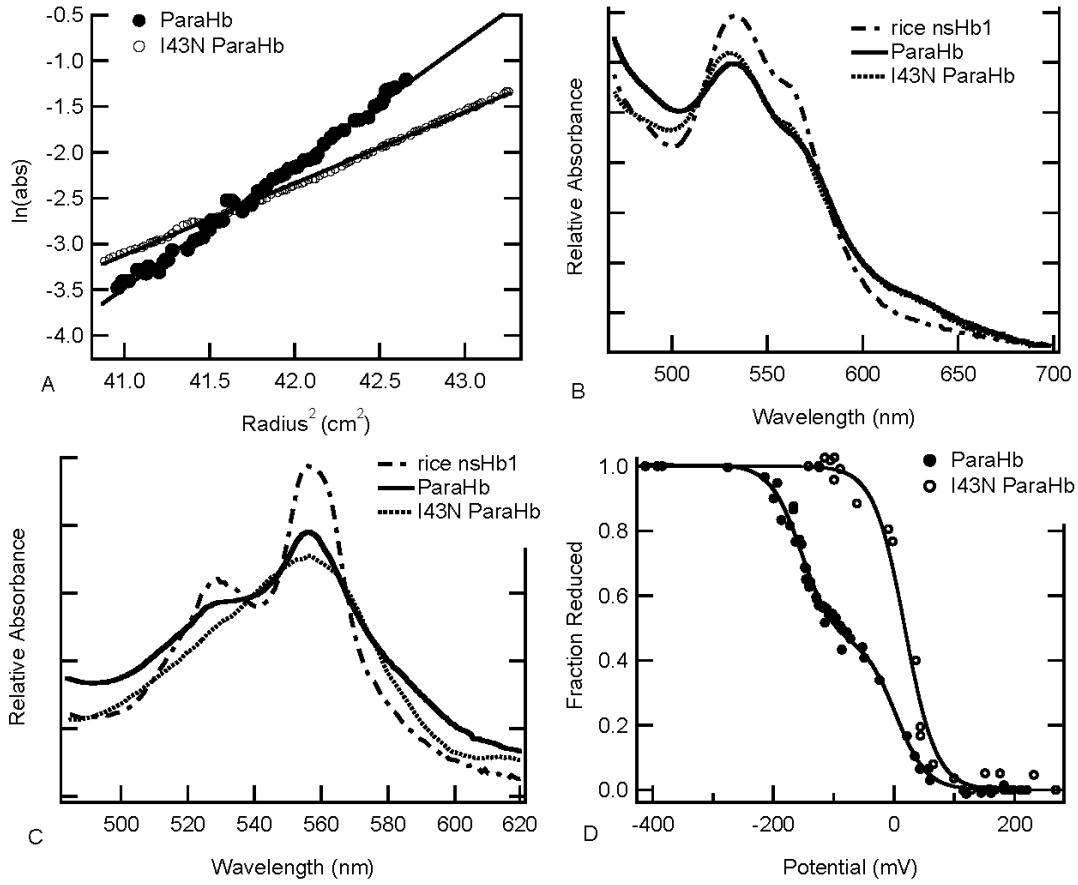
ParaHb
I43N ParaHb
ln(abs)
Radius^2 (cm^2)
A
rice nsHb1
ParaHb
I43N ParaHb
Relative Absorbance
Wavelength (nm)
B
rice nsHb1
ParaHb
I43N ParaHb
Relative Absorbance
Wavelength (nm)
C
ParaHb
I43N ParaHb
Fraction Reduced
Potential (mV)
D

Figure 5.

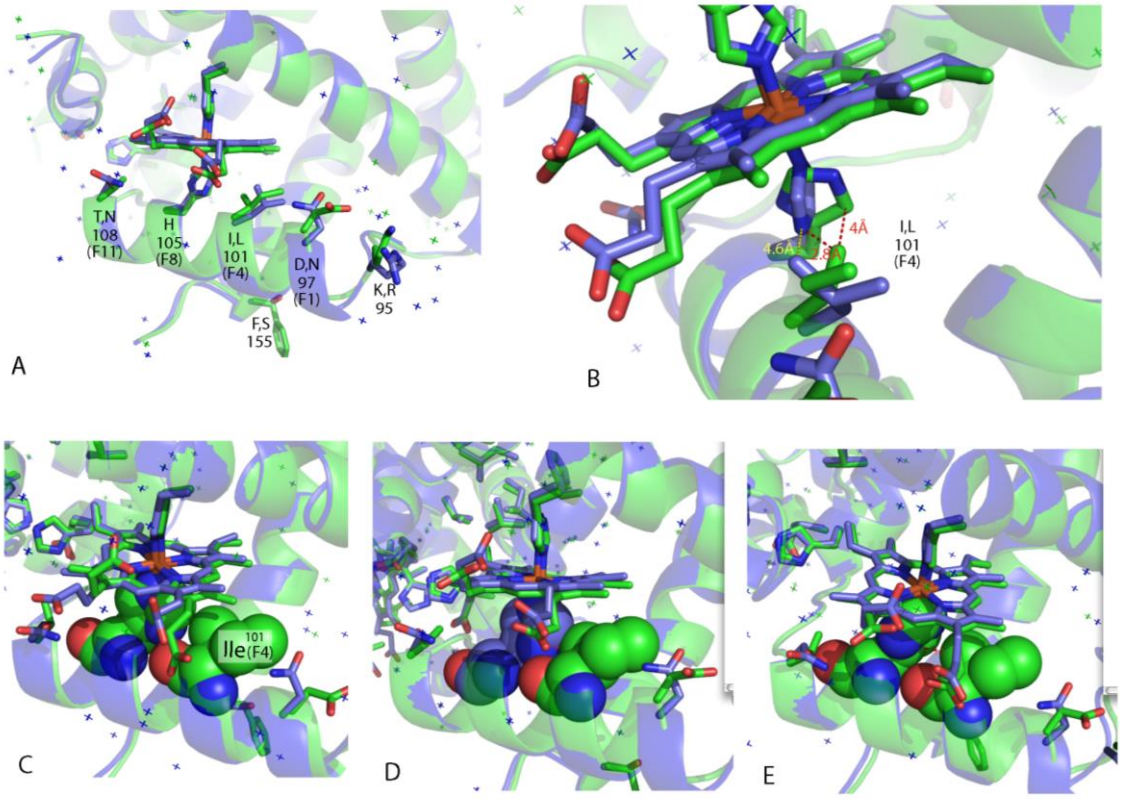
T,N
108
(F11)
H
105
(F8)
I,L
101
(F4)
D,N
97
(F1)
K,R
95
F,S
155
A
4Å
I,L
101
(F4)
B
Ile 101 (F4)
C
D
E

CHAPTER 4.

PLANT AND CYANOBACTERIAL HEMOGLOBINS REDUCE NITRITE TO NITRIC OXIDE UNDER ANOXIC CONDITIONS

Modified from a paper published in *Biochemistry*

Ryan Sturms, Alan A. DiSpirito, and Mark S. Hargrove

Abstract

The ability of ferrous hemoglobins to reduce nitrite to form nitric oxide has been demonstrated for hemoglobins from animals including myoglobin, blood cell hemoglobin, neuroglobin, and cytoglobin. In all cases, the rate constants for the bimolecular reactions with nitrite are relatively slow, with maximal values of ~ 5 $M^{-1}s^{-1}$ at pH 7. Combined with the relatively low concentrations of nitrite found in animal blood plasma (normally no greater than 13 μM), these slow reaction rates are unlikely to contribute significantly to hemoglobin oxidation, nitrite reduction, or NO production. Plants and cyanobacteria, however, must contend with much higher (mM) nitrite concentrations necessitated by assimilatory nitrogen metabolism during hypoxic growth, such as the conditions commonly found during flooding or in waterlogged soil. Here we report rate constants for nitrite reduction by a ferrous plant hemoglobin (rice nonsymbiotic hemoglobin 1) and a ferrous cyanobacterial hemoglobin from *Synechocystis* that are more than 10-times faster than those observed for animal hemoglobins. These rate constants, along with the relatively high concentrations of

nitrite present during hypoxia, suggest that plant and cyanobacterial hemoglobins could serve as anaerobic nitrite reductases *in vivo*.

Introduction

Hemoglobins (Hbs) with unknown functions have been found in most organisms. A hypothetical role common to many of them is nitric oxide (NO) scavenging (*1*), which is grounded in the established contribution of Hbs to nitric oxide dioxygenase (HbO_2 + NO → metHb + NO_3^-) (NOD) activity in bacterial flavohemoglobins (*2*), the effects of blood cell Hb on NO metabolism (*3*), and the general reactivity of oxy, deoxy, and ferric hemoglobins with NO (*4*). In plants, NOD function for Hbs (*5, 6*) is supported by increases in Hb expression in response to nitrate, nitrite, and nitric oxide (*7*), increases in NO scavenging ability in plants over-expressing Hb (*8, 9*), decreases in the levels of NO-sensitive enzymes in plants with down-regulated Hb (*10*), and the encouragement of cell growth by cyanobacterial Hb in the presence of high concentrations of reactive nitrogen species (*11*).

The importance of NO scavenging is clear in bacteria and yeast, where the organisms must defend themselves against oxidative bursts from the immune systems of their hosts (*1, 2*). The role of Hb NOD activity in plants and animals could involve scavenging to mitigate cell damage resulting from elevated NO levels during hypoxia, and could affect NO-mediated signaling. Alternatively, as has been proposed for myoglobin (Mb), red blood cell Hb, and neuroglobin in animals, Hbs could be responsible for NO production from reduction of nitrite (*12, 13*). However, the relatively

low rates of NO production by wild type and native animal Hbs (*14, 15*), and the modest (low μM) levels of nitrite typically found in mammalian tissues (*16*) diminish the likelihood that nitrite reductase activity is a major function of these proteins.

The metabolism of nitrogen is quite different in autotrophs such as plants and cyanobacteria, which must assimilate nitrogen through the reduction of nitrate under conditions ranging from normoxic to anoxic. In these organisms nitrate and nitrite can accumulate to very high (mM) concentrations (*17*), particularly when oxygen concentrations are low (*18*). Such conditions are associated with plant Hb up-regulation (*19, 20*), and thus reactions of nitrate and nitrite with plant and cyanobacterial Hbs are of potential physiological significance. Here we test the reactions of class 1 rice non-symbiotic Hb (rice nsHb1) (*21*) and the Hb from the cyanobacterium *Synechocystis* (SynHb) (*22-24*) with nitrate and nitrite. These Hbs are not oxygen transporters and have hypothetical roles in nitrogen metabolism. Our results show that the deoxyferrous forms of each react rapidly with nitrite to form ferric Hb and ferrous-nitrosyl Hb in a fixed ratio, indicative of nitric oxide production from the reduction of nitrite by ferrous Hb.

Materials and Methods

Protein expression and purification for rice nsHb1 and SynHb were carried out by previously described methods (*23, 25*), and horse heart myoglobin (Mb) was prepared by dissolving the lyophilized protein (Sigma) in 0.1 M sodium phosphate, pH 7.0, followed by centrifugation and desalting over a G-25 column equilibrated in the same buffer. Deoxyferrous protein samples were prepared under anaerobic conditions by

adding a liquid stock of 100 mM sodium dithionite (DT) in a slight excess of protein concentration and then passing the sample over a medium G-25 desalting column (to remove excess sodium dithionite) that was poured and equilibrated in an anaerobic chamber (95% argon and 5% hydrogen, Coy Laboratories). Deoxyferrous samples were sealed in air-tight cuvettes, confirmed using a USB 200 spectrophotometer (Ocean Optics), and diluted to 15 μM final concentration using deoxygenated 100 mM potassium phosphate buffer at pH7.

Aliquots from an anaerobic 100 mM sodium nitrite solution were added to the cuvette using a gas-tight Hamilton syringe to achieve the experimental nitrite concentrations. Reaction progress was monitored by observing the decrease in deoxyferrous heme at 558 nm for rice nsHb1, and at 559 nM for SynHb. These time courses were collected using the "scanning kinetics" mode on a Cary 50 spectrophotometer. The reactions in Figure 3, including the reactivity of ferric Hbs with nitrite, those bound to different ligands, and the comparative reaction of deoxyferrous proteins with 100 μM nitrate, were conducted under the same conditions as the reactions with nitrite, and monitored in the same way.

Single exponential fits of the reaction progress were carried out using Igor Pro, and the k_{obs} values at each [nitrite] were plotted against nitrite concentration and fitted to a line to measure observed bimolecular rate constants. Analyses of the endpoint spectra in Figure 1 were performed by adding together the ferric and ferrous-nitrosyl components for each Hb in Igor Pro.

Results

The reaction of rice nsHb1 and SynHb with nitrite- Sodium nitrite reacts with ferrous deoxy blood cell Hb to produce a combination of ferric and ferrous nitrosyl-Hb ($Hb^{Fe(II)}NO$) (*12, 13, 26*). To determine if such a reaction occurs with rice nsHb1 and SynHb, the deoxy forms of each were reacted with nitrite under anaerobic conditions. Figures 1A and 1B show the spectral changes associated with the reaction at 50 µM nitrite collected at 30 second intervals, demonstrating that each is oxidized relatively rapidly compared with other Hbs (*12*) at this nitrite concentration. Figures 1C and 1D show the absorbance spectra for each Hb at the end of the reaction along with the spectra of the ferric and HbNO components for each. The endpoint spectrum for each Hb could be fit to the sum of its respective ferric and HbNO components to measure the contribution of each form to the products at equilibrium. In the case of rice nsHb1, the final ratio is 60% ferric and 40% HbNO, which is consistent with what is observed for murine neuroglobin and Human Hb in this reaction(*15, 26*). For SynHb, the final spectrum is composed of 50% ferric and 50% HbNO, corresponding exactly to the final product predicted and observed for other members of the globin family (*26, 27*).

Kinetics of the reaction of rice nsHb1 and SynHb with nitrite- Measurements of the reaction of neuroglobin, Mb, and blood cell Hb have shown a range of observed rate constants for the wild type proteins that are relatively slow (0.12 - 6 $M^{-1}s^{-1}$ for neuroglobin and blood cell Hb, and 2.9-5.6 $M^{-1}s^{-1}$ for Mb) (*12, 15, 27*). To measure the rate constant for the reactions with rice nsHb1 and SynHb, time courses for the nitrite-induced progression of each ferrous Hb to its equilibrium endpoint were measured as a

function of nitrite concentration (Figure 2). A comparison of the time courses for reaction of rice nsHb1, SynHb, and Mb (the fastest of the Hbs previously reported wild type Hbs (*12*)) at 100 μM nitrite is shown in Figure 2A, demonstrating that the two autotroph Hbs are significantly faster than Mb. Figure 2B shows the dependence of the observed rate constant on nitrite concentration, yielding observed bimolecular rate constants for rice nsHb1 and SynHb of 166 and 130 $M^{-1}s^{-1}$, and a value for Mb of 11 s^{-1}.

Specificity of the reaction of rice nsHb1 and SynHb with nitrite- Hbs will participate in many reactions due to the innate reactivity of the heme iron. To test the specificity of the Hb/nitrite reaction with rice nsHb1 and SynHb, we have reacted nitrite with the ferric ($Hb^{Fe(III)}$), CO-bound ($Hb^{Fe(II)}CO$), and oxygenated ($Hb^{Fe(II)}O_2$) species of each along with the same derivatives of Mb. Additionally, the ferrous forms of each protein were reacted with nitrate. Figure 3 shows the progress of these reactions with 100 μM nitrite (or nitrate) after 300 s. Only the reaction of nitrite with the deoxyferrous form of each Hb occurs with any degree of completion on this time scale.

Discussion

Doyle (*26*) and others (*14, 15*) have previously investigated the mechanism of the reduction of nitrite by several animal deoxyferrous Hbs. Based on the pH dependence of the reaction, it is thought that the protonated form of nitrite, nitrous acid (HNO_2), is the species that reacts directly with Hb. But the equilibrium between nitrite and nitrous acid is rapid, and does not limit the relatively slow bimolecular reaction with Hbs. Thus, it is convenient to report the reaction with respect to nitrite concentration, as has become the

custom in the literature. With this understanding, the reaction of nitrite with Hbs can be described by the following reactions and Equation 1.

$$Hb^{Fe(II)} + NO_2^- + H^+ \xrightarrow{k_{NO_2^-}} Hb^{Fe(III)} + NO + OH^- \quad \text{Reaction 1.}$$

$$Hb^{Fe(II)} + NO \xrightarrow{k_{NO}} Hb^{Fe(II)}NO \quad \text{Reaction 2.}$$

Reactions 1 and 2 are simplified by two assumptions. First, Reaction 1 is rate limiting, and probably proceeds by the formation of $Hb^{Fe(III)}NO$, followed by NO release. As long as NO release is rapid relative to k_{NO2}^-, (as is the case with ferric Mb and neuroglobin, where k_{-NO} = 12 s^{-1} and 6.2 s^{-1} (*12*), respectively), this will not prevent NO binding to deoxyferrous Hb (Reaction 2). The second assumption is the irreversibility of Reaction 2, which is valid on these time scales because of the rapid (~ 100 μM^{-1} s^{-1}) bimolecular rate constant for NO binding to ferrous Hbs (*28*), and the extremely slow dissociation rate constant (~ 10^{-4} s^{-1}). The resulting high affinity for NO by ferrous Hbs is such that NO will always be bound at equilibrium under any reasonable experimental conditions.

The relatively slow rate of Reaction 1 compared to Reaction 2 means that two $Hb^{Fe(II)}$ molecules are consumed in the reaction with each NO_2^- (one in Reaction 1, and the second upon binding to NO in Reaction 2). This lead to Equation 1, which describes the expected velocity of the overall reaction as measured by monitoring the disappearance of deoxyferrous Hb.

$$\frac{-dHb^{Fe(II)}}{dt} = 2k_{NO_2^-}[Hb^{Fe(II)}][NO_2^-] \quad \text{Equation 1.}$$

Equation 1 shows that "k_{obs}", as measured in Figure 2B by following the disappearance of ferrous Hb in the absence of sodium dithionite (DT), is actually equal to $2k_{NO2}^-$. In the presence of DT (which rapidly reduces the $Hb^{Fe(III)}$ produced in Reaction 1), k_{obs} will equal k_{NO2}^-, and should be half of the value measured in its absence, as observed by others for Mb and Hb (*29, 30*). As such, our value of 11 $M^{-1}s^{-1}$ for Mb in the absence of DT is consistent with the value of 2.9 s^{-1} reported in its presence (*12*).

To directly test this relationship, the reaction of nitrite with SynHb was carried out in the presence of 3 mM sodium dithionite (DT), and included in Figure 2B. As expected, the slope in the presence of DT (68 $M^{-1}s^{-1}$) is half that observed in its absence (130 $M^{-1}s^{-1}$). Such consideration means that the actual rate of reduction of nitrite (k_{NO2-}) by rice nsHb and SynHb are 83 and 68 $M^{-1}s^{-1}$, respectively. These rates are the highest observed for a native or wild type Hb by at least an order of magnitude.

The consequences of rapid, tight NO rebinding to ferrous Hb is that, absent other factors, nitrite reduction by Hb is not an efficient means for generating free NO. In fact, to be useful for other purposes, NO produced in blood cells would also have to avoid binding to the previously existing high concentration of ferrous Hb, and reacting with oxyHb, which would result in its destruction. The latter two reactions occur on microsecond time scales at the ~20 mM Hb concentrations in erythrocytes (*31*), whereas nitrite reduction by Hb occurs in minutes to hours at low nitrite concentrations. If fact, spectral analysis was chosen in our experiments as the primary means of product observation because attempts to directly measure NO release using an NO electrode were unsuccessful. In efforts to measure NO production, others have adjusted

experimental parameters specifically to minimize the extent of NO binding to the remaining deoxyferrous Hb, and even then observed relatively low levels of free NO gas (*27*).

The consequences of Hb hexacoordination for nitrite reduction- Rice nsHb1, SynHb, neuroglobin, and cytoglobin are all "hexacoordinate" hemoglobins, meaning that the distal histidine reversibly coordinates the heme iron (*32*). The hemes of ferrous neuroglobin and SynHb bind tightly to the distal histidine ($K_{H2} > 100$, where K_{H2} is the association equilibrium constant for histidine coordination in the ferrous oxidation state), but those of rice nsHb and cytoglobin bind relatively weakly ($K_{H2} < 100$). Yet ferrous neuroglobin and cytoglobin react very slowly with nitrite (*15*), and rice nsHb1 and SynHb react much more rapidly. Furthermore, pentacoordinate E7L neuroglobin (where the distal histidine is replaced with leucine) is a very effective nitrite reductase (*12*), but pentacoordinate Mb and blood cell Hb are not.

The only correlation between the strength of hexacoordination and reactions with nitrite is found in the plots of k_{obs} vs. [nitrite] for SynHb (Figure 2B), and murine neuroglobin (*15*). Both of these plots have non-zero y-intercepts of similar magnitude ($0.004\ s^{-1}$), and both Hbs have large values of K_{H2}. It is possible that this phenomenon reflects some aspect of the nitrite reaction mechanism with hexacoordinate Hbs, but there is no clear relationship between overall nitrite reductase activity and the equilibria or kinetics of intramolecular heme coordination.

The physiological significance of Hb nitrite reductase activity in plants and cyanobacteria- A current hypothesis for plant and cyanobacterial Hbs is that they

scavenge NO or peroxynitrite to detoxify these or other reactive oxygen species (ROS), which are particularly damaging under hypoxic conditions, like those encountered during soil waterlog (*6, 11, 18*). When bound to oxygen, these Hbs are certainly capable of reacting with NO to form nitrate (*4, 5*), and over-expression of plant nsHbs has been shown to reduce NO levels *in vivo* (*8, 9*). The results presented here suggest that under conditions of extreme hypoxia, plant and cyanobacterial Hbs could also function as nitrite reductases. Since these organisms often face such anoxic conditions (*11, 18*), during which nitrate and nitrite concentrations can rise to mM levels and pH can drop several tenths of a unit (*33, 34*), it is likely that this activity is of physiological relevance, where it might help in preventing ROS generation from excess nitrite, or in the continuation of nitrate assimilation. In fact, it is under just such conditions that cyanobacterial Hb knockouts show the largest amount of ROS buildup (*11*).

There are a few questions that must be addressed in consideration of this hypothesis. 1) Why would plants want an alternative nitrite reductase active under anoxic conditions? 2) Could Hbs have a dual function as NO scavengers in the presence of oxygen, and nitrite reductases during anoxia? 3) How are plant Hbs reduced *in vivo*, and how could they maintain catalytic nitrite reduction in the presence of potential inhibition by the NO they produce?

During hypoxia, nitrite can accumulate to toxic levels (*17, 35, 36*). Plant Hbs could help to reduce nitrite levels under such conditions, using the reductive power accumulated as a result of anaerobic glycolysis. However, $Hb^{Fe(II)}NO$ formed in the reaction would inhibit catalytic nitrite reduction, and there would need to be either a

mechanism *in vivo* for its removal prior to Hb binding, or $Hb^{Fe(II)}NO$ must react further to regenerate free Hb. Long-term plant survival requires continuation of protein synthesis even under anoxic conditions (*37, 38*). It is possible that $Hb^{Fe(II)}NO$ is an intermediate in the production of a further reduced nitrogen oxide, which could lead to the ammonia needed for protein synthesis in the absence of O_2.

It is also possible that Hbs are NO scavengers when oxygenated, and nitrite reductases under anoxic conditions, or a combination of the two if partially saturated with oxygen. Igamberdiev *et al.* (*6*) have presented a strong argument for NOD activity during fermentative growth, during which Hb reduction is achieved by reduced monodehydroascorbate reductase (*39*). Oxygen binding follows, and the oxyHb scavenges NO using the NOD reaction. Under anoxic conditions, the NOD reaction will not occur, and the resulting deoxyferrous Hb could function as a nitrite reductase. However, if the Hb were partially oxygenated (for rice nsHb1 this would be $[O_2] \sim 2$ nM, and for SynHb ~ 20 nM (*32*)), it is possible that nitrite reduction could lead to NO that is subsequently scavenged by reacting with oxyHb.

Regardless of whether plant and cyanobacterial Hbs are NO scavengers or nitrite reductases, their rates of activity are certainly limited by the rates of reduction of each ferric Hb *in vivo* (*4, 39*). Even in the case of monodehydroascorbate reductase, the most likely candidate for Hb reduction in plant roots, the rate of reduction is slower than that observed here for the nitrite reductase reaction. Thus, it is important to characterize the reductase half-reactions carefully when evaluating the proposed activity of any Hb reactions involving changes in heme iron oxidation state. It will also be necessary to

compare nitrite reductase activities in the other classes of plant Hbs (*21*), such as the leghemoglobins, which are not associated with surviving hypoxia. Results from such experiments will test the specificity of the reaction, and will be an important consideration in evaluating the physiological significance of Hb nitrite reductase activity in these organisms.

References

1. Gardner, P. R. (2005) Nitric oxide dioxygenase function and mechanism of flavohemoglobin, hemoglobin, myoglobin and their associated reductases, *J Inorg Biochem 99*, 247-266.

2. Gardner, P. R., Gardner, A. M., Martin, L. A., and Salzman, A. L. (1998) Nitric oxide dioxygenase: an enzymic function for flavohemoglobin, *Proc Natl Acad Sci U S A 95*, 10378-10383.

3. Doherty, D. H., Doyle, M. P., Curry, S. R., Vali, R. J., Fattor, T. J., Olson, J. S., and Lemon, D. D. (1998) Rate of reaction with nitric oxide determines the hypertensive effect of cell-free hemoglobin, *Nat Biotechnol 16*, 672-676.

4. Smagghe, B. J., Trent, J. T., 3rd, and Hargrove, M. S. (2008) NO dioxygenase activity in hemoglobins is ubiquitous in vitro, but limited by reduction in vivo, *PLoS One 3*, e2039.

5. Perazzolli, M., Dominici, P., Romero-Puertas, M. C., Zago, E., Zeier, J., Sonoda, M., Lamb, C., and Delledonne, M. (2004) Arabidopsis nonsymbiotic hemoglobin AHb1 modulates nitric oxide bioactivity, *Plant Cell 16*, 2785-2794.

6. Igamberdiev, A. U., and Hill, R. D. (2004) Nitrate, NO and haemoglobin in plant adaptation to hypoxia: an alternative to classic fermentation pathways, *J. Exp. Bot. 55*, 2473-2482.

7. Ohwaki, Y., Kawagishi-Kobayashi, M., Wakasa, K., Fujihara, S., and Yoneyama, T. (2005) Induction of class-1 non-symbiotic hemoglobin genes by nitrate, nitrite and nitric oxide in cultured rice cells, *Plant Cell Physiol 46*, 324-331.

8. Dordas, C., Hasinoff, B. B., Igamberdiev, A. U., Manac'h, N., Rivoal, J., and Hill, R. D. (2003) Expression of a stress-induced hemoglobin affects NO levels produced by alfalfa root cultures under hypoxic stress, *Plant J 35*, 763-770.

9. Seregelyes, C., Igamberdiev, A. U., Maassen, A., Hennig, J., Dudits, D., and Hill, R. D. (2004) NO-degradation by alfalfa class 1 hemoglobin (Mhb1): a possible link to PR-1a gene expression in Mhb1-overproducing tobacco plants, *FEBS Lett 571*, 61-66.

10. Igamberdiev, A. U., Stoimenova, M., Seregelyes, C., and Hill, R. D. (2006) Class-1 hemoglobin and antioxidant metabolism in alfalfa roots, *Planta 223*, 1041-1046.

11. Scott, N. L., Xu, Y., Shen, G., Vuletich, D. A., Falzone, C. J., Li, Z., Ludwig, M., Pond, M. P., Preimesberger, M. R., Bryant, D. A., and Lecomte, J. T. (2010) Functional and structural characterization of the 2/2 hemoglobin from Synechococcus sp. PCC 7002, *Biochemistry 49*, 7000-7011.

12. Tiso, M., Tejero, J., Basu, S., Azarov, I., Wang, X., Simplaceanu, V., Frizzell, S., Jayaraman, T., Geary, L., Shapiro, C., Ho, C., Shiva, S., Kim-Shapiro, D. B., and Gladwin, M. T. (2011) Human neuroglobin functions as a redox regulated nitrite reductase, *J Biol Chem*.

13. Gladwin, M. T., Grubina, R., and Doyle, M. P. (2009) The new chemical biology of nitrite reactions with hemoglobin: R-state catalysis, oxidative denitrosylation, and nitrite reductase/anhydrase, *Acc Chem Res 42*, 157-167.

14. Shiva, S., Huang, Z., Grubina, R., Sun, J., Ringwood, L. A., MacArthur, P. H., Xu, X., Murphy, E., Darley-Usmar, V. M., and Gladwin, M. T. (2007) Deoxymyoglobin is a nitrite reductase that generates nitric oxide and regulates mitochondrial respiration, *Circ Res 100*, 654-661.

15. Petersen, M. G., Dewilde, S., and Fago, A. (2008) Reactions of ferrous neuroglobin and cytoglobin with nitrite under anaerobic conditions, *J Inorg Biochem 102*, 1777-1782.

16. Moshage, H., Kok, B., Huizenga, J. R., and Jansen, P. L. (1995) Nitrite and nitrate determinations in plasma: a critical evaluation, *Clin Chem 41*, 892-896.

17. Ferrari, T. E., and Varner, J. E. (1971) Intact tissue assay for nitrite reductase in barley aleurone layers, *Plant Physiol 47*, 790-794.

18. Gupta, K. J., Fernie, A. R., Kaiser, W. M., and van Dongen, J. T. (2011) On the origins of nitric oxide, *Trends Plant Sci.*, in press.

19. Taylor, E. R., Nie, X. Z., MacGregor, A. W., and Hill, R. D. (1994) A cereal haemoglobin gene is expressed in seed and root tissues under anaerobic conditions, *Plant Mol Biol 24*, 853-862.

20. Hunt, P. W., Klok, E. J., Trevaskis, B., Watts, R. A., Ellis, M. H., Peacock, W. J., and Dennis, E. S. (2002) Increased level of hemoglobin 1 enhances survival of hypoxic stress and promotes early growth in Arabidopsis thaliana, *Proc Natl Acad Sci U S A 99*, 17197-17202.

21. Smagghe, B. J., Hoy, J. A., Percifield, R., Kundu, S., Hargrove, M. S., Sarath, G., Hilbert, J. L., Watts, R. A., Dennis, E. S., Peacock, W. J., Dewilde, S., Moens, L., Blouin, G. C., Olson, J. S., and Appleby, C. A. (2009) Review: correlations between oxygen affinity and sequence classifications of plant hemoglobins, *Biopolymers 91*, 1083-1096.

22. Couture, M., Das, T., Savard, P., Ouellet, Y., Wittenberg, J., Wittenberg, B., Rousseau, D., and Guertin, M. (2000) Structural investigations of the hemoglobin of the cyanobacterium Synechocystis PCC6803 reveal a unique distal heme pocket, *Eur. J. Biochem. 267*, 4770-4780.

23. Hvitved, A. N., Trent, J. T., III, Premer, S. A., and Hargrove, M. S. (2001) Ligand binding and hexacoordination in Synechocystis hemoglobin, *J. Biol. Chem. 276*, 34714-34721.

24. Scott, N., and LeComte, J. (2000) Cloning, expression, purification, and preliminary characterization of a putative hemoglobin from the cyanobacterium Synechocystis sp. PCC 6803, *Protein Sci. 3*, 587-597.

25. Halder, P., Trent, J. T., III., and Hargrove, M. S. (2007) The Influence of the Protein Matrix on Histidine Ligation in Ferric and Ferrous Hexacoordinate Hemoglobins, *PROTEINS: Structure, Function, and Bioinformatics 66*, 172-182.

26. Doyle, M. P., LePoire, D. M., and Pickering, R. A. (1981) Oxidation of hemoglobin and myoglobin by alkyl nitrites inhibition by oxygen, *J Biol Chem 256*, 12399-12404.

27. Huang, Z., Shiva, S., Kim-Shapiro, D. B., Patel, R. P., Ringwood, L. A., Irby, C. E., Huang, K. T., Ho, C., Hogg, N., Schechter, A. N., and Gladwin, M. T. (2005) Enzymatic function of hemoglobin as a nitrite reductase that produces NO under allosteric control, *J Clin Invest 115*, 2099-2107.

28. Van Doorslaer, S., Dewilde, S., Kiger, L., Nistor, S. V., Goovaerts, E., Marden, M. C., and Moens, L. (2003) Nitric oxide binding properties of neuroglobin. A characterization by EPR and flash photolysis, *J Biol Chem 278*, 4919-4925.

29. Grubina, R., Huang, Z., Shiva, S., Joshi, M. S., Azarov, I., Basu, S., Ringwood, L. A., Jiang, A., Hogg, N., Kim-Shapiro, D. B., and Gladwin, M. T. (2007)

Concerted nitric oxide formation and release from the simultaneous reactions of nitrite with deoxy- and oxyhemoglobin, *J Biol Chem 282*, 12916-12927.

30. Salhany, J. M. (2008) Kinetics of reaction of nitrite with deoxy hemoglobin after rapid deoxygenation or predeoxygenation by dithionite measured in solution and bound to the cytoplasmic domain of band 3 (SLC4A1), *Biochemistry 47*, 6059-6072.

31. Olson, J. S., Foley, E. W., Rogge, C., Tsai, A. L., Doyle, M. P., and Lemon, D. D. (2004) No scavenging and the hypertensive effect of hemoglobin-based blood substitutes, *Free Radic Biol Med 36*, 685-697.

32. Kakar, S., Hoffman, F. G., Storz, J. F., Fabian, M., and Hargrove, M. S. (2010) Structure and reactivity of hexacoordinate hemoglobins, *Biophys Chem 152*, 1-14.

33. Roberts, J. K., Andrade, F. H., and Anderson, I. C. (1985) Further Evidence that Cytoplasmic Acidosis Is a Determinant of Flooding Intolerance in Plants, *Plant Physiol 77*, 492-494.

34. Roberts, J. K., Callis, J., Jardetzky, O., Walbot, V., and Freeling, M. (1984) Cytoplasmic acidosis as a determinant of flooding intolerance in plants, *Proc Natl Acad Sci U S A 81*, 6029-6033.

35. Dry, I., Wallace, W., and Nicholas, D. J. D. (1981) Role of ATP in nitrite reduction in roots of wheat and pea, *Planta 152*, 234-238.

36. Wellbrun, A. R. (1990) Why are atomospheric oxides of nitrogen usually phytotoxic and not alternative fertilizers?, *New Phytol 115*, 395-429.

37. Subbaiah, C. C., and Sachs, M. M. (2009) *Responses to Oxygen Deprivation and Potential for Enhanced Flooding Toloerance in Maize*, Springer Science.

38. Rhoads, D. M., Umbach, A. L., Subbaiah, C. C., and Siedow, J. N. (2006) Mitochondrial reactive oxygen species. Contribution to oxidative stress and interorganellar signaling, *Plant Physiol 141*, 357-366.

39. Igamberdiev, A. U., Bykova, N. V., and Hill, R. D. (2006) Nitric oxide scavenging by barley hemoglobin is facilitated by a monodehydroascorbate reductase-mediated ascorbate reduction of methemoglobin, *Planta 223*, 1033-1040.

Figure legends

Figure 1. The reaction of rice nsHb1 and SynHb with nitrite. The spectral changes associated with Rice nsHb1 (A) and SynHb (B) oxidation are shown at 30 second intervals following the addition of 50 µM sodium nitrite. Figures 1C and 1D show ferric and ferrous nitrosyl (HbNO) reference spectra, the final experimental spectrum, and a sum of the reference spectra to determine the contribution of each species to the final experimental spectrum for rice nsHb1 and SynHb respectively.

Figure 2. The kinetics of the reaction of rice nsHb1 and SynHb with nitrite. (A) Time courses for the reaction with each Hb and Mb at 100 µM nitrite. The absorbance change is normalized to that associated with the transition from each deoxyferrous Hb to its end point spectrum. (B) The observed reaction rates for each Hb are presented as a function of [nitrite]. Linear fits of these plots yield observed bimolecular rate constants of 166, 130, and 11 $M^{-1}s^{-1}$ respectively. Also included are the reaction rates for SynHb in the presence of sodium dithionite (DT), demonstrating that the slope is half that observed without DT.

Figure 3. The reactivity of nitrite and nitrate with other forms of rice nsHb1, SynHb, and Mb. The deoxyferrous (Hb), CO (HbCO), ferric (metHb), and oxy (oxyHb) forms of each Hb were reacted with 100 µM nitrite, and the reaction progress measured after 300 s. Each deoxyferrous Hb was also reacted with 100 µM nitrate over

the same period of time. In each case, only the reaction of deoxyferrous Hb with nitrite shows any appreciable reaction.

Figure 1.

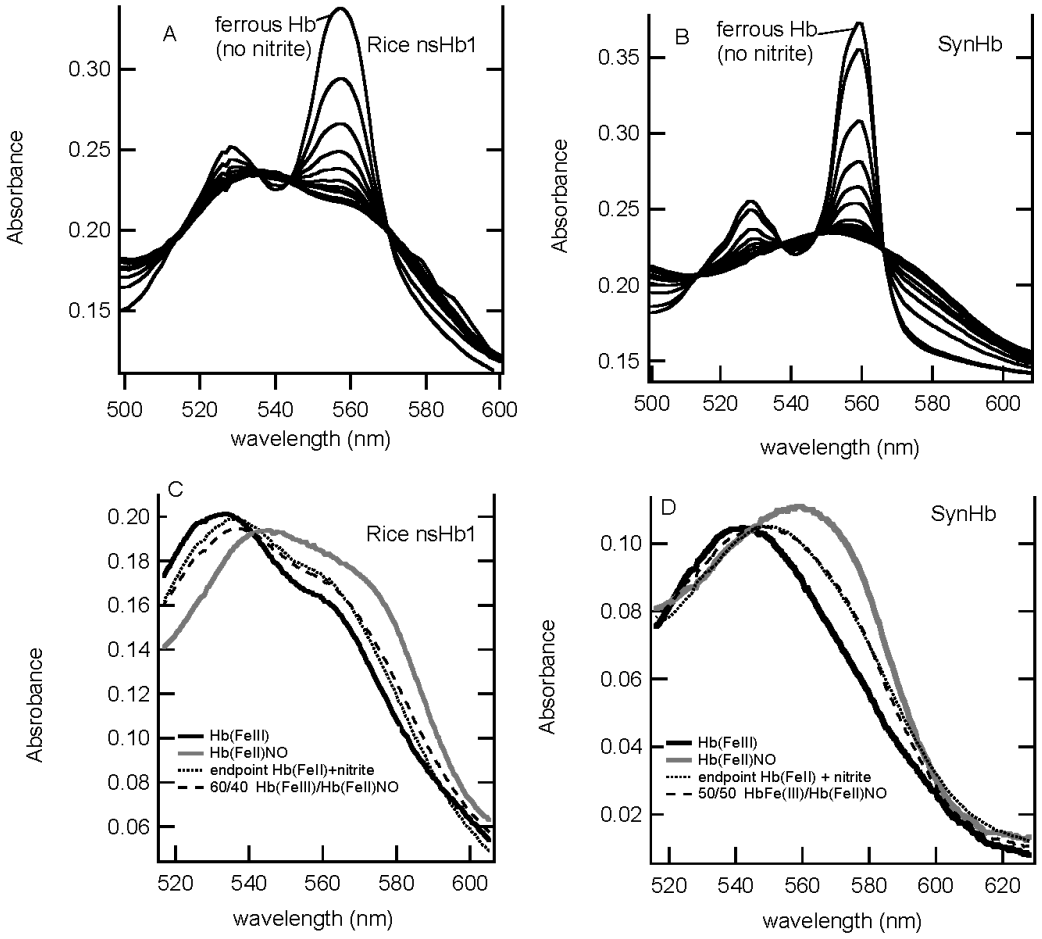

Figure 2.

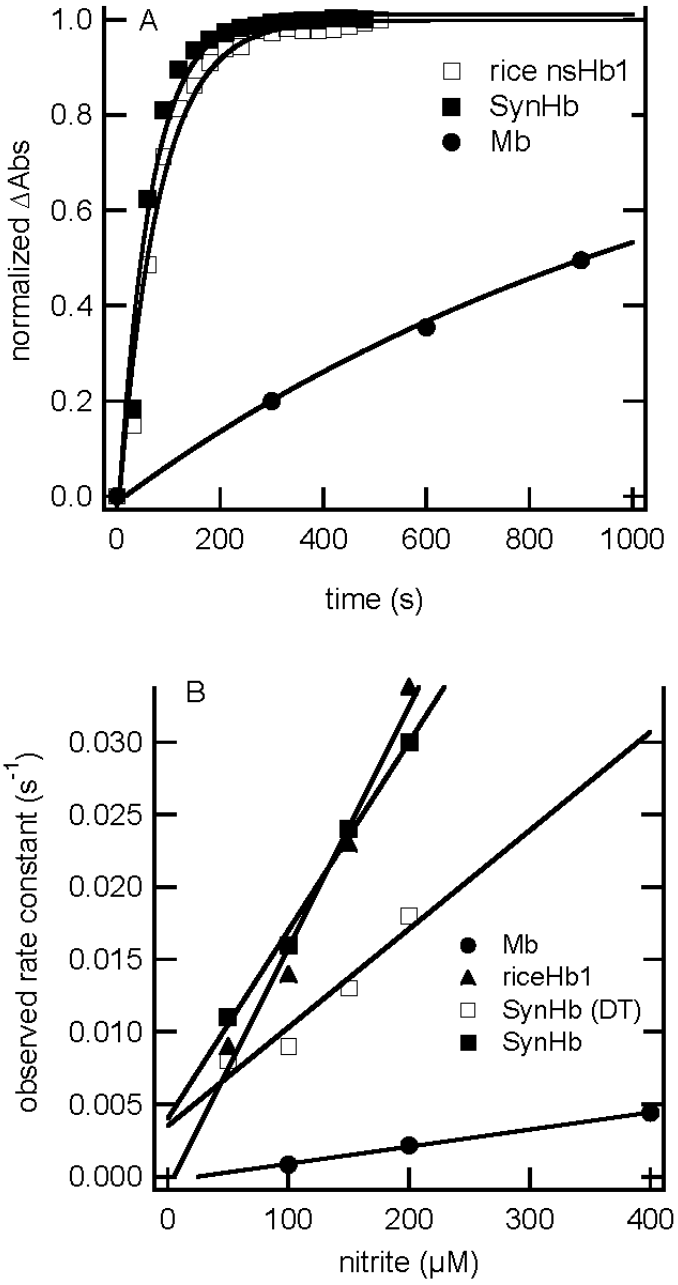
A
1.0
0.8
0.6
0.4
0.2
0.0
normalized ΔAbs
0
200
400
600
800
1000
time (s)
rice nsHb1
SynHb
Mb
B
0.030
0.025
0.020
0.015
0.010
0.005
0.000
observed rate constant (s-1)
0
100
200
300
400
nitrite (μM)
Mb
riceHb1
SynHb (DT)
SynHb

Figure 3.

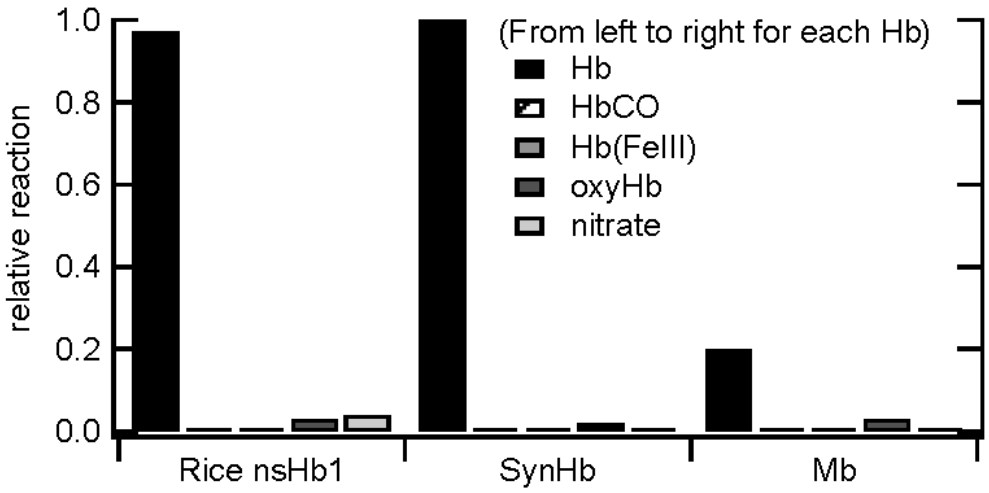
1.0
0.8
0.6
0.4
0.2
0.0
relative reaction
(From left to right for each Hb)
Hb
HbCO
Hb(FeIII)
oxyHb
nitrate
Rice nsHb1
SynHb
Mb

CHAPTER 5.
PLANT AND CYANOBACTERIAL HEMOGLOBINS RAPIDLY REDUCE HYDROXYLAMINE TO PRODUCE AMMONIUM

Modified from a paper published in *Biochemistry*

Ryan Sturms, Alan A. DiSpirito, D. Bruce Fulton, and Mark S. Hargrove

Abstract

Plants often face hypoxic stress as a result of flooding and waterlogged soils. During these periods, they must continue ATP production and nitrogen assimilation for use in protein synthesis if they are to survive. The normal pathway of reductive nitrogen assimilation in non-legumes, the combined reactions of nitrate and nitrite reductase, can be inhibited during low oxygen conditions that are associated with the buildup of toxic metabolites such as nitrite and nitric oxide, so the plant must also have a means of detoxifying these molecules. Compared with animal hemoglobins, plant and cyanobacterial hemoglobins are uniquely adept at reducing nitrite to nitric oxide under anaerobic conditions. Here we test their ability to reduce hydroxylamine, a proposed intermediate of nitrite reductase, under anaerobic conditions. We find that class 1 rice nonsymbiotic hemoglobin (rice nsHb1) and the hemoglobin from the cyanobacterium *Synechocystis* (SynHb) catalyze the reduction of hydroxylamine to ammonium at rates 100 to 2,500 times faster than animal hemoglobins including myoglobin, neuroglobin, cytoglobin, and blood cell hemoglobin. These results support the hypothesis that plant and cyanobacterial hemoglobins contribute to anaerobic nitrogen metabolism in support of nitrogen assimilation and/or anaerobic respiration.

Introduction

Plants routinely face hypoxic and anoxic conditions, and survival varies greatly across different species, plant ages, and the lengths of oxygen deprivation (*1, 2*). In order to survive these challenges, plants must generate ATP, continue ammonium production in support of protein synthesis, and cope with nitrite (NO_2^-) and nitric oxide (NO) toxicity (*3-5*). The mechanisms by which NO_2^- and NO accumulation occur are not entirely understood, but may result from the activities of nitrate reductase (NR) (*6, 7*) and nitrite reductase (NiR) (*8*), as well as the reduction of nitrite by mitochondria and a membrane-bound nitrite/nitric oxide reductase (NiNOR) (*9, 10*). Thus, in plants, hypoxia results in the production of nitrite and NO, which are harmful metabolites reflecting the failure to completely reduce nitrate to ammonium.

Hypoxia, nitrate, nitrite, and NO are known to up-regulate a specific class of plant hemoglobin (class 1 nonsymbiotic hemoglobins, or nsHbs (*11*)), which increases survival in the absence of oxygen (*5, 12, 13*). The role of nsHbs in survival during hypoxia has previously been attributed to the scavenging and detoxification of NO, and the concomitant oxidation of NADH to keep glycolysis functioning under these conditions (*5*). The proposed mechanism of NO scavenging is the "nitric oxide dioxygenase" (NOD) reaction, which is common to hemoglobins (Hbs) in general (*14, 15*).

$$Hb^{2+}O_2 + NO \xrightarrow{NOD} Hb^{3+} + NO_3^- \quad (1)$$

Oxygen is required for the NOD reaction, as well as a source of electrons to reduce the resulting ferric Hb. The source of reduction in plants as been attributed to NADH and the enzyme monodehydroascorbate reductase (*16*).

It is counterintuitive however, to waste the reductive power of NADH on the oxidation of NO, if it could instead be coupled to production of ammonium and/or ATP. Furthermore, when oxygen levels are below ~ 2 nM (the K_D for oxygen binding to class 1 nsHbs (*11*)), the co-substrate of the NOD reaction is absent and the reaction cannot proceed. These ideas led us to test the possibility that nsHb might instead reduce nitrite in support of ammonium production during hypoxia. Those results show that plant and cyanobacterial Hbs reduce nitrite to NO very rapidly compared to animal Hbs (*17*). However, converting nitrite to NO in isolation makes little sense metabolically as the NO produced binds to the remaining ferrous Hb preventing continued nitrite reduction. Thus, for nitrite reduction to be a plausible hypothesis for the function of nsHb, it must influence additional chemistry associated with the overall goal of ammonium or dinitrogen production.

The sequential reduction of nitrite to ammonium involves the one-electron reduction of nitrite to NO, three-electron reduction of NO to NH_2OH (hydroxylamine, or HA), and the two-electron reduction of HA to ammonium, NH_4^+. It has long been known that deoxyferrous blood cell Hb reacts with HA to form N_2, N_2O, and ammonium, and that the percentage of ammonium formed can be increased dramatically in the presence of an excess of reductant (*18, 19*). However, the reaction between HA

and deoxyferrous blood cell Hb is very slow, having a bimolecular rate constant of 0.01 $mM^{-1}s^{-1}$ (*19*), making blood cell Hb an unlikely candidate to serve as a HA reductase.

In the current work, we examine the ability of a deoxyferrous class 1 nsHb, rice nsHb1, to catalyze the reduction of HA. We compare this activity to that of three animal Hbs (myoglobin, neuroglobin, and cytoglobin), and a Hb from another photosynthetic autotroph, the cyanobacterium *Synechocystis* (SynHb). Our results show that deoxyferrous rice nsHb1 and SynHb convert HA specifically to ammonium at rates 100 to 2,500-times faster than the animal Hbs. These results complement those of nitrite reduction by rice nsHb1 and SynHb (*17*), and support the hypothesis that they serve as an alternative means of reducing nitrogen metabolites and continuing ammonium production during hypoxia.

EXPERIMENTAL PROCEDURES

Protein and reagent preparation. Hbs were expressed, purified, and converted to the deoxyferrous forms as described previously (*17*, *20*, *21*). These include rice nsHb1, SynHb, human neuroglobin, human cytoglobin, and horse heart myoglobin. Anaerobic buffers were prepared by boiling for 5 minutes followed by argon purging until cooled to room temperature, followed by equilibration in the anaerobic chamber overnight (95% argon and 5% hydrogen, Coy Laboratories). All dry chemical reagents were weighed outside of the anaerobic chamber, deoxygenated and dissolved inside the chamber in anaerobic buffer. ^{15}N-hydroxylamine, ^{15}N-ammonia and ^{15}N-urea were purchased from Cambridge Isotope Laboratories.

Equilibrium reactions. Anaerobic titrations of deoxyferrous Hbs with HA were carried out by adding a stock solution of 1 mM HA to a stirred cuvette containing deoxyferrous Hb in the anaerobic chamber, and monitoring the equilibrated visible absorbance spectra with an Ocean Optics USB 2000 spectrophotometer. All reactions were carried out in 0.1 M phosphate buffer, pH 7.0, and room temperature. The progress of oxidation associated with these isosbestic transitions can be followed as the normalized decrease in absorbance at 557 nm.

NMR Experiments. NMR experiments were carried out on a Bruker DRX500 NMR spectrometer at the Iowa State University Biomolecular NMR Facility using a Nalorac 5 mm broadband probe configured for ^{15}N detection. 1D ^{15}N spectra were collected at 25° C with inverse-gated ^{1}H decoupling. ^{15}N chemical shifts are referenced to urea as an indirect reference to liquid NH_3. Data were collected and processed using Bruker TopSpin 1.3 software, and Bruker data files were exported to Igor Pro for further analysis. Samples were prepared in the anaerobic chamber and sealed before being removed. NMR spectra were acquired from several minutes to several hours after sample preparation with little difference observed in the resulting spectra. To measure the yield of conversion of HA to ammonium (Figure 2C), 10 mM ^{15}N-urea was added just prior to measurement of NMR spectra, as an internal standard for peak integration. Thus, the values on the y-axis of Figure 2C are the peak area at 21 ppm divided by peak area at 77 ppm (for ^{15}N-urea). Each HA reduction reaction in Figure 2C contained the [HA] indicated on the x-axis, 2 μM Hb (either rice nsHb1 or SynHb), and 200 mM

sodium dithionite (DT). As demonstrated in Figure 2A, DT alone has no effect on the ^{15}N-NMR spectrum of ^{15}N-HA on these times scales.

Kinetics measurements. Kinetic traces for the reaction of HA with Hbs were measured using a Bio-Logic stopped flow SFM-400 reactor, a MOS-250 scanning spectrophotometer, and Biokine software. All reactions were carried out in 0.1 M phosphate buffer, pH 7.0, and room temperature. The reactor and all associated solutions were housed in the anaerobic chamber. Reactions were carried out under pseudo-first order conditions by mixing deoxyferrous Hbs with equal volumes of HA to achieve final concentrations of 50 μM, 100 μM, 150 μM, 200 μM, and 500 μM HA. Reaction time courses were monitored at 557 nm, and fitted to an exponential curve in Igor Pro to determine rate constants at each concentration (k_{obs}). These observed rate constants were plotted versus [HA] and fitted to a line to determine observed bimolecular rate constants (Figure 3B).

RESULTS

The reaction of HA with rice nsHb, SynHb, and Mb- Previous studies have demonstrated that deoxyferrous blood cell Hb reacts slowly with HA to catalyze a two-electron reduction to ammonium, along with the production of some N_2 and a small amount of N_2O (*18, 19*). To determine if a reaction also occurs with plant and cyanobacterial Hbs, the deoxyferrous forms of rice nsHb1, SynHb, and Mb were combined with HA under anaerobic conditions. Figure 1 shows absorbance spectra associated with these titrations. In each case the Hb (with concentrations in the 15 to 25 μM range) reacts stoichiometrically with HA, indicating that the K_D for binding must be

no greater than ~ 1 µM. Furthermore, in each case the reaction is complete at a molar ratio of 0.5 HA/Hb, indicating a two-electron reduction of HA. These results are consistent with those observed for blood cell Hb (*19*), leading to the hypothesis that the major product of the reaction is ammonium.

Ammonium is product of HA reduction- The progress of the reactions associated with Figure 1 was measured by monitoring heme absorbance, which is convenient at µM concentrations. One product of the reaction is ferric Hb; the other, hypothesized to be ammonium, is presumably also produced and present at µM concentrations. Ammonium is difficult to detect directly at these low levels, so the product concentration was increased to concentrations necessary for detection via ^{15}N-NMR spectroscopy with an acquisition time of 15 minutes (i.e. 20 mM ^{15}N). Because ammonium does not appear to bind the resulting ferric Hb (as indicated by the ferric endpoint absorbance spectra in Figure 1), it was reasoned that increasing product concentration might simply be a matter of adding more HA and reductant, and letting the Hb catalyze the formation of higher product concentrations.

To test this possibility, 50 mM ^{15}N-HA was mixed with 2 µM rice nsHb1, or 2 µM SynHb in the presence of 100 mM sodium dithionite (DT, serving as the reductant). As a control to ensure that DT alone does not reduce HA, the ^{15}N-NMR spectrum of ^{15}N-HA was measured in the absence and presence of 100 mM DT, and the chemical shift was found be the same (90 ppm) (Figure 2A, upper panel). However, when the mixture included 2 µM rice nsHb1 or SynHb, all of the ^{15}N is converted to a product with a chemical shift of 21 ppm, identical to that of ammonium (Figure 3A, lower panel).

Thus, in the presence of a reductant, rice nsHb1 and SynHb catalyzed the complete conversion of HA to ammonium.

The ^{15}N chemical shift is determined by the shielding of the nitrogen nucleus, and is generally directly proportional to its oxidation number. To verify the specificity of product formation, we also acquired ^{15}N-NMR spectra over a large chemical shift range, including the locations of peaks for nitrogen compounds with more positive oxidation numbers than HA and ammonium (Figure 2B). No such peaks were observed, suggesting that ammonium is the principal soluble product of HA reduction by these Hbs. To test for the presence of gaseous products, GCMS was used to examine the headspace above the reaction. A small amount of N_2 could be detected, but accounted for less than 1% of the total product, (data not shown).

Quantification of ammonium production from HA- A standard curve for the ^{15}N-NMR peak area was used to determine the yield of ammonium produced from HA by rice nsHb1 and SynHb (Figure 2C). The results for rice nsHb1 and SynHb were identical, with each Hb converting HA to ammonium with a yield of ~80%. In all samples, NMR detected no other soluble products, and only trace amounts of N_2 were detectable by GCMS.

The reverse reaction, and the reaction of HA with ferric Hbs were also measured. Addition of ammonium to ferric Hb did not affect the Hb absorption spectrum, and did not affect the ^{15}N-NMR signal of ^{15}N-ammonium. HA was also equally unreactive with ferric Hb as measured spectrally, or as the effect of ferric Hb on the ^{15}N-HA spectrum. Thus, no reverse reaction, or reaction with ferric Hb, is detectable.

Kinetics of ammonium production from HA- Time courses for the reactions of HA and deoxyferrous rice nsHb1, SynHb, myoglobin, neuroglobin, and cytoglobin were measured in a stopped flow reactor housed in the anaerobic chamber. Figure 3A shows a comparison of time courses for each Hb at 150 µM [HA], monitoring the oxidation of the deoxyferrous Hb. The reactions with rice nsHb1 and SynHb are nearly complete in two seconds, while those of Mb, Ngb, and Cgb are no more than 10% complete over this period of time. Observed bimolecular rate constants for reactions with rice nsHb1, SynHb, and Mb were measured from the slopes of the plots of concentration dependence of the reaction (Figure 3B). Rice nsHb1 and SynHb have observed bimolecular rate constants for HA reduction that are two orders of magnitude faster than Mb, with values of 25 $mM^{-1}s^{-1}$ and 28 $mM^{-1}s^{-1}$, respectively, compared to 0.25 $mM^{-1}s^{-1}$.

Over the range of [HA] shown in Figure 3B, k_{obs} increases linearly with [HA]. However, at higher [HA] (> 500µM) some deviation from linearity is observed (data not shown) that is consistent with previous reports of the reaction with blood cell Hb (*18, 19*). In addition to the reaction with the deoxyferrous forms of each Hb in Figure 3, oxy, CO, and ferric forms of each were reacted with 150 µM HA, but no spectral changes were detected for any of these derivatives.

DISCUSSION

The results presented in this study demonstrate that deoxyferrous rice nsHb1 and SynHb are capable of reducing HA to ammonium at rates much faster than other Hbs. In comparison to the fastest animal Hbs tested, myoglobin (0.25 $mM^{-1}s^{-1}$), the observed bimolecular rate constants for rice nsHb1 (25 $mM^{-1}s^{-1}$) and SynHb (28 $mM^{-1}s^{-1}$) are at

least 100-times faster. We have recently reported that deoxyferrous rice nsHb1 and SynHb are also particularly effective at reducing nitrite to NO (*17*). Thus, rice nsHb1 and SynHb are adept at catalyzing two reactions involved in the conversion of nitrite to ammonium.

Other enzymes that will reduce nitrite to ammonium are the siroheme nitrite reductases (NiR) in plants and cyanobacteria (*22, 23*), and the bacterial cytochrome c nitrite reductases (ccNiR)(*24*). NiR participates in the second step of assimilatory nitrate utilization, reducing nitrite to ammonium principally for amino acid production. NiR uses a [4Fe:4S] cluster and a siroheme prosthetic group to carry out the six electron reduction presumably via sequential one electron reductions and the formation of enzyme bound NO and HA intermediates, though these molecules are not normally released from the enzyme (*25, 26*). However, when reductant is limited these enzyme-bound intermediates may be released (*27*). NiR also reacts directly with HA (*28*), albeit with lower activity (*23, 27*).

ccNiR is responsible for dissimilatory nitrite ammonification in support of anaerobic respiration in many Gram-negative bacteria. It exists in the periplasmic space as a homodimer of 70 kD subunits, each containing five heme groups. Four of the hemes are *bis*-histidine hexacoordinated, and the other is pentacoordinate with a lysine side chain binding one axial position of the heme iron (*29*). Like NiR, ccNiR does not normally release NO or HA, but will reduce exogenous HA with lower activity than nitrite (*30, 31*).

Hbs and nitrogen metabolism in plants and cyanobacteria- Previous studies pertaining to the functions of plant and cyanobacterial Hbs describe the increased expression of Hb in response to hypoxia, nitrate, and nitrite (*12*, *13*), their effects on NO concentrations (*32*-*35*), and the toxicity of nitrate and nitric oxide to cyanobacteria lacking a wild type Hb (*36*). These studies, taken together, have been interpreted as supporting a role for nsHbs as NO scavengers, which use the NOD mechanism to oxidize NO and regenerate NAD^+ in support of anaerobic respiration (*35*, *37*). However, plant and cyanobacterial Hbs do not catalyze the NOD reaction any better than other Hbs for which it is not the primary function (*15*), so there is no experimental evidence distinctively in support of this role. Additionally, under extreme hypoxic conditions, the NOD reaction cannot proceed due to the lack of oxygen.

Here, and in one previous publication (*17*), we have demonstrated that plant nsHbs and SynHb reduce nitrite and HA at rates much faster than other Hbs under anaerobic conditions. There are three reasons why plants and cyanobacteria might benefit from nitrite and HA reduction by their Hbs during hypoxia: 1) To assimilate nitrogen in support of continued amino acid synthesis in an assimilatory manner, 2) to remove the toxic metabolites nitrite and NO (and possibly HA) by reducing them to ammonium, and 3) to serve as an electron sink in support of anaerobic metabolism by coupling respiratory and/or glycolytic electrons to ammonium production. It is possible that nsHbs support any or all of these roles. Furthermore, all three functions would likely cause the aforementioned phenotypes that have previously been attributed solely

to the NOD reaction, and could be linked to the observed nitrite-driven ATP synthesis in plant roots (*37, 38*).

It is possible that nsHbs could carry out the NOD reaction when oxygen is present, and catalyze reductive nitrogen chemistry in its absence. Data in support of this possibility include the fact that, while the rate of NOD activity for nsHb and SynHb is no faster than other Hbs, it is probably suitable for NO scavenging (~ 100 s^{-1} (*15*)). In addition, HA and nitrite reduction rates are ~ 0 when nsHb1 and SynHb are oxygenated. Thus, they are suited exclusively for one activity or the other depending on the level of oxygenation. In this way, oxygen itself could serve as a switch between respiratory (or glycolytic NADH) electrons being delivered to it or to nsHbs.

What is the mechanism of HA reduction by nsHbs? The experiments presented here do not provide a mechanism for HA reduction by Hbs. They only demonstrate that the reaction occurs, and that ammonium is the major product. Thus, we cannot describe the rate law and can only present observed rate constants. However, the simplest reaction fitting our stoichiometry is:

$$2Hb^{2+} + NH_2OH + 2H^+ \longrightarrow 2Hb^{3+} + NH_4^+ + OH^- \quad (2)$$

The spectra associated with the reaction (Figure 1) show no intermediates, suggesting that reduction of HA and release of ammonium are very rapid compared to binding, or that the reaction occurs in the outer sphere, with the reactants never binding the heme

iron (such as the reaction between Hb and DT (*39*)). On the other hand, the reaction is inhibited by oxygen and CO, suggesting an inner-sphere mechanism.

An important question concerning this reaction is how Hb^{2+} delivers two electrons to a single molecule of HA. This could happen either through a geminate or a dissociative mechanism. In the geminate mechanism, the two electrons are delivered to HA while it is bound to the same Hb molecule. This would require the addition of an electron to the HA-Hb^{2+} complex followed by dissociation of ammonium. The dissociative mechanism would have a partially reduced intermediate dissociate from Hb^{3+} and find another Hb^{2+} to provide the second electron. The fact that no intermediates or products other than ammonium have been observed, and that there are no known stable products resulting from the one-electron reduction of HA suggests that the reaction proceeds via the geminate reduction mechanism.

Further consideration of a geminate two-electron reduction by Hb raises the question of how an individual Hb^{2+} delivers two electrons to HA. In the presence of excess exogenous reductant (as in the catalytic reactions with DT in Figure 2) one could suppose that DT rapidly reduces the HA-Hb^{2+} complex. However, this cannot explain how the reaction proceeds with only Hb^{2+} (in the absence of DT, as in Figures 1 and 3). In these reactions, where all the electrons must come from Hb^{2+}, there must be rapid transfer of electrons from free Hb^{2+} to HA-Hb^{2+} to complete the reaction.

Such inter-Hb electron transfer has been directly measured for horse-heart myoglobin, with a rate constant of 3,000 $M^{-1}s^{-1}$ (*40*). At the concentration where we measured the kinetics of HA reduction by myoglobin (~20 μM Mb), this would predict a

rate of electron transfer between myoglobin molecules of 0.06 s^{-1}. Furthermore, it predicts that at higher [HA] concentrations the reaction should become limited by the rate of electron transfer, reaching (for myoglobin) an asymptote near 0.06 s^{-1}. Measurement of the observed rate constant for [HA] above 500 µM shows a deviation from linearity, but no asymptote near 0.06 s^{-1} is observed (k_{obs} for 20 mM Mb and 2.5 mM [HA] = 0.43 s^{-1}). This suggests that inter-molecular electron transfer is not a limiting factor or that the presence of HA somehow facilitates electron transfer between Hbs.

Potential roles of Hb hexacoordination in HA reduction- Rice nsHb1 and SynHb are hexacoordinate Hbs (41), meaning that their heme irons are coordinated by six ligands in the ferric and ferrous oxidation states. The sources of coordination are the four equatorial pyrrole nitrogens of the heme porphyrin and two axial histidine side chains. One of the histidine side chains (the "distal" histidine) can dissociat from the heme iron to allow binding of exogenous ligands like oxygen, CO, NO, and (possibly) nitrite and HA. Just being hexacoordinate does not mean that a Hb will rapidly reduce nitrite or HA, as neuroglobin and cytoglobin are both hexacoordinate and relatively slow at these reactions. In fact, removing the distal histidine from neuroglobin by mutation greatly increases the rate of nitrite reduction (42).

There are three features of hexacoordinate Hbs that could contribute to catalytic HA reduction. First is the fact that heme hexacoordination increases the rate of electron transfer and heme reduction by lowering the activation energy associated with the change in oxidation state (*39*). This is because the heme iron, with histidines bound in

both axial positions, remains low spin in both the ferrous and ferric oxidation states. It is probably no coincidence that four of the five hemes in ccNiR are *bis*-histidine hexacoordinated (29, 43). If electron transfer to re-reduce the Hb is rate limiting, hexacoordination could increase the limit compared to pentacoordinate Hbs such as Mb.

Second, distal histidine coordination of the heme iron could provide energy for rapidly displacing the positively charged ammonium ion formed from HA reduction. The partial positive charge on its side chain could also serve to attract negatively charged molecules like nitrite, while helping to displace ammonium through charge repulsion. Third, hexacoordination could serve to prevent HA from reacting with the ferric Hb. HA has been shown to react with ferric siroheme in NiR to form NO (*26*). Coordination of the distal histidine in hexacoordinate Hbs is generally much stronger in the ferric oxidation state than in the ferrous (*21*), and could serve as a mechanism to block any reaction with the ferric Hb and ensure that nitrogen metabolism continues in the reductive direction.

REFERENCES

1. Fukao, T., and Bailey-Serres, J. (2004) *Trends Plant Sci*. **9**, 449-456.

2. Singh, N. T., Vig, A. C., and Singh, R. (1985) *Fert Res*. **6**, 111-120.

3. Botrel, A., and Kaiser, W. M. (1997) *Planta*. **201**, 496-501.

4. Ferrari, T. E., and Varner, J. E. (1971) *Plant Physiol*. **47**, 790-794.

5. Igamberdiev, A. U., and Hill, R. D. (2004) *J. Exp. Bot.* **55**, 2473-2482.

6. Rockel, P., Strube, F., Rockel, A., Wildt, J., and Kaiser, W. M. (2002) *Journal of Experimental Botany*. **53**, 103-110.

7. Yamasaki, H., and Sakihama, Y. (2000) *Febs Letters*. **468**, 89-92.

8. Gupta, K. J., Fernie, A. R., Kaiser, W. M., and van Dongen, J. T. (2011) *Trends Plant Sci.*, in press.

9. Stohr, C., and Stremlau, S. (2006) *Journal of Experimental Botany*. **57**, 463-470.

10. Stohr, C., and Ullrich, W. R. (2002) *Journal of Experimental Botany*. **53**, 2293-2303.

11. Smagghe, B. J., Hoy, J. A., Percifield, R., Kundu, S., Hargrove, M. S., Sarath, G., Hilbert, J. L., Watts, R. A., Dennis, E. S., Peacock, W. J., Dewilde, S., Moens, L., Blouin, G. C., Olson, J. S., and Appleby, C. A. (2009) *Biopolymers*. **91**, 1083-1096.

12. Hunt, P. W., Klok, E. J., Trevaskis, B., Watts, R. A., Ellis, M. H., Peacock, W. J., and Dennis, E. S. (2002) *Proc Natl Acad Sci U S A*. **99**, 17197-17202.

13. Ohwaki, Y., Kawagishi-Kobayashi, M., Wakasa, K., Fujihara, S., and Yoneyama, T. (2005) *Plant Cell Physiol*. **46**, 324-331.

14. Eich, R. F., Li, T., Lemon, D. D., Doherty, D. H., Curry, S. R., Aitken, J. F., Mathews, A. J., Johnson, K. A., Smith, R. D., Phillips, G. N., Jr., and Olson, J. S. (1996) *Biochemistry*. **35**, 6976-6983.

15. Smagghe, B. J., Trent, J. T., 3rd, and Hargrove, M. S. (2008) *PLoS One*. **3**, e2039.

16. Igamberdiev, A. U., Bykova, N. V., and Hill, R. D. (2006) *Planta*. **223**, 1033-1040.

17. Sturms, R., Dispirito, A. A., and Hargrove, M. S. (2011) *Biochemistry*. **50**, 3873-3878.

18. Colter, J. S., and Quastel, J. H. (1950) *Arch Biochem*. **27**, 368-389.
19. Bazylinski, D. A., Arkowitz, R. A., and Hollocher, T. C. (1987) *Arch Biochem Biophys*. **259**, 520-526.

20. Doyle, M. P., LePoire, D. M., and Pickering, R. A. (1981) *J Biol Chem*. **256**, 12399-12404.

21. Halder, P., Trent, J. T., III., and Hargrove, M. S. (2007) *PROTEINS: Structure, Function, and Bioinformatics*. **66**, 172-182.

22. Guerrero, M., Vega, J., and Losada, M. (1981) *Ann. Rev. Plant Physiol*. **32**, 169-204.

23. Hewitt, E. J. (1975) *Ann. Rev. Plant Physiol.* **26**, 73-100.

24. Burlat, B., Gwyer, J. D., Poock, S., Clarke, T., Cole, J. A., Hemmings, A. M., Cheesman, M. R., Butt, J. N., and Richardson, D. J. (2005) *Biochem Soc Trans*. **33**, 137-140.

25. Kuznetsova, S., Knaff, D. B., Hirasawa, M., Lagoutte, B., and Setif, P. (2004) *Biochemistry*. **43**, 510-517.

26. Kuznetsova, S., Knaff, D. B., Hirasawa, M., Setif, P., and Mattioli, T. A. (2004) *Biochemistry*. **43**, 10765-10774.

27. Vega, J. M., and Kamin, H. (1977) *J Biol Chem*. **252**, 896-909.

28. Hirasawa, M., Tripathy, J. N., Sommer, F., Somasundaram, R., Chung, J. S., Nestander, M., Kruthiventi, M., Zabet-Moghaddam, M., Johnson, M. K., Merchant, S. S., Allen, J. P., and Knaff, D. B. (2010) *Photosynth Res*. **103**, 67-77.

29. Einsle, O., Messerschmidt, A., Stach, P., Bourenkov, G. P., Bartunik, H. D., Huber, R., and Kroneck, P. M. (1999) *Nature*. **400**, 476-480.

30. Kajie, S., and Anraku, Y. (1986) *Eur J Biochem*. **154**, 457-463.

31. Silveira, C. M., Besson, S., Moura, I., Moura, J. J., and Almeida, M. G. (2010) *Bioinorganic Chemistry and Applications*.

32. Dordas, C., Hasinoff, B. B., Igamberdiev, A. U., Manac'h, N., Rivoal, J., and Hill, R. D. (2003) *Plant J*. **35**, 763-770.

33. Perazzolli, M., Dominici, P., Romero-Puertas, M. C., Zago, E., Zeier, J., Sonoda, M., Lamb, C., and Delledonne, M. (2004) *Plant Cell*. **16**, 2785-2794.

34. Seregelyes, C., Igamberdiev, A. U., Maassen, A., Hennig, J., Dudits, D., and Hill, R. D. (2004) *FEBS Lett*. **571**, 61-66.

35. Igamberdiev, A. U., Seregelyes, C., Manac'h, N., and Hill, R. D. (2004) *Planta*. **219**, 95-102.

36. Scott, N. L., Xu, Y., Shen, G., Vuletich, D. A., Falzone, C. J., Li, Z., Ludwig, M., Pond, M. P., Preimesberger, M. R., Bryant, D. A., and Lecomte, J. T. (2010) *Biochemistry*. **49**, 7000-7011.

37. Stoimenova, M., Igamberdiev, A. U., Gupta, K. J., and Hill, R. D. (2007) *Planta*. **226**, 465-474.

38. Gupta, K. J., Stoimenova, M., and Kaiser, W. M. (2005) *J Exp Bot*. **56**, 2601-2609.

39. Weiland, T., Kundu, S., Trent, J., Hoy, J., and Hargrove, M. (2004) *J. Am. Chem. Soc.* **126**, 11930-11935.

40. Brunel, C., Bondon, A., and Simonneaux, G. (1992) *Biochim Biophys Acta*. **1101**, 73-78.

41. Kakar, S., Hoffman, F. G., Storz, J. F., Fabian, M., and Hargrove, M. S. (2010) *Biophys Chem*. **152**, 1-14.

42. Tiso, M., Tejero, J., Basu, S., Azarov, I., Wang, X., Simplaceanu, V., Frizzell, S., Jayaraman, T., Geary, L., Shapiro, C., Ho, C., Shiva, S., Kim-Shapiro, D. B., and Gladwin, M. T. (2011) *J Biol Chem*.

43. Bamford, V. A., Angove, H. C., Seward, H. E., Thomson, A. J., Cole, J. A., Butt, J. N., Hemmings, A. M., and Richardson, D. J. (2002) *Biochemistry*. **41**, 2921-2931.

FIGURE LEGENDS

FIGURE 1. Titrations of deoxyferrous Hbs with HA. A) rice nsHb1 (16 µM). B) SynHb (16 µM). C) Mb (24 µM). All titrations exhibit sharp deviations from linearity at [HA]/[Hb] = 0.5, at which point the titration reaches 100 percent completion. This shows that the reactions proceed by a mechanism in which two Hbs are oxidized by one HA. In each case the spectral transition is from deoxyferrous Hb^{2+} to ferric Hb^{3+}.

FIGURE 2. A) ^{15}N-NMR spectra of $^{15}NH_2OH$ in the presence and absence of sodium dithionite (DT) (upper panel), the product of the reaction of 50 mM $^{15}NH_2OH$ with ~ 2µM nsHb1 or SynHb in the presence of 100 mM DT (middle panel), and $^{15}NH_4^+$ as a control (lower panel). B) An expanded ^{15}N-NMR spectrum of the reaction of $^{15}NH_2OH$ with rice nsHb1 (or SynHb) demonstrating that $^{15}NH_4^+$ is the only detectable soluble product. C) A standard curve of $^{15}NH_4^+$ peak area compared to the $^{15}NH_4^+$ peaks generated by the reaction of $^{15}NH_2OH$ with ~2 µM rice nsHb1 (closed squares) and SynHb (open squares) in the presence of 100 mM DT. These results demonstrate that the reaction is both catalytic and specific, with at least 80 % of starting $^{15}NH_2OH$ converted to $^{15}NH_4^+$.

FIGURE 3. A) Time courses for the reaction of deoxyferrous rice nsHb1, SynHb, Mb, Cgb, and Ngb with 150 µM HA, as measured by the oxidation of the Hb (as in Figure 1). B) The dependence of the reaction rate constant (k_{obs}) on [HA] for rice nsHb1, SynHb, and Mb, demonstrating that reaction rates for rice nsHb1 and SynHb are two orders of magnitude

faster than Mb, having pseudo first order rates of 25 $mM^{-1}s^{-1}$ and 28 $mM^{-1}s^{-1}$, respectively, compared to 0.25 $\mu M^{-1}s^{-1}$.

Figure 1.

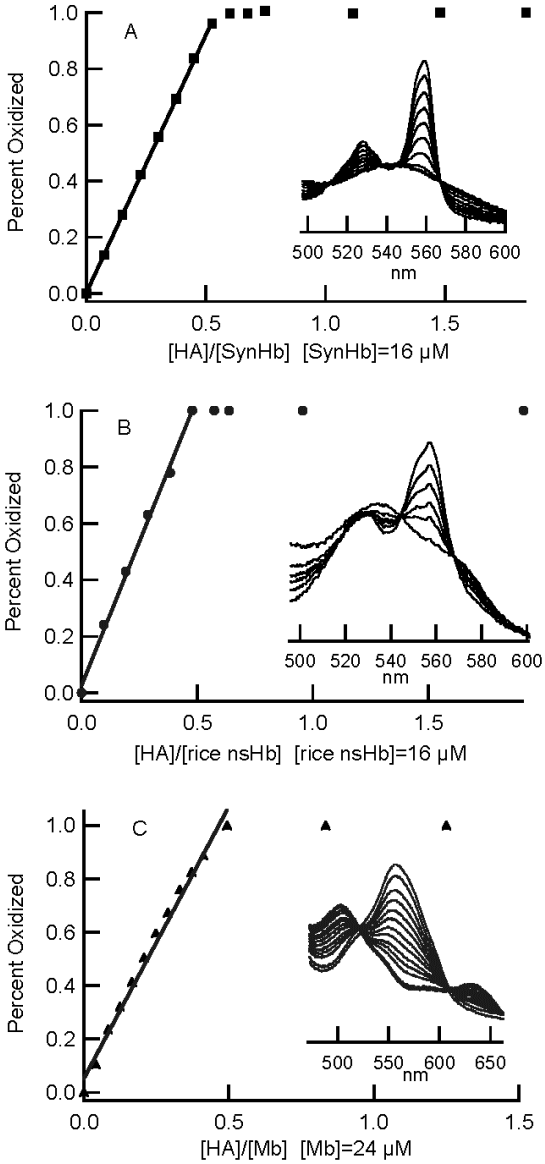

Figure 2.

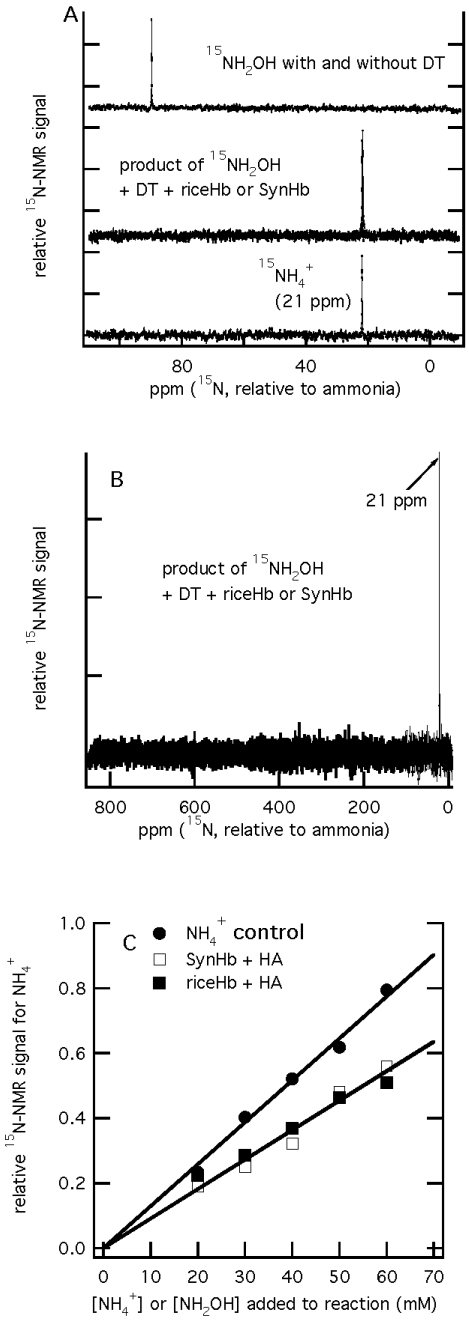
A
$^{15}NH_2OH$ with and without DT
product of $^{15}NH_2OH$
+ DT + riceHb or SynHb
$^{15}NH_4^+$
(21 ppm)
relative ^{15}N-NMR signal
80
40
0
ppm (^{15}N, relative to ammonia)
B
21 ppm
product of $^{15}NH_2OH$
+ DT + riceHb or SynHb
relative ^{15}N-NMR signal
800
600
400
200
0
ppm (^{15}N, relative to ammonia)
C
NH_4^+ control
SynHb + HA
riceHb + HA
relative ^{15}N-NMR signal for NH_4^+
1.0
0.8
0.6
0.4
0.2
0.0
0
10
20
30
40
50
60
70
[NH_4^+] or [NH_2OH] added to reaction (mM)

Figure 3.

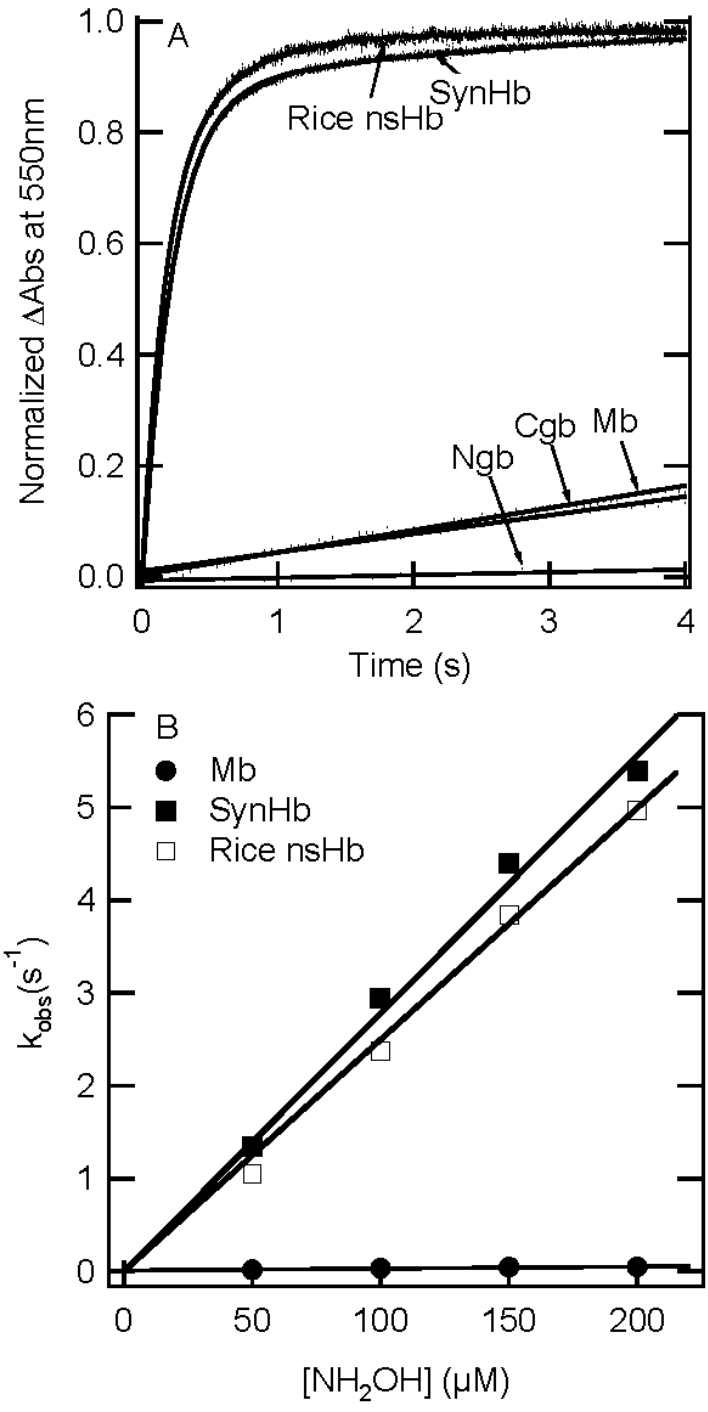
A
Normalized ΔAbs at 550nm
1.0
0.8
0.6
0.4
0.2
0.0
0
1
2
3
4
Time (s)
SynHb
Rice nsHb
Cgb
Mb
Ngb
B
Mb
SynHb
Rice nsHb
$k_{obs}(s^{-1})$
6
5
4
3
2
1
0
0
50
100
150
200
$[NH_2OH]$ (μM)

CHAPTER 6.

ELECTRON SELF EXCHANGE RATES IN MYOGLOBIN AND RICE HEMOGLOBIN MEASURED USING DEUTEROHEME SUBSTITUTED GLOBINS CORRELATE WITH RATES OF NITRITE AND HYDROXYLAMINE REDUCTION

A manuscript to be submitted to *Biochemistry*

Ryan Sturms, Alan DiSpirito, Mark Hargrove

Introduction

Globin proteins have been shown to carry out the one electron reduction of nitrite to nitric oxide and the two electron reduction of hydroxylamine to ammonium. Of the published rates for these reactions, the class one non-symbiotic hemoglobins carry out both reactions at rates much faster than any of the wild type mammalian globins studied [(1-5)]. In our study of the reduction of hydroxylamine by deoxy hemoglobin, we postulate two mechanisms by which hemoglobin could reduce hydroxylamine without forming any detectable intermediate. The first would be a dissociative mechanism, in which hydroxylamine is reduced by one electron from one ferrous hemoglobin, resulting in ferric hemoglobin and a one electron reduced intermediate followed by dissociation of this intermediate from the protein and a subsequent second one electron reduction from another ferrous hemoglobin. The second mechanism is an associative mechanism, in which hydroxylamine associates with and is reduced by one electron by ferrous hemoglobin followed by an intermolecular electron transfer event between the resulting ferric hemoglobin that is associated with the hydroxylamine intermediate and a second

ferrous hemoglobin. This transfer would provide the two electrons necessary to complete the reaction and would not produce a free intermediate [2]. Because there are no known, stable, one electron reduced intermediates of hydroxylamine, we hypothesize that the second mechanism is more likely. This study aims to address the question of whether differences in the rates of electron self-exchange between rice non-symbiotic hemoglobin and myoglobin can account for the differences observed in the bimolecular rate of hydroxylamine reduction between them.

Electron self-exchange rates are typically measured using either ruthenium modified proteins [2], photo excitation or, in myoglobin, by the addition of a bulky ligand, trimethylphosphine [6], to the protein all of which introduce into the system, unwanted modifications. We introduce a new technique for measuring spectrophotometrically, the rate of electron self-exchange using proteins that are reconstituted using deuteroheme. This substitution of deuteroheme, in which the vinyl groups are not present, for protoheme results in minimal differences in redox potential [7] but provides approximately a ten nanometer blue shift in absorbance. This shift allows direct spectral monitoring of the exchange of electrons between unliganded, non-photo excited molecules.

Materials and Methods

Preparation of proteins

Rice nsHb1 was produced as previously described [8]. Horse heart myoglobin was obtained from Sigma and desalted using a G-25 column prior to use.

Deutero-heme containing myoglobin was prepared by generating apo-myoglobin through the method of lowering the pH to 2 using 0.1M hydrochloric acid and extracting the heme using ice cold methyl ethyl ketone. This was followed by dialysis into 0.1 M potassium phosphate buffer pH7. Deutero-heme was reincorporated by adding deutero-heme (Frontier Scientific) dissolved in 0.1M sodium hydroxide to the apo protein.

Deutero-heme containing rice nsHb1 was generated by adding a 2-fold excess of (neutral pH) deutero-heme to 100 µL of 2 mM hemoglobin. This was diluted 5:1 with 6 M guanidine chloride, and concentrated back to ~ 500 µl. this was run over G25 resin equilibrated in 6 M guanidine chloride, concentrated back to ~ 500 µL, followed by addition of another 2-fold excess of deutero-heme in 6 M guanidine chloride and incubated for 1 hour at 4 degrees C. The sample was then dialyzed into 0.1M phosphate pH 7 overnight at 4 degrees C. The dialyzed sample was centrifuged to remove precipitant and run over G25 resin equilibrated in 0.1 M phosphate pH 7. The final sample was concentrated and verified using a Cary 50 spectrophotometer.

Determination of extinction coefficients

Extinction coefficients for all deutero-heme containing proteins were determined by dissolving a known amount of deutero- hemin in 6M guanidine chloride. 1 crystal of sodium cyanide was added to this and the absorbance was measured at 424nm. Using $A=\text{Ɛ}cl$, Ɛ for cyanide bound free deutero-heme was determined. All free hemin concentration values were determined by weight. Holo protein was then diluted to 1 mL with 6M guanidine chloride to release the deutero-heme. This solution was treated with sodium cyanide, and the absorbance at 424 nm recorded. Using the Ɛ determined for

cyanide bound free deutero-heme, the concentration of deutero-heme contained in the sample was determined. This information was used to calculate Ɛ for incorporated deutero-heme by measuring the absorbance of the same amount of holo-protein diluted with 1 mL of phosphate buffer pH 7.

Mixing experiments.

Mixing experiments were performed in a sealed split chamber cell (Starna Cells). Equal concentrations, in heme, of ferrous proto-heme, prepared by reducing with an excess of dithionite and passing over a G25 column equilibrated with anaerobic buffer inside of an anaerobic chamber (Coy) and argon purged ferric deutero-heme containing proteins were placed in each of the chambers of the split cell inside of an anaerobic chamber (Coy). The cuvettes were sealed and brought out of the chamber to a Cary 50 Bio spectrophotometer and initial spectra were acquired. The cells were inverted and the contents of each chamber mixed. The reaction was followed at 30 second intervals using the scanning kinetics mode on the Cary 50. Kinetic traces were generated by following the decrease of the peak associated with ferrous proto-heme. Mixing experiments with rice nsHb1 in the stopped flow were carried out on a Bio-logic SFM-400 housed inside the anaerobic chamber. Similarly, equal concentrations, in heme, of each protein were mixed and reaction progress was followed at by monitoring the decrease in absorbance associated with the disappearance of ferrous proto-heme.

Concentration dependence

The concentration dependence of the reactions was determined by plotting the initial velocity, approximately the first 10 percent of the expected absorbance change, of

the reaction measured using the kinetics mode on a Cary 50 Bio spectrophotometer or a Bio-Logic SFM 400 stopped-flow reactor housed inside of an anaerobic chamber and fit to a line using Igor pro software, against the product of the concentrations of the reactants.

Results

Absorbance Spectra of Proto- and Deuteroheme-Containing Proteins

Absorbance spectra for ferric and ferrous forms of proto- and deuteroheme containing myoglobin, and rice nsHb1 proteins were collected. Figure 1 shows the extinction coefficient of these absorbance spectra plotted as a function of wavelength. The incorporation of the deuteroheme prosthetic group results in a blue shift of the absorbance spectra of approximately 10 nm for each protein. This results in a soret peak with a maximum value at 393 nm for ferric deutero-myoglobin, 401 nm for ferric deutero-rice nsHb1. The ferrous soret peaks are similarly shifted with peaks at 420 nm, 411 nm, for deutero-myoglobin, and deutero-rice nsHb1 respectively. These maxima, their associated extinction coefficients, and the maxima and extinction coefficients for the protoheme containing proteins are summarized in Table 1.

Exchange of electrons following mixing

By taking advantage of the differences in absorption maxima between the proto-ferrous proteins and the deutero-ferric proteins and a split, sealed cuvette, we were able to generate combined starting spectra that were the combination of 50 percent proto-ferrous protein and 50 percent deutero-ferric protein. These observed spectra for myoglobin and rice nsHb1, along with a theoretical spectrum for the same ratios of

proteins, generated by linear combinations of the individual component spectra from Figure 1 are shown in panels a and b of Figure 2.

Panels c and d of Figure 2 show the spectral changes associated with the mixing of the individual components. Of particular note is the first spectrum acquired after mixing for both myoglobin and rice nsHb1. In each case this was acquired thirty seconds after mixing. In the case of myoglobin, there is relatively little change in the absorbance spectrum. However, in the case of rice nsHb1 the change in absorbance during the first thirty seconds following mixing accounts for nearly half of the total absorbance change associated with this approach to equilibrium.

Panels e and f of Figure 2 show the observed and calculated final spectra for each set of proteins. This shows that upon completion of the reaction, the final mixture of proteins is composed of approximately 25 percent of each deutero-ferric, deutero-ferrous, proto-ferric, and proto-ferrous protein, with a small amount of excess oxidation likely due to imperfect seals on the cuvette.

Figure 3 addresses the question of whether there is a difference in the time scales of the self-exchange of electrons in myoglobin versus rice nsHb1 at a given concentration of protein. By plotting the absorbance at the wavelength associated with a maximum for the proto-ferrous protein versus time we observe a significant difference in the time to half completion for the two systems at 10 μM individual protein concentration. $T_{1/2}$ for the exchange of electrons in myoglobin is approximately 60 minutes while the $T_{1/2}$ for the exchange of electrons in rice nsHb1 is approximately 1 minute. Furthermore, the initial absorbance change in rice nsHb1 observed in Figure 2

was re-collected using a stopped-flow reactor. In addition to the $T_{1/2}$ for the exchange of electrons, we observe that both reactions follow a biphasic time course.

Concentration Dependence of Electron Self-Exchange

The dependence of the initial velocity of this exchange of electrons was measured by following the reaction at the absorbance maximum associated with proto-ferrous protein using the kinetics mode on a Cary 50 Bio spectrophotometer or in a Bio-Logic SFM-400 stopped-flow reactor. These results are shown in Figure 4 and demonstrate that there is a dependence on the rate of electron self-exchange in this system on total protein concentration. These data can be plotted versus the product of the concentrations of each individual reactant and fit to a line to extract a second order rate constant for the initial velocity of electron self-exchange measured using deuteroheme substituted proteins. These values are 75 $M^{-1}s^{-1}$ for myoglobin and 1.6 x 10^3 $M^{-1}s^{-1}$ for rice nsHb1.

Discussion

Using Deuteroheme Substituted Proteins as a Tool for Measuring Ground State, Unliganded Electron Self-Exchange in Heme Proteins

Other techniques that are commonly used to measure the rates of electron transfer and self-exchange in heme proteins typically include some kind of external factor in the measurement. A commonly used technique is to modify heme proteins like myoglobin using pentamineruthenium modified proteins [(9-11)] and then measure transfer from an excited donor to the modified protein. This modification and the subsequent measurements are accomplished using laser flash photolysis techniques which resulted

in myoglobin that is predominately modified at histidine residue 48[11]. However, other complications of this preparative technique arises from the fact that there are multiple histidine residues that can be modified non-selectively with each modification giving a different rate of electron transfer [11]. Furthermore, this technique relies on photo-excitation of a donor, resulting in a significant energy difference in the system [11]. This difference would set up an artificial driving force for the transfer that would not be present in a ground state system.

More recently, nuclear magnetic resonance spectroscopy has been used to measure rates of electron self-exchange in heme proteins, specifically myoglobin [6] and *Synechocystis* cyanoglobin [12]. In myoglobin, this technique requires the addition of the ligand trimethylphosphine to the solution because of the association and dissociation of a bound water molecule to the heme iron of myoglobin upon change in oxidation state and the significant reorganizational energy barrier that this creates [6, 9]. The rate of electron self-exchange measured in this system is 3.1×10^3 $M^{-1}s^{-1}$ which is significantly faster than the rate we measure for the unliganded protein but is likely influenced by the addition of the trimethylphosphine. The measurement for *Synechocystis* cyanoglobin does not require addition of this ligand due to the coordination of the heme iron by the distal histidine in both oxidation states [12]. The rate measured by NMR spectroscopy for this reaction is 1.4×10^3 $M^{-1}s^{-1}$ [12], which is on the same order of magnitude as the rate we measure for rice non-symbiotic hemoglobin. This is consistent then, with the rates of nitrite and hydroxylamine reduction by *Synechocystis* cyanoglobin being nearly the same as the rates observed for rice non-symbiotic hemoglobin [2, 3].

A goal of this study was to measure the electron self-exchange rates using proteins that are minimally modified, in the ground state and without introducing ligands into the system. To accomplish this, we use the spectroscopic properties and differences of hemin and deutero hemin incorporated into globin proteins. Upon reconstitution with deuteroheme, the absorbance spectra of both myoglobin and rice nsHb1 display a blue shift of approximately 10 nm in both oxidation states. This difference allows us to create a solution in which we can differentiate four species of a single protein through spectral deconvolution.

Differences in Electron Self-Exchange Rates Correlate with Rates of Hydroxylamine Reduction

In regards to the rates observed for the self-exchange reaction that we monitored for myoglobin, our rates are significantly slower than the rates observed by NMR analysis using the trimethylphosphine ligand [(6)], which may be due to the effects of the ligand. When the rates that we measure for myoglobin and rice nsHb1 are compared with each other, we see significant differences in both the $T_{1/2}$ of the reaction at ~10 micromolar individual protein concentration and in the second order rate constant that is extracted from a plot of initial velocity versus product of protein concentration. Based on previous reports [(9)], this difference would be expected between these two proteins given that myoglobin exists with a high spin heme iron in both oxidation states and rice nsHb1 exists with predominately low spin heme iron in both oxidation state [(13-16)]. This difference in electron self-exchange is thus correlated with the rate of hydroxylamine reduction by these proteins.

The observed second order rate constants for electron self-exchange cannot, however fully explain the rates of hydroxylamine reduction since they are approximately 4 and 15 fold slower than the rates of hydroxylamine reduction observed for myoglobin and rice nsHb1 respectively. This difference may be due to the hydroxylamine ligand providing some driving force for the transfer of electrons. Alternatively, the rates of electron self-exchange in these systems may only reflect the propensity of the respective proteins to serve as electron acceptors and that in a physiological setting an external reductase provides electrons which are used by hemoglobin to reduce hydroxylamine and intermolecular transfer of electrons between hemoglobins never occurs. To test this would require the identification of an external reductase and an observation method for the reaction other than following the oxidation of hemoglobin.

References

1. Petersen, M. G., Dewilde, S., and Fago, A. (2008) Reactions of ferrous neuroglobin and cytoglobin with nitrite under anaerobic conditions, *Journal of Inorganic Biochemistry 102*, 1777-1782.

2. Sturms, R., DiSpirito, A. A., Fulton, D. B., and Hargrove, M. S. (2011) Hydroxylamine reduction to ammonium by plant and cyanobacterial hemoglobins, *Biochemistry 50*, 10829-10835.

3. Sturms, R., DiSpirito, A. A., and Hargrove, M. S. (2011) Plant and cyanobacterial hemoglobins reduce nitrite to nitric oxide under anoxic conditions, *Biochemistry 50*, 3873-3878.

4. Tiso, M., Tejero, J., Basu, S., Azarov, I., Wang, X., Simplaceanu, V., Frizzell, S., Jayaraman, T., Geary, L., Shapiro, C., Ho, C., Shiva, S., Kim-Shapiro, D. B., and Gladwin, M. T. (2011) Human neuroglobin functions as a redox-regulated nitrite reductase, *The Journal of Biological Chemistry 286*, 18277-18289.

5. Tiso, M., Tejero, J., Kenney, C., Frizzell, S., and Gladwin, M. T. (2012) Nitrite reductase activity of nonsymbiotic hemoglobins from Arabidopsis thaliana, *Biochemistry 51*, 5285-5292.

6. Brunel, C., Bondon, A., and Simonneaux, G. (1992) Electron-transfer self-exchange kinetics of trimethylphosphine horse-heart myoglobin, *Biochimica et Biophysica Acta 1101*, 73-78.

7. Brunori, M., Saggese, U., Rotilio, G. C., Antonini, E., and Wyman, J. (1971) Redox equilibrium of sperm-whale myoglobin, Aplysia myoglobin, and Chironomus thummi hemoglobin, *Biochemistry 10*, 1604-1609.

8. Goodman, M. D., and Hargrove, M. S. (2001) Quaternary structure of rice nonsymbiotic hemoglobin, *The Journal of Biological Chemistry 276*, 6834-6839.

9. Crutchley, R. J., Ellis, W. R., and Gray, H. B. (1985) Long-distance electron transfer in pentaammineruthenium (histidine-48)-myoglobin. Reorganizational energetics of a high-spin heme, *Journal of the American Chemical Society 107*, 5002-5004.

10. Gray, H. B., and Winkler, J. R. (1996) Electron Transfer in Proteins, *Annual Review of Biochemistry 65*, 537-561.

11. Winkler, J. R., and Gray, H. B. (1992) Electron transfer in ruthenium-modified proteins, *Chemical Reviews 92*, 369-379.

12. Preimesberger, M. R., Pond, M. P., Majumdar, A., and Lecomte, J. T. (2012) Electron self-exchange and self-amplified posttranslational modification in the hemoglobins from Synechocystis sp. PCC 6803 and Synechococcus sp. PCC 7002, *Journal of biological inorganic chemistry : JBIC : a publication of the Society of Biological Inorganic Chemistry 17*, 599-609.

13. Arredondo-Peter, R., Hargrove, M. S., Sarath, G., Moran, J. F., Lohrman, J., Olson, J. S., and Klucas, R. V. (1997) Rice hemoglobins. Gene cloning, analysis, and O2-binding kinetics of a recombinant protein synthesized in Escherichia coli, *Plant Physiology 115*, 1259-1266.

14. Della Longa, S., Pin, S., Cortes, R., Soldatov, A. V., and Alpert, B. (1998) Fe-heme conformations in ferric myoglobin, *Biophysical Journal 75*, 3154-3162.

15. Roder, H., Berendzen, J., Bowne, S. F., Frauenfelder, H., Sauke, T. B., Shyamsunder, E., and Weissman, M. B. (1984) Comparison of the magnetic properties of deoxy- and photodissociated myoglobin, *Proceedings of the National Academy of Sciences of the United States of America 81*, 2359-2363.

16. Sturms, R., Kakar, S., Trent, J., 3rd, and Hargrove, M. S. (2010) Trema and parasponia hemoglobins reveal convergent evolution of oxygen transport in plants, *Biochemistry 49*, 4085-4093.

Tables.

Table 1. Soret Absorbance maxima and extinction coefficients for proto-and deuteroheme containing proteins.

Protein	Soret Absorbance Maximum (nm)	Ɛ ($mM^{-1}cm^{-1}$)
Proto-myoglobin ferric	408	179
Proto-myoglobin ferrous	435	121
Proto-rice nsHb1 ferric	410	117
Proto-rice nsHb1 ferrous	424	157
Deutero-myoglobin ferric	393	99
Deutero-myoglobin ferrous	421	61
Deutero-rice nsHb1 ferric	401	70
Deutero-rice nsHb1 ferrous	411	80

Figure Legends.

Figure 1. Component Spectra of Proto- and Deuteroheme Myoglobin (a) and Rice nsHb1 (b)

Figure 2. a, b) observed (solid) and theoretical (dotted) starting spectra for mixtures of 50 percent proto-ferrous and 50 percent deutero-ferric Myoglobin and Rice nsHb1 respectively. c, d) spectral transitions upon mixing. e, f) observed (solid) and theoretical (dotted) final spectra following mixing for Myoglobin and Rice nsHb1.

Figure 3. Time course for the exchange of electrons in protoheme and deuteroheme containing Myoglobin and Rice nsHb1.

Figure 4. Concentration dependence of initial velocity of electron self-exchange in protoheme and deuteroheme containing Myoglobin and Rice nsHb1.

Figure 1.

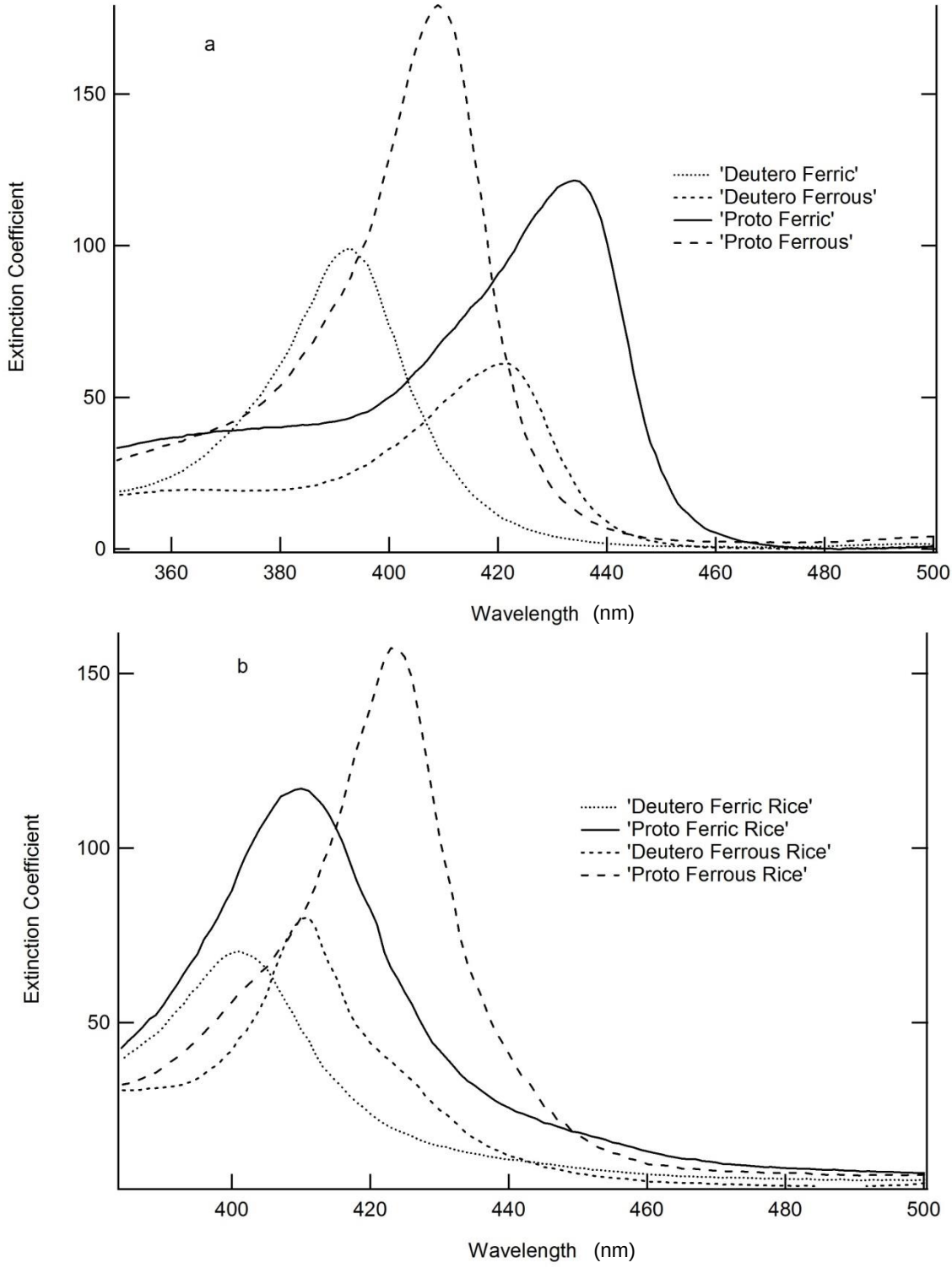
a
Extinction Coefficient
150
100
50
0
360
380
400
420
440
460
480
500
Wavelength (nm)
'Deutero Ferric'
'Deutero Ferrous'
'Proto Ferric'
'Proto Ferrous'
b
Extinction Coefficient
150
100
50
400
420
440
460
480
500
Wavelength (nm)
'Deutero Ferric Rice'
'Proto Ferric Rice'
'Deutero Ferrous Rice'
'Proto Ferrous Rice'

Figure 2.

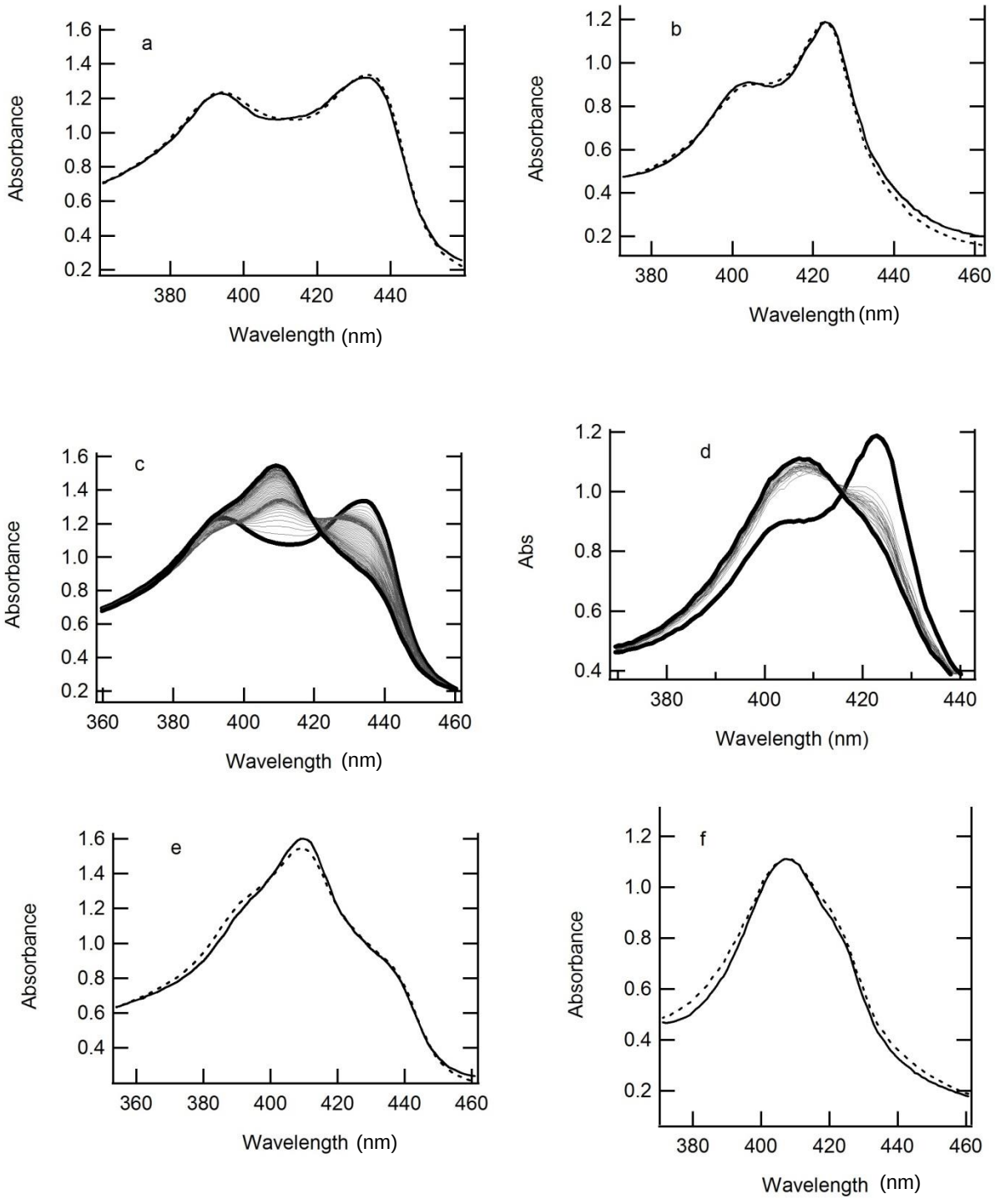
a
Absorbance
Wavelength (nm)
b
Absorbance
Wavelength (nm)
c
Absorbance
Wavelength (nm)
d
Abs
Wavelength (nm)
e
Absorbance
Wavelength (nm)
f
Absorbance
Wavelength (nm)

Figure 3.

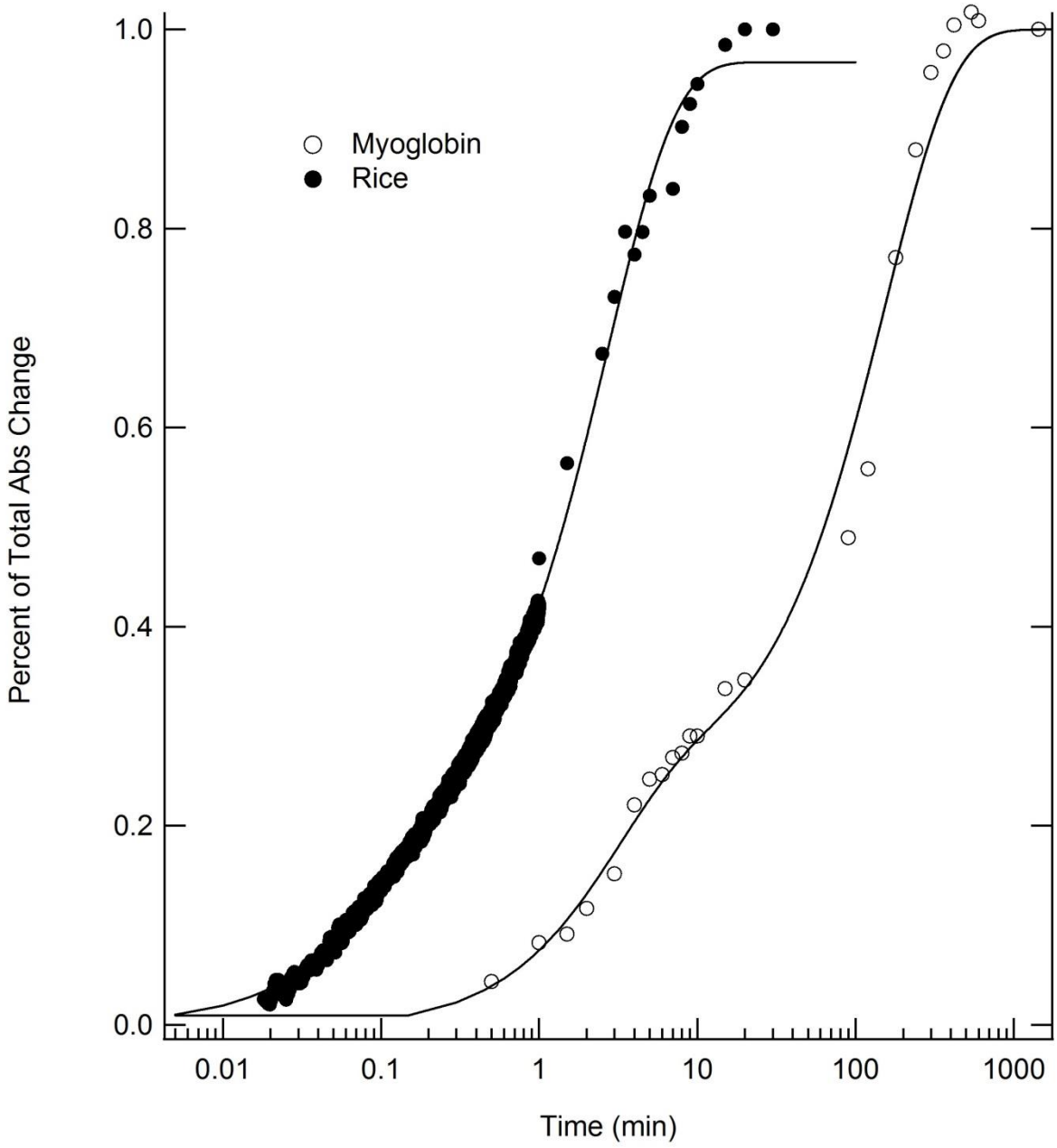
Myoglobin
Rice
Percent of Total Abs Change
Time (min)
0.0
0.2
0.4
0.6
0.8
1.0
0.01
0.1
1
10
100
1000

Figure 4.

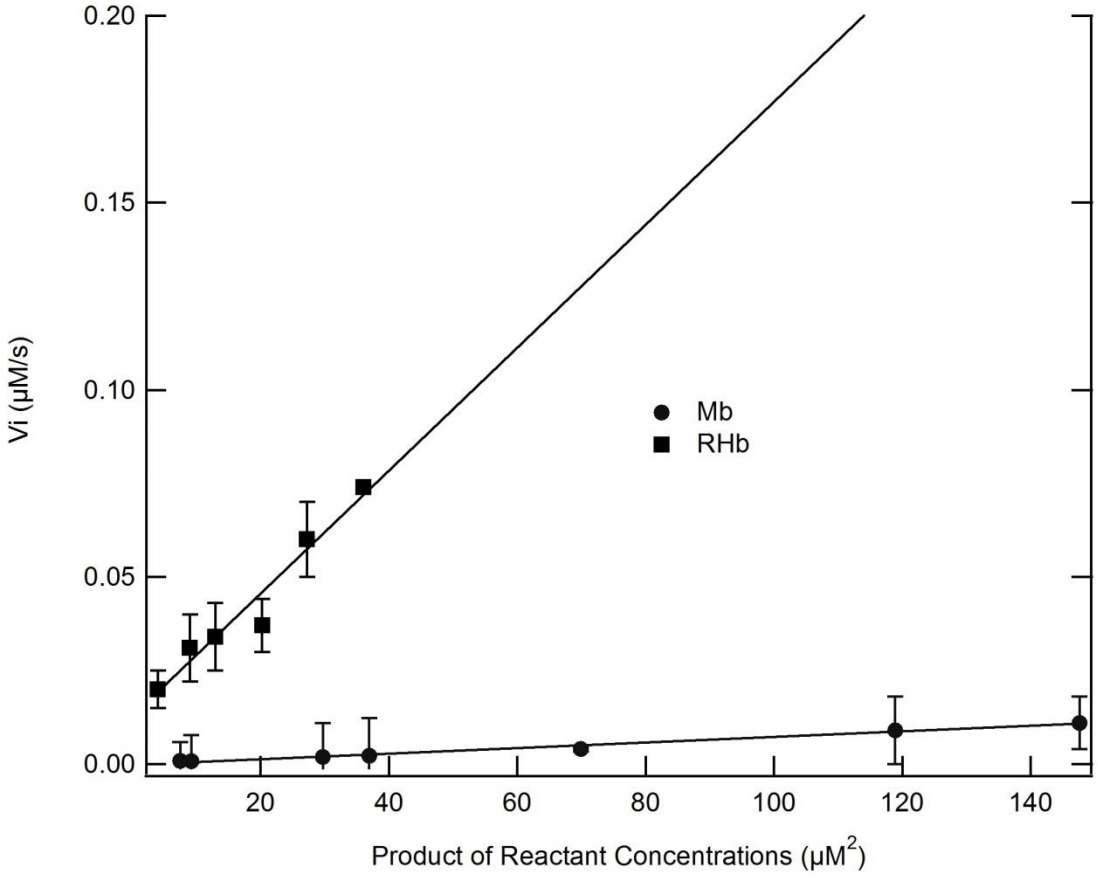
0.20
0.15
0.10
0.05
0.00
Vi (μM/s)
Mb
RHb
20
40
60
80
100
120
140
Product of Reactant Concentrations (μM^2)

CHAPTER 7.

A ROLE FOR FRACTIONAL HEXACOORDINATION AND DIMERIZATION IN PLANT NON-SYMBIOTIC HEMOGLOBINS

Ryan Sturms, Mark Hargrove

A manuscript to be submitted to *Biochemistry*

Abstract

Classical oxygen transport hemoglobins exist with five coordinate bonds to the heme iron. Class 1 non-symbiotic hemoglobins in plants have been observed to exist as a population with a fraction of that population having a sixth coordinate bond from a distal histidine residue at the seventh position on the E-helix. Furthermore, rice non-symbiotic hemoglobin has been shown to exist as a transient dimer with oxidation and ligand state dependent equilibrium dissociation constants. The possible physiological implications of these structural elements of non-symbiotic hemoglobin are explored in this work. The three dimensional crystal structures of bacterial dissimilatory nitrite reductases have revealed that these enzymes contain multiple heme prosthetic groups that are arranged in such a manner as to have one or more with two axial histidine ligands resulting in six coordinate bonds and one heme with an open binding site for nitrogenous ligands. Following binding of the nitrogenous ligand to the five-coordinate heme, intermolecular electron transfer occurs from the six-coordinate heme(s) to the reaction site. This results in the reduction of the bound nitrogenous ligand in a dissimilatory manner. The fractional hexacoordination observed in rice non-symbiotic hemoglobin could functionally mimic this structural feature of dissimilatory nitrite

reductases and provide a mechanism for non-symbiotic hemoglobin to function in such a capacity in plants. Through mutational studies, we have evaluated the role that fractional hexacoordination in rice non-symbiotic hemoglobin plays in the rates of nitrite and hydroxylamine reduction. Additionally, we have tested the impact of transient dimer formation on these same reactions. We observe that either by abolishing or increasing hexacoordination in rice non-symbiotic hemoglobin, the rate of the two electron reduction of hydroxylamine is impaired by up to 100 fold. Further, we observe that disruption of the ability of rice non-symbiotic hemoglobin to form a transient dimer impairs the rate of hydroxylamine reduction by 10 fold. Mixing experiments reveal that the flow of electrons in this system is indeed from the hexacoordinate heme to the pentacoordinate heme.

Introduction

Non-symbiotic plant hemoglobins (nsHbs) have recently been shown to effectively carry out the one electron reduction of nitrite to nitric oxide and the two electron reduction of hydroxylamine to ammonium [(1-3)]. The physiological role of these reactions however, remains to be fully understood. One hypothesis is that these proteins function as nitric oxide producers during conditions of severe hypoxia, providing an alternative pathway to generate nitric oxide that is used in signaling pathways [(3)]. An alternative hypothesis is that hemoglobins are carrying out the reduction of nitrite and potentially hydroxylamine in a manner similar to the nitrogen reduction reactions used for anaerobic respiratory purposes found in bacteria [(4-12)].

The dissimilatory reduction of nitrogen to ammonium in a respiratory manner is one process in the biogeochemical nitrogen cycle[13]. Structural characterization of some of the enzymes that are involved in this process have revealed active sites that make use of two or more heme prosthetic groups to transfer electrons to a nitrogenous ligand, forming ammonium [4-6, 10, 12, 14, 15].The addition of nitrogenous molecules, including nitrite and nitrate, to plants exposed to prolonged hypoxic conditions has shown the ability to improve plant survivability during these stresses but the mechanisms of this effect are still an area of active investigation[16]. Plant nsHbs have shown that they are capable of efficiently carrying out the reductive reactions that would be required to observe the beneficial effects of nitrite seen in previous studies [1-3]and this study aims to elucidate the mechanism by which nsHbs carry out these reactions, particularly multi-electron reductions.

The multi-heme enzymes that are used by bacteria in dissimilatory nitrogen metabolism have, through three dimensional crystal structures, shown that one heme site is typically coordinated by 5 bonds leaving an empty binding site at one axial position[17]. The other heme moieties present in the enzyme then have six coordinate bonds with both axial ligands commonly occurring as histidine and coming from the protein. These hemes serve as electron donors to the pentacoordinate binding site where the reductive chemistry takes place [4-6, 8-10, 12, 17]. Plant nsHbs have previously been shown to exist in a state of fractional hexacoordination [18], a state which would functionally mimic the active site architecture of the bacterial enzymes which participate in reductive nitrogen chemistry. In this study, we examine both the influence of

quaternary structure of nsHbs, shown to be able to form transient dimers in solution[19], and the effects of fractional hexacoordination on the rates of reduction of the nitrogenous ligands nitrite and hydroxylamine.

We hypothesize that by perturbing the coordination of the heme iron in rice nsHb1 we will be able to affect the rates of nitrite and hydroxylamine reduction in the following ways. The one electron reduction of nitrite is predicted to be unchanged in the pentacoordinate and monomeric mutants due to the maintenance of an open binding site and the requirement for only a single electron and reduction of nitrite by the hexacoordinate mutant will be slowed since there is no open binding site. With respect to hydroxylamine, we hypothesize that there would be little to no effect of the monomeric mutant on the rate of reduction given that the equilibrium dissociation constant for ferrous wild type rice nsHb1 is approximately 600 micro molar and the reactions are being observed at much lower protein concentrations. We further hypothesize that both of the coordination mutants will impair the rate of reduction of hydroxylamine.

Materials and Methods

Protein Preparation- All proteins were grown and purified as previously described. Mutants were chosen based on the lack of or additional degree of hexacoordination [20]. The observed fraction of hexacoordinate protein, the observed values for distal histidine coordination, and the equilibrium dissociation constants for dimerization are summarized in Table 1.

Reductive Reactions- All reactions were carried out as described previously [1, 2]. Briefly, ferrous deoxy protein was generated in an anaerobic chamber (Coy Laboratories). This protein was mixed with either nitrite or hydroxylamine and the change in absorbance was monitored as a function of time using either a Cary 50 Bio spectrophotometer with the kinetics or scanning kinetics modes or a Bio-Logic SFM 400 stopped flow reactor attached to an Ocean Optics DH-2000 light source using the strip chart function in SpectraSuite (Ocean Optics). All data was analyzed using Igor Pro software.

Mixing Reactions- Mixing reactions were carried out using wild type rice nsHb1 and rice H73L proteins. Reactions were done in both ferrous wild type to ferric H73L and ferrous H73L to ferric wild type directions. Ferrous deoxy protein was generated by reducing with dithionite in an anaerobic chamber. Excess dithionite was removed by passing over a G-25 column equilibrated in anaerobic potassium phosphate buffer pH 7. Ferric proteins were similarly passed over a G-25 column equilibrated in anaerobic potassium phosphate buffer pH 7. Extinction coefficients were determined as described in chapter six. Spectra were collected as a function of time before and following mixing in a sealed split cuvette (Starna Cells) using the scanning kinetics mode of a Cary 50 Bio spectrophotometer. Theoretical spectra were generated by combining individual component spectra for each species present.

Results

Nitrite Reduction- The reduction of nitrite to NO and the concomitant formation of ferric hemoglobin was measured as described previously [2] by following the decrease

in absorbance at 557 nm associated with the conversion of ferrous deoxy protein for the pentacoordinate H73L mutant, the more hexacoordinate F40A mutant, and the monomeric S49A mutant of rice nsHb1. The time courses for these reactions are shown in Figure 1a and the concentration dependence on nitrite for the reactions is shown in Figure 1b. We observe that there is almost no effect of the pentacoordinate mutation on this reaction, suggesting that rice nsHb1 in the pentacoordinate form is able to easily bind nitrite and subsequently reduce it by one electron. In contrast, the F40A mutant, which increases hexacoordination, shows a profound effect on the rate of nitrite reduction. This mutation causes the reaction to proceed at a rate similar to the rate observed for myoglobin[(2)]. This demonstrates that the increase in hexacoordination directly affects the rate of nitrite reduction. Furthermore, the monomeric S49A mutant of rice nsHb1 shows a slight effect on the rate of nitrite reduction. These rates, along with other representative pentacoordinate and hexacoordinate mammalian globins are summarized in Table 2.

Hydroxylamine Reduction- The reduction of hydroxylamine by two electrons to form ammonium ion and two ferric hemoglobins was followed as previously reported [(1)] by monitoring the decrease in absorbance at 557 nm associated with oxidation of ferrous deoxy protein. The time courses and the dependence of the observed rate of reaction on hydroxylamine concentration are shown in Figure 2 a and b respectively. These plots demonstrate that both coordination mutants have a significant effect on the observed rate of the reaction. The pentacoordinate H73L mutant shows a 100 fold increase in $t_{1/2}$ and

a corresponding decrease in the pseudo-first order rate constant to 0.2 $mM^{-1}s^{-1}$. This decrease is nearly the same as that observed for horse heart myoglobin[(2)].

The more hexacoordinate F40A mutant shows a biphasic reaction time course with a fast, albeit 3 fold slower than wild type, phase comprising approximately 60 percent of the reaction. The slow phase comprising the remaining 40 percent of the reaction has a rate constant on the order of that observed for myoglobin and rice H73L, 0.6 $mM^{-1}s^{-1}$. The monomeric mutant also shows a change in the rate of hydroxylamine reduction from the wild type protein. The S49A mutant has a monophasic time course and a rate constant that is 10 fold slower than the wild type protein, 2.5 $mM^{-1}s^{-1}$. These rates are summarized in Table 3.

Electron Flow- A possible explanation for the reduced rates of catalysis that are observed in the pentacoordinate mutant protein is that intermolecular electron exchange is unable to occur. To test this hypothesis, mixing experiments using the same split cell apparatus described in chapter 6 was employed. In this case mixing was carried out in two directions, from ferrous wild type rice nsHb1 to ferric rice H73L and in the complementary ferrous H73L to ferric wild type directions. The results are shown in Figure 3. What we observe is that electron transport in the ferrous wild type to ferric H73L direction occurs on approximately the same time scale as electron self-exchange in deuteroheme substituted rice nsHb1. However in the opposite direction the electron exchange occurs on the same time scale as the electron self-exchange in deuteroheme substituted myoglobin reported in chapter six. Furthermore, we observe that electron transfer from the ferrous wild type protein to the ferric H73L mutant is complete while

the reverse transfer reaches an equilibrium with four species present, indicating that the equilibrium for this reaction lies on the side of ferrous H73L protein.

Discussion

Nitrite Reduction- The results presented for the reduction of nitrite by rice nsHb1 mutants are consistent with our hypotheses of a largely unaffected rate by removing the coordination by the distal histidine and by disrupting dimerization. The rate is unchanged from wild type for the pentacoordinate H73L mutant [(2)], and decreased by only 2 fold for the monomeric S49A mutant. This slightly decreased rate is still on the same scale as rates measured for other plant nsHbs [(3)]. The observed results are also consistent with our hypothesis of a decreased rate of reduction by the hexacoordinate F40A mutant, possibly indicative of an occlusion of the binding site for nitrite at the sixth axial ligand position and a dependence on distal histidine dissociation followed by ligand binding. This dependence would follow one of the scenarios described in Smagghe et al [(18)].

Hydroxylamine Reduction- In the case of hydroxylamine reduction for the monomeric S49A mutant, we would expect that there would be little change to the rate of hydroxylamine reduction based on the relatively high equilibrium dissociation constant of the wild type rice nsHb1 dimer in the ferrous oxidation state of 600 micromolar [(19)]. What we actually observe in this case however, is a tenfold decrease in the rate constant. This decrease in rate constant suggests that even though wild type rice has a high equilibrium dissociation constant in the ferrous oxidation state, the ability to transiently dimerize is still an integral part of the reaction mechanism. This may be due

to rates of intermolecular electron transfer between the individual monomers which would provide the second electron for hydroxylamine reduction to ammonium. In a completely monomeric system, inter-heme distances might, on average, increase which would, according to Marcus theory, lead to a slower rate of intermolecular electron transfer [(21)]. This hypothesis will be further tested by examining the rates of electron self-exchange in rice S49A using the deuteroheme substitution method described in chapter six.

In the case of both coordinate mutants, we would expect that rates of hydroxylamine reduction would slow. For the hexacoordinate mutant, we observe a biphasic time course with both phases being significantly slower than the wild type rate of hydroxylamine reduction. This suggests that by blocking the entrance of the ligand into the active site, the rate of hydroxylamine reduction is reduced. I hypothesize that the second, slow phase is limited by the dissociation of the distal histidine from the heme iron. Preliminary results show a loss in amplitude of absorbance change associated with the fast phase and a deviation from linearity for the slow phase at high (10 and 13 millimolar) concentrations of hydroxylamine (data not shown). Additional measurements at high concentrations of hydroxylamine on the hexacoordinate mutant, the wild type protein, and hexacoordinate mammalian globins will further probe the role of k_{-H} on the rates of hydroxylamine reduction.

The pentacoordinate H73L mutant also shows a decreased rate of hydroxylamine reduction compared to the wild type protein. The measured rate of reaction is on the order of that observed for myoglobin [(1)]. Analysis of dissimilatory reductases has shown

that the role of the b_5 type heme centers found in these enzymes is to transfer electrons to the active site, while the role of the pentacoordinate centers is to serve as a binding site for the ligand [4-6, 8-10, 12, 17]. If hemoglobin functions in an analogous way, the H73L mutant would maintain the open binding site required for hydroxylamine reduction, but removing the fraction of hexacoordinate heme in the protein would impact this multi-electron reduction reaction by eliminating the heme center which efficiently provides a second electron. In order to test this hypothesis we performed mixing experiments with reduced wild type and ferric H73L rice nsHbs, and the complementary ferrous H73L and ferric wild type rice nsHbs.

The results of these mixing experiments demonstrate that electrons flow from ferrous wild type rice nsHb to ferric H73L rice nsHb at nearly the rate as the electron self-exchange for wild type rice nsHb reported in chapter six. However, they also show that, the transfer of electrons to ferric wild type rice nsHb from ferrous rice H73L occurs on the same time scale as the self-exchange reported for myoglobin in chapter six. When these results are taken together with previous reports of the redox potentials of these proteins and the role of hexacoordination in reduction kinetics [20, 22], they lead to the following hypothesis for the role of fractional hexacoordination and dimerization in plant nsHbs.

By maintaining a population of proteins which are able to transiently dimerize[19] and which have fractional hexacoordination, plant nsHbs provide both an open binding site for nitrogenous ligands and an electron donor capable of efficient inter-hemoglobin electron transfer required for multi-electron reduction reactions. Furthermore, the

pentacoordinate center maintains a more positive redox potential, favoring the flow of electrons in the direction of reduced hexacoordinate heme to ferric pentacoordinate, ligand bound heme, again analogous to bacterial reductases[17]. The resulting ferric hexacoordinate heme then favors re-reduction by an external source [22] which would result in a resetting of the system following catalysis. Further experimentation to prove or disprove this hypothesis is required, including identification of an *in vivo* source of hemoglobin re-reduction, *in vivo* detection of hydroxylamine, and determining the steps following generation of nitric oxide from nitrite by hemoglobin.

References

1. *Sturms, R., DiSpirito, A. A., Fulton, D. B., and Hargrove, M. S. (2011) Hydroxylamine reduction to ammonium by plant and cyanobacterial hemoglobins, Biochemistry 50, 10829-10835.*

2. *Sturms, R., DiSpirito, A. A., and Hargrove, M. S. (2011) Plant and cyanobacterial hemoglobins reduce nitrite to nitric oxide under anoxic conditions, Biochemistry 50, 3873-3878.*

3. *Tiso, M., Tejero, J., Kenney, C., Frizzell, S., and Gladwin, M. T. (2012) Nitrite reductase activity of nonsymbiotic hemoglobins from Arabidopsis thaliana, Biochemistry 51, 5285-5292.*

4. *Einsle, O. (2011) Structure and function of formate-dependent cytochrome c nitrite reductase, NrfA, Methods in Enzymology 496, 399-422.*

5. *Einsle, O., Messerschmidt, A., Stach, P., Bourenkov, G. P., Bartunik, H. D., Huber, R., and Kroneck, P. M. (1999) Structure of cytochrome c nitrite reductase, Nature 400, 476-480.*

6. *Einsle, O., Stach, P., Messerschmidt, A., Simon, J., Kroger, A., Huber, R., and Kroneck, P. M. (2000) Cytochrome c nitrite reductase from Wolinella succinogenes. Structure at 1.6 A resolution, inhibitor binding, and heme-packing motifs, The Journal of Biological Chemistry 275, 39608-39616.*

7. *Kern, M., Eisel, F., Scheithauer, J., Kranz, R. G., and Simon, J. (2010) Substrate specificity of three cytochrome c haem lyase isoenzymes from Wolinella*

succinogenes: unconventional haem c binding motifs are not sufficient for haem c attachment by NrfI and CcsA1, Molecular Microbiology 75, 122-137.

8. *Kern, M., and Simon, J. (2009) Electron transport chains and bioenergetics of respiratory nitrogen metabolism in Wolinella succinogenes and other Epsilonproteobacteria, Biochimica et Biophysica Acta 1787, 646-656.*

9. *Pittman, M. S., Elvers, K. T., Lee, L., Jones, M. A., Poole, R. K., Park, S. F., and Kelly, D. J. (2007) Growth of Campylobacter jejuni on nitrate and nitrite: electron transport to NapA and NrfA via NrfH and distinct roles for NrfA and the globin Cgb in protection against nitrosative stress, Molecular Microbiology 63, 575-590.*

10. *Stach, P., Einsle, O., Schumacher, W., Kurun, E., and Kroneck, P. M. (2000) Bacterial cytochrome c nitrite reductase: new structural and functional aspects, Journal of Inorganic Biochemistry 79, 381-385.*

11. *Atkinson, S. J., Mowat, C. G., Reid, G. A., and Chapman, S. K. (2007) An octaheme c-type cytochrome from Shewanella oneidensis can reduce nitrite and hydroxylamine, FEBS Letters 581, 3805-3808.*

12. *Mowat, C. G., Rothery, E., Miles, C. S., McIver, L., Doherty, M. K., Drewette, K., Taylor, P., Walkinshaw, M. D., Chapman, S. K., and Reid, G. A. (2004) Octaheme tetrathionate reductase is a respiratory enzyme with novel heme ligation, Nature Structural & Molecular Biology 11, 1023-1024.*

13. *Simon, J., and Klotz, M. G. (2013) Diversity and evolution of bioenergetic systems involved in microbial nitrogen compound transformations, Biochimica et Biophysica Acta (BBA) - Bioenergetics 1827, 114-135.*

14. *Allen, J. W., Watmough, N. J., and Ferguson, S. J. (2000) A switch in heme axial ligation prepares Paracoccus pantotrophus cytochrome cd1 for catalysis, Nature Structural Biology 7, 885-888.*

15. *Bamford, V. A., Angove, H. C., Seward, H. E., Thomson, A. J., Cole, J. A., Butt, J. N., Hemmings, A. M., and Richardson, D. J. (2002) Structure and spectroscopy of the periplasmic cytochrome c nitrite reductase from Escherichia coli, Biochemistry 41, 2921-2931.*

16. *Oliveira, H. C., Salgado, I., and Sodek, L. (2013) Involvement of nitrite in the nitrate-mediated modulation of fermentative metabolism and nitric oxide production of soybean roots during hypoxia, Planta 237, 255-264.*

17. *Todorovic, S., Rodrigues, M. L., Matos, D., and Pereira, I. A. (2012) Redox properties of lysine- and methionine-coordinated hemes ensure downhill electron transfer in NrfH(2)A(4) nitrite reductase, The Journal of Physical Chemistry. B.*

18. *Smagghe, B. J., Sarath, G., Ross, E., Hilbert, J. L., and Hargrove, M. S. (2006) Slow ligand binding kinetics dominate ferrous hexacoordinate hemoglobin reactivities and reveal differences between plants and other species, Biochemistry 45, 561-570.*

19. *Goodman, M. D., and Hargrove, M. S. (2001) Quaternary structure of rice nonsymbiotic hemoglobin, The Journal of Biological Chemistry 276, 6834-6839.*

20. *Smagghe, B. J., Kundu, S., Hoy, J. A., Halder, P., Weiland, T. R., Savage, A., Venugopal, A., Goodman, M., Premer, S., and Hargrove, M. S. (2006) Role of phenylalanine B10 in plant nonsymbiotic hemoglobins, Biochemistry 45, 9735-9745.*

21. *Gray, H. B., and Malmstrom, B. G. (1989) Long-range electron transfer in multisite metalloproteins, Biochemistry 28, 7499-7505.*

22. *Weiland, T. R., Kundu, S., Trent, J. T., 3rd, Hoy, J. A., and Hargrove, M. S. (2004) Bis-histidyl hexacoordination in hemoglobins facilitates heme reduction kinetics, J Am Chem Soc 126, 11930-11935.*

23. *Tiso, M., Tejero, J., Basu, S., Azarov, I., Wang, X., Simplaceanu, V., Frizzell, S., Jayaraman, T., Geary, L., Shapiro, C., Ho, C., Shiva, S., Kim-Shapiro, D. B., and Gladwin, M. T. (2011) Human neuroglobin functions as a redox-regulated nitrite reductase, The Journal of Biological Chemistry 286, 18277-18289.*

Tables.

Table 1. Biophysical Characteristics of Proteins

Protein	k_H	k_{-H}	K_H	F_{Hex}	$K_{D\ dimerization}$
Rice nsHb1	75	40	1.9	0.65	610 µM *
Rice H73L				0	-
Rice F40A	200	4.3	47	~1	-
Rice S49A	-	-	-	-	monomeric **

values taken from references [18-20]
*value for deoxy ferrous protein
**value for ferric protein
- value not determined

Table 2. Nitrite Reduction Rates for Rice nsHb Mutants and Representative Mammalian Globins

Protein	$k_{Nitrite}$ ($M^{-1}s^{-1}$)
Wild Type Rice nsHb1	166*
Rice H73L	162
Rice F40A	14
Rice S49A	90
Myoglobin	11*
Neuroglobin	0.24**

*value taken from reference [2]
**value calculated from reference[23]

Table 3. Hydroxylamine Reduction Rates for Rice nsHb Mutants

Protein	$k_{Hydroxylamine}$ ($mM^{-1}s^{-1}$)
Wild Type Rice nsHb1	25*
Rice H73L	0.2
Rice F40A	7.7**
	0.6***
Rice S49A	2.4

*value taken from reference[1]
**comprises 60 percent of reaction
***comprises 40 percent of reaction

Figure Legends

Figure 1. Reactions of deoxy ferrous hemoglobin with nitrite. A) Time courses for the reaction of deoxy ferrous hemoglobin with 100 micromolar nitrite. Wild Type Rice nsHb1 (closed squares), Rice H73L (closed circles), Rice S49A (open squares), Rice F40A (crosses). **B)** Plot of observed rate constant versus nitrite concentration. Markers are the same with the addition of Myoglobin (open circles). Error bars are +/- one standard deviation.

Figure 2. Reactions of deoxy ferrous hemoglobin with hydroxylamine. . A) Time courses for the reaction of deoxy ferrous hemoglobin with 100 micromolar hydroxylamine. **B)** Plot of observed rate constant versus hydroxylamine concentration. Wild Type Rice nsHb1 (closed squares), Rice H73L (closed circles), Rice S49A (open squares), Rice F40A (crosses), Myoglobin (open circles). Error bars are +/- one standard deviation.

Figure 3. Electron transfer in wild type rice nsHb and rice H73L. A) Component spectra of each individual protein plotted as extinction coefficient versus wavelength. Wild type rice nsHb is black, rice H73L is red. **B)** Starting and final observed (solid line) spectra along with calculated (dotted line) spectra for ferrous wild type rice nsHb with ferric rice H73L at equal concentrations. The theoretical starting spectrum is composed of 40 percent ferrous wild type rice nsHb, 10 percent ferric wild type rice nsHb and 45 percent ferric rice H73L. The theoretical final spectrum is composed of 50 percent ferric wild type rice nsHb, 35 percent ferrous rice H73L, and 15 percent ferric rice H73L. **C)** Spectral transition observed for mixing ferrous wild type rice nsHb with

ferric rice H73L at equal concentrations. **D)** Starting and final observed (solid line) spectra along with calculated (dotted line) spectra for ferrous rice H73L with ferric wild type rice nsHb. Starting theoretical spectrum is 50 percent ferrous rice H73L, 40 percent ferric wild type rice nsHb, and 10 percent ferrous rice nsHb. Final theoretical spectrum is 40 percent ferrous rice H73L, 10 percent ferric rice H73L, 30 percent ferric wild type rice nsHb and 20 percent ferrous wild type rice nsHb. **E)** Spectral transition observed for mixing ferrous rice H73L with ferric wild type rice nsHbs. **F)** Time courses for both reactions. Transfer from ferrous wild type to ferric H73L is represented by open circles and transfer from ferrous H73L to ferric wild type is represented by closed circles.

Figure 1.

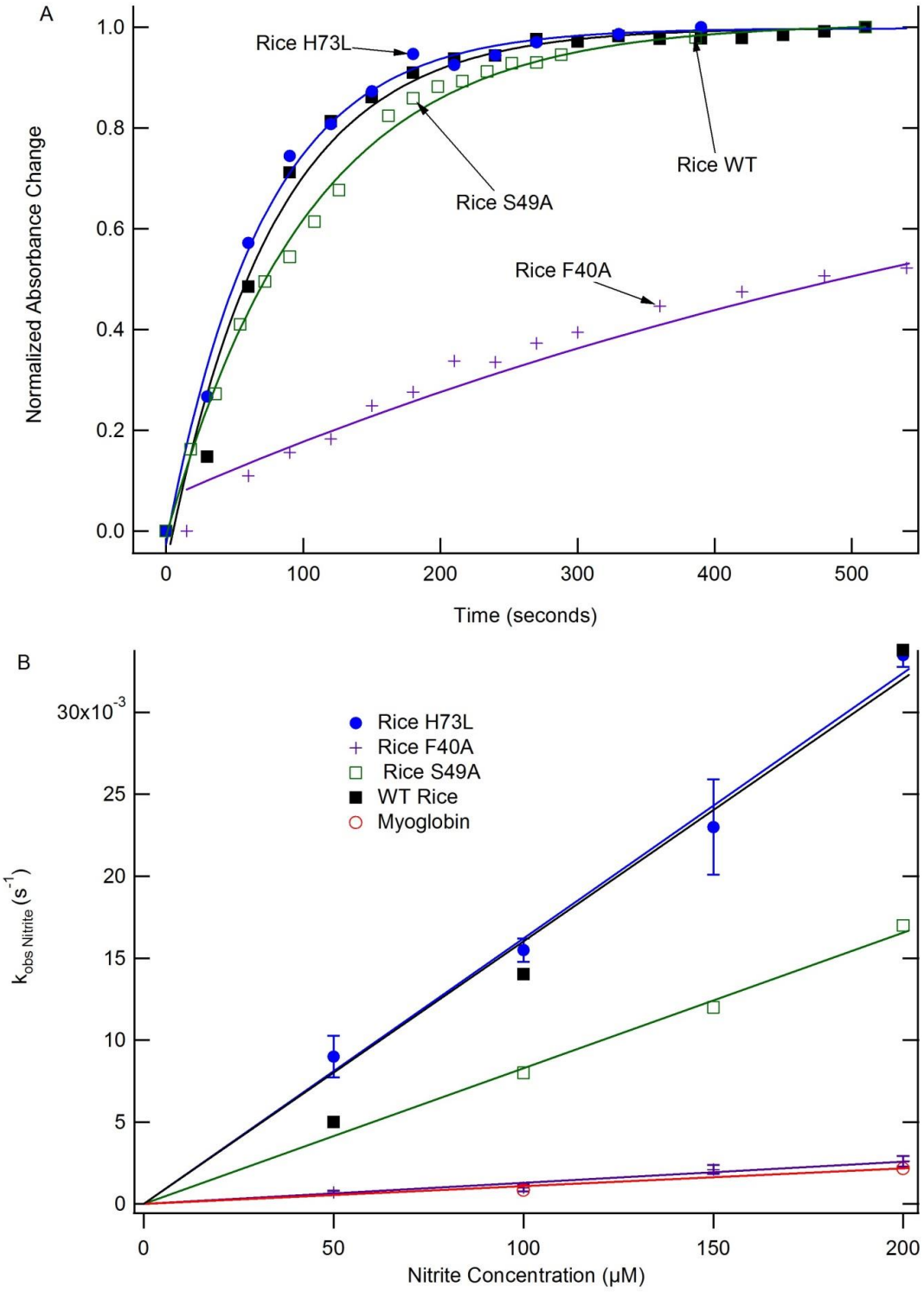
A
Normalized Absorbance Change
Time (seconds)
Rice H73L
Rice S49A
Rice WT
Rice F40A
B
$k_{obs\ Nitrite}$ (s^{-1})
$30x10^{-3}$
Nitrite Concentration (μM)
Rice H73L
Rice F40A
Rice S49A
WT Rice
Myoglobin

Figure 2.

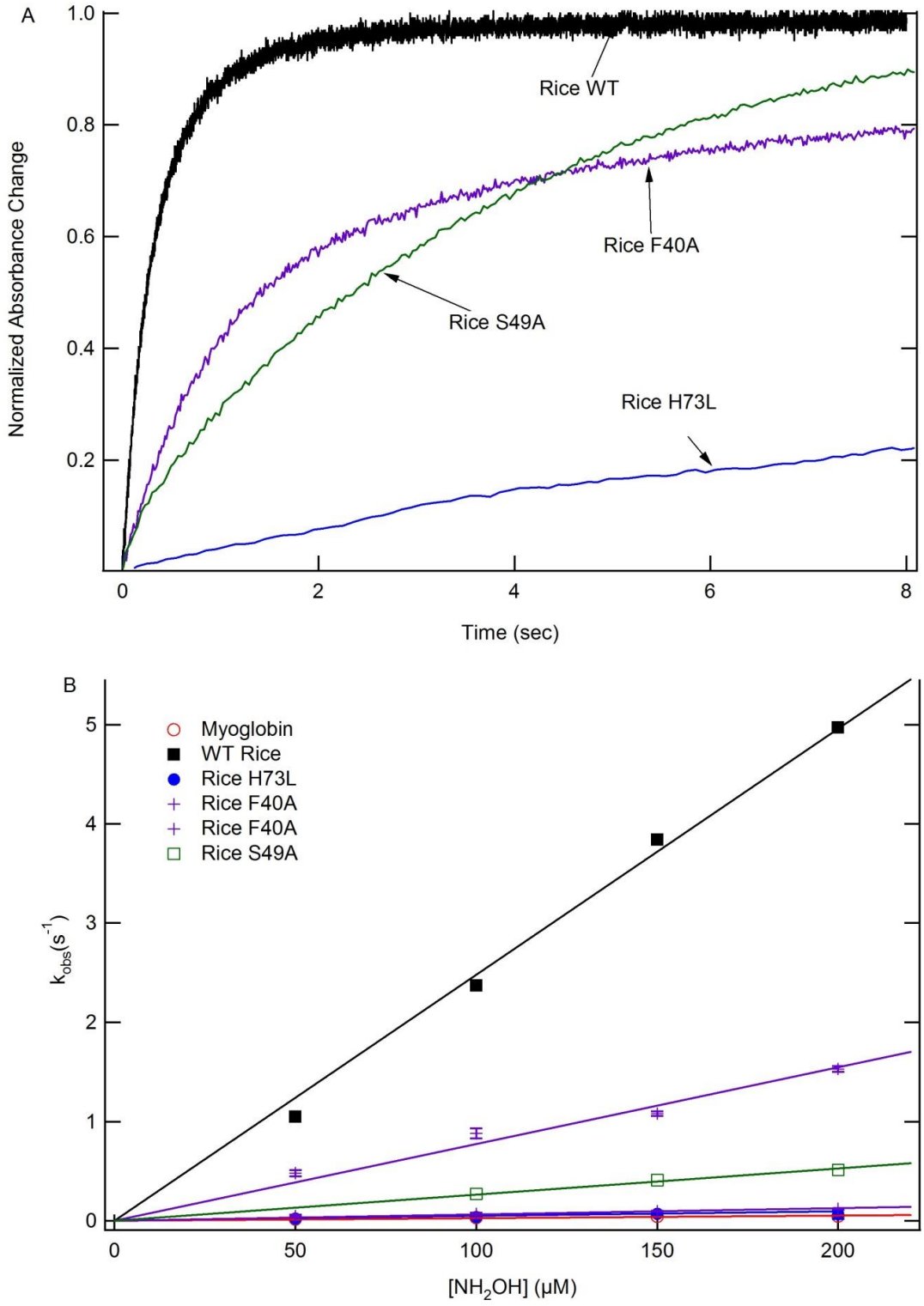
A
Normalized Absorbance Change
Time (sec)
Rice WT
Rice F40A
Rice S49A
Rice H73L
B
Myoglobin
WT Rice
Rice H73L
Rice F40A
Rice F40A
Rice S49A
$k_{obs}(s^{-1})$
$[NH_2OH]$ (μM)

Figure 3.

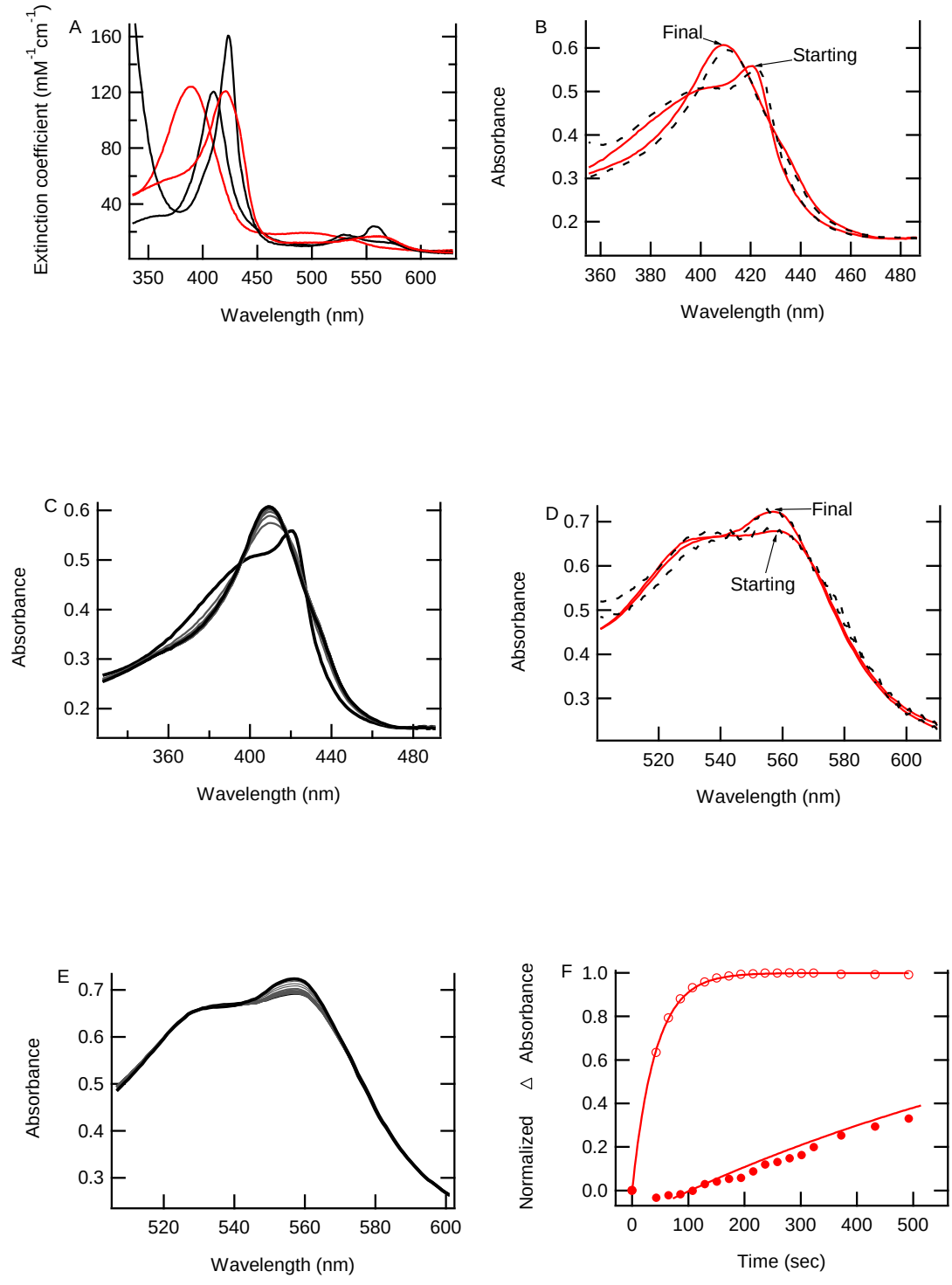
A
Extinction coefficient (mM-1cm-1)
160
120
80
40
350
400
450
500
550
600
Wavelength (nm)
B
Absorbance
0.6
0.5
0.4
0.3
0.2
Final
Starting
360
380
400
420
440
460
480
Wavelength (nm)
C
Absorbance
0.6
0.5
0.4
0.3
0.2
360
400
440
480
Wavelength (nm)
D
Absorbance
0.7
0.6
0.5
0.4
0.3
Final
Starting
520
540
560
580
600
Wavelength (nm)
E
Absorbance
0.7
0.6
0.5
0.4
0.3
520
540
560
580
600
Wavelength (nm)
F
Normalized △ Absorbance
1.0
0.8
0.6
0.4
0.2
0.0
0
100
200
300
400
500
Time (sec)

CHAPTER 8.

CONCLUSIONS

The discovery of hexacoordinate non-symbiotic hemoglobins in plants provided a new direction for the field of hemoglobin biochemistry. Even now, more than 15 years after the discovery of non-symbiotic hemoglobin in barley [(1)], the field is still searching for *in vivo* functions of these proteins. I have presented in this dissertation *in vitro* studies that have laid the biochemical groundwork for further investigation of the hypothesis that class 1 non-symbiotic hemoglobins are able to function in an anaerobic respiratory system within the plant. I have also presented ligand binding kinetics and structural analysis to help understand the convergent evolution of the familiar oxygen transport function of hemoglobins.

The pair of hemoglobin proteins from *Trema* and *Parasponia* provides a unique system for studying the evolution of oxygen transport in class 1 non-symbiotic hemoglobins. This class is normally not associated with oxygen transport due to typical hexacoordination of the heme iron, a generally high affinity for oxygen, and a slow oxygen dissociation rate constant[(2, 3)]. However, phylogenetic studies show that both *Trema* and *Parasponia* hemoglobins belong to the class 1 family of non-symbiotic hemoglobins. The results I presented showed that these two hemoglobins, despite differing by only 11 amino acids, have significantly different oxygen dissociation rate constants, in turn influencing the oxygen affinity and allowing the hemoglobin from *Parasponia* to function as an oxygen transporter while these same characteristics in the hemoglobin from *Trema* are typical of non-symbiotic hemoglobins.

Questions that are yet to be addressed from the kinetic and structural analyses of these proteins include: Which amino acid residues are responsible for the change in oxygen dissociation rate constants and thus oxygen affinity? This question would be addressed by future research in which mutant proteins for each species are generated. Pertinent first mutants to make would be those close to the distal heme pocket including the isoleucine at position 101 in *Parasponia* Hb. This residue is a leucine in *Trema* hemoglobin, and the crystal structure suggests that there may be some steric clash between this residue and the distal histidine residue in *Parasponia* hemoglobin that is not present in *Trema* hemoglobin.

Furthermore, the factors involved in creating a tight dimer for these proteins could continue to be explored. It was observed that a histidine at position 114 and a glutamate at position 113 form a hydrogen bond in both *Parasponia* and *Trema* hemoglobins. This hydrogen bonding pair is not present in rice hemoglobin, an alanine is in the place of the glutamate, so a mutational study in which the alanine is replaced with glutamate would begin to address if this interaction indeed plays a role in dimerization.

This pair of proteins from *Trema* and *Parasponia* demonstrates that oxygen transport proteins can arise from the class 1 non-symbiotic hemoglobins that are found in plants. However, the traditional ligand binding kinetics and crystal structures presented in chapters two and three do not address what the primordial function of the other class 1 non-symbiotic hemoglobins, which are not oxygen transport proteins, is. It has been observed that expression of class 1 non-symbiotic hemoglobins is up regulated during

times of hypoxic stress as well as during conditions of nitrosative stress including exposure to nitric oxide [4, 5]. In combination with work that described hemoglobins and flavohemoglobin as efficient nitric oxide dioxygenases [6-13], these data led some groups to suggest that non-symbiotic hemoglobins, in concert with mono-dehydroascorbate reductases (MDHAR) function in an "alternative to classical fermentation" to continue energy production during hypoxic stresses [9, 10].

However, this hypothesis does not test the effectiveness of MDHAR at actually reducing hemoglobin, nor does it test the activity of MDHAR towards nitric oxide. This hypothesis also does not take into account that during times of water saturated soil, available oxygen concentrations can approach 0 [14]. This would remove from the "NOD fermentation" system an integral component, oxygen, and render this proposed mechanism for NAD+ regeneration ineffective. Another hypothesis for the primordial function of non-symbiotic hemoglobins is that they function as anaerobic nitrite reductases with the end goal of producing nitric oxide as a signaling molecule [15]. This hypothesis though, fails to address other sources of nitric oxide and how they may impact the importance of hemoglobin serving as an NO producer for signaling purposes.

The hypothesis presented, and tested as feasible in this dissertation is that non-symbiotic hemoglobins, because of their unique fractional hexacoordination of their heme prosthetic groups, function in the hypoxic and anoxic root tissue of plants to support continued respiration with a nitrogenous ligand serving as the terminal electron acceptor. These types of respiratory systems are found in other kingdoms of life including bacteria and fungi [16-18]. These systems include both denitrification, in which

nitrate or nitrite are reduced to a gaseous ligand, and ammonification, in which nitrite or hydroxylamine are reduced to ammonium. The reductive reactions that plant non-symbiotic hemoglobins catalyze for the nitrogenous species, nitrite and hydroxylamine, are steps that would be required for both schemes of anaerobic nitrogen respiration.

In order to prove whether or not this type of anaerobic respiration mediated by hemoglobins is occurring in plants and is responsible for the increased tolerance to hypoxia when plants are treated with nitrite much more research needs to be done. Questions that remain are significant and are no easy task to answer. They include, at the biochemical level, determining if there is a mechanism for getting past ferrous-nitrosyl hemoglobin. Without such a mechanism, regardless of what it is, this would effectively be a dead end reaction since nitric oxide binds rapidly to ferrous hemoglobin and would thus poison the system for further catalysis. Furthermore, an *in vivo* source of reduction for hemoglobin must be identified. *In vitro* studies used dithionite as an external reductant for catalytic turnover of nitrogenous ligands but this molecule is not present in plant cells. Continued catalysis *in vivo* then would require some other source of electrons to "reset" the hemoglobin catalyst once it has been oxidized.

At the mechanistic level, limitations of and influences on the reactions by the distal histidine ligand remain to be fully explored. This can be accomplished by studying the rates of nitrite and hydroxylamine reduction at high ligand concentrations to try to observe an upper limit where the reaction rate becomes concentration independent. Additionally, the electron self-exchange rates in rice S49A and rice H73L will help to

further clarify the mechanism by which rice nsHb is able to efficiently transfer electrons amongst itself.

Finally at the physiological level, knock out studies will be instrumental in demonstrating the significance of this proposed respiratory system. Protocols have already been published for evaluating the effects that treatment with nitrite has on a plant during hypoxic stress and these protocols could be extended to the study of plants lacking hemoglobin. By comparing these markers in plants containing hemoglobin against plants with hemoglobin knocked out we could begin to investigate and evaluate the hypoxic nitrogen respiration reactions that may be carried out by non-symbiotic hemoglobin.

The study of plant non-symbiotic hemoglobins will continue to provide new and exciting discoveries in the basic biochemistry that plants use to survive. Class two and class three hemoglobins remain largely uninvestigated, and class one hemoglobins are still an active area of research and debate. With new sequences and new globins being discovered at a rapid pace with the help of bioinformatics techniques, there are many opportunities for future research in the field of hemoglobins.

References

1. Duff, S. M., Wittenberg, J. B., and Hill, R. D. (1997) Expression, purification, and properties of recombinant barley (Hordeum sp.) hemoglobin. Optical spectra and reactions with gaseous ligands, *The Journal of Biological Chemistry 272*, 16746-16752.

2. Kakar, S., Hoffman, F. G., Storz, J. F., Fabian, M., and Hargrove, M. S. (2010) Structure and reactivity of hexacoordinate hemoglobins, *Biophysical Chemistry 152*, 1-14.

3. Hoy, J. A., Robinson, H., Trent, J. T., 3rd, Kakar, S., Smagghe, B. J., and Hargrove, M. S. (2007) Plant hemoglobins: a molecular fossil record for the evolution of oxygen transport, *Journal of Molecular Biology 371*, 168-179.

4. Ohwaki, Y., Kawagishi-Kobayashi, M., Wakasa, K., Fujihara, S., and Yoneyama, T. (2005) Induction of class-1 non-symbiotic hemoglobin genes by nitrate, nitrite and nitric oxide in cultured rice cells, *Plant & Cell Physiology 46*, 324-331.

5. Seregelyes, C., Mustardy, L., Ayaydin, F., Sass, L., Kovacs, L., Endre, G., Lukacs, N., Kovacs, I., Vass, I., Kiss, G. B., Horvath, G. V., and Dudits, D. (2000) Nuclear localization of a hypoxia-inducible novel non-symbiotic hemoglobin in cultured alfalfa cells, *FEBS Letters 482*, 125-130.

6. Gardner, P. R., Gardner, A. M., Martin, L. A., Dou, Y., Li, T., Olson, J. S., Zhu, H., and Riggs, A. F. (2000) Nitric-oxide dioxygenase activity and function of flavohemoglobins. sensitivity to nitric oxide and carbon monoxide inhibition, *The Journal of Biological Chemistry 275*, 31581-31587.

7. Gardner, P. R., Gardner, A. M., Martin, L. A., and Salzman, A. L. (1998) Nitric oxide dioxygenase: an enzymic function for flavohemoglobin, *Proceedings of the National Academy of Sciences of the United States of America 95*, 10378-10383.

8. Igamberdiev, A. U., Baron, K., Manac'h-Little, N., Stoimenova, M., and Hill, R. D. (2005) The haemoglobin/nitric oxide cycle: involvement in flooding stress and effects on hormone signalling, *Annals of Botany 96*, 557-564.

9. Igamberdiev, A. U., Bykova, N. V., Shah, J. K., and Hill, R. D. (2010) Anoxic nitric oxide cycling in plants: participating reactions and possible mechanisms, *Physiologia Plantarum 138*, 393-404.

10. Igamberdiev, A. U., and Hill, R. D. (2004) Nitrate, NO and haemoglobin in plant adaptation to hypoxia: an alternative to classic fermentation pathways, *Journal of Experimental Botany 55*, 2473-2482.

11. Igamberdiev, A. U., Seregelyes, C., Manac'h, N., and Hill, R. D. (2004) NADH-dependent metabolism of nitric oxide in alfalfa root cultures expressing barley hemoglobin, *Planta 219*, 95-102.

12. Pathania, R., Navani, N. K., Gardner, A. M., Gardner, P. R., and Dikshit, K. L. (2002) Nitric oxide scavenging and detoxification by the Mycobacterium tuberculosis haemoglobin, HbN in Escherichia coli, *Molecular Microbiology 45*, 1303-1314.

13. Smagghe, B. J., Trent, J. T., 3rd, and Hargrove, M. S. (2008) NO dioxygenase activity in hemoglobins is ubiquitous in vitro, but limited by reduction in vivo, *PloS One 3*, e2039.

14. Jackson, M., and Attwood, P. (1996) Roots of willow (Salix viminalis L.) show marked tolerance to oxygen shortage in flooded soils and in solution culture, *Plant Soil 187*, 37-45.

15. Tiso, M., Tejero, J., Kenney, C., Frizzell, S., and Gladwin, M. T. (2012) Nitrite reductase activity of nonsymbiotic hemoglobins from Arabidopsis thaliana, *Biochemistry 51*, 5285-5292.

16. Shoun, H., and Tanimoto, T. (1991) Denitrification by the fungus Fusarium oxysporum and involvement of cytochrome P-450 in the respiratory nitrite reduction, *Journal of Biological Chemistry 266*, 11078-11082.

17. Simon, J., and Klotz, M. G. (2013) Diversity and evolution of bioenergetic systems involved in microbial nitrogen compound transformations, *Biochimica et Biophysica Acta (BBA) - Bioenergetics 1827*, 114-135.

18. Verbaendert, I., Boon, N., De Vos, P., and Heylen, K. (2011) Denitrification is a common feature among members of the genus Bacillus, *Systematic and Applied Microbiology 34*, 385-391.